2009

Nitric Oxide Synthase in Confined Environments;Detection and Quantification of Nitric Oxide Released from Cells and Modified Liposomes Using a Sensitive Metal Catalyst-Pedot Modified Carbon Fiber Electrode

P. A. Reshani H. Perera
Cleveland State University

NITRIC OXIDE SYNTHASE IN CONFINED ENVIRONMENTS: DETECTION AND QUANTIFICATION OF NITRIC OXIDE RELEASED FROM CELLS AND MODIFIED LIPOSOMES USING A SENSITIVE METAL CATALYST-PEDOT MODIFIED CARBON FIBER ELECTRODE

P. A. RESHANI H. PERERA

Graduate Chemist

College of Sciences, Institute of Chemistry,

Colombo, Sri Lanka

June, 2001

Bachelor of Science, Specialization in Chemistry

University of Colombo, Colombo, Sri Lanka

December, 2002

Submitted in partial fulfillment of the requirements for the degree

DOCTOR OF PHILOSOPHY IN CLINICAL AND BIOANALYTICAL CHEMISTRY

at the

CLEVELAND STATE UNIVERSITY

December, 2009

This dissertation has been approved for the department of Chemistry and the College of Graduate Studies by:

_____

Dissertation Committee Chairperson, Dr. Mekki Bayachou
Department of Chemistry, Cleveland State University

_____

Dissertation Committee Member, Dr. Robert Wei
Department of Chemistry, Cleveland State University

_____

Dissertation Committee Member, Alan Riga
Department of Chemistry, Cleveland State University

_____

Dissertation Committee Member, Dr. Xue-Long Sun
Department of Chemistry, Cleveland State University

_____

Dissertation Committee Member, Dr. Orhan Talu
Department of Chemical and Biomedical Engineering, Cleveland State University

ACKNOWLEDGEMENTS

First and foremost I offer my sincerest gratitude to my supervisor, Dr. Mekki Bayachou, who has supported me throughout my thesis with his patience and knowledge whilst allowing me the room to work in my own way. I could not have completed this project without him.

I must aknowledge all of my committee members, Dr. Robert Wei, Dr. Alan Riga, Dr. Xue-Long Sun, and Dr. Orhan Talu**.**

I am grateful and proud to have Dr. Robert Wei in my committee. You provided me unflinching encouragement and support in various ways for my thesis. I have also benefited for my project by advice and guidance that you gave.

I am grateful in every possible way to Dr. Alan Riga, for his advice, supervision, and crucial contribution to my project. I am extremely thankful for your support and advice given for my project and also my personal life.

I owe my deepest gratitude to Dr. Xue-Long Sun, you offered me much advice and insight throughout my work. I am thankful for always helping me out for my research work and allowing me to use your lab and instruments for my project.

Dr. Orhan Talu, it is an honor for me to have you in my committee. You have made available your support in a number of ways. Thank you for providing me with valuable insight for this project.

I would like to show my gratitude to Dr. Girish Shukla in Biology Department for allowing me to use his lab for my research work.

Collective and individual acknowledgments are also owed to my colleagues, Indika, Jean, John, Pubudu, Charbel, Ling, Saleem, Bhagya, and Lalitha. My special thanks go to Indika, because of him we ended up in Cleveland.

Words fail me to express my appreciation to my husband Pubudu and my little son Haridu whose dedication, love and persistent confidence in me, has taken the load off my shoulder. I would like to give my appreciation again to Pubudu for the support given me in the lab as well as at home. I gratefully thank my parents Nimala and Wickrama for supporting me throughout all my studies, showing me the joy of intellectual pursuit ever since I was a child. I would like to show my gratitude to my parents in-law for their support in past few years.

Finally, I would like to thank Department of Chemistry, CSU and everybody who supported me in any way to the success of my thesis, as well as expressing my apology that I could not mention personally one by one.

DEDICATION

This dissertation is dedicated to:

My son Haridu, husband Pubudu, and for my Parents

NITRIC OXIDE SYNTHASE IN CONFINED ENVIRONMENTS: DETECTION AND QUANTIFICATION OF NITRIC OXIDE RELEASED FROM CELLS AND MODIFIED LIPOSOMES USING A SENSITIVE METAL CATALYST-PEDOT MODIFIED CARBON FIBER ELECTRODE

ABSTRACT

P. A. RESHANI H. PERERA

Nitric oxide (NO) is a freely diffusible, gaseous free radical, associated with many physiological and pathological processes that include neuronal signaling, immune response, and inflammatory response. NO is produced from L-arginine in an NADPH-dependent reaction catalyzed by a family of nitric oxide synthase (NOS) enzymes. A deficiency in NO plays a role in hypertension, hyperglycaemia, and arteriosclerosis, among other pathological states. Conversely, increased NO levels contribute to arthritis, septic shock, and hypotention. Therefore, measuring and quantifying NO production in biological systems and matrices may be vital in elucidating physiological and pathological processes. The goal of this work is to develop an ultra-sensitive and selective electrochemical sensor taking advantage of NO-sulfur chemistry. In particular, electropolymerizing 3,4-ethylenedioxythiophene (EDOT) monomers on the surface of our electrodes yield a suitable sulfur-based polymer PEDOT to be used as an affinity matrix for NO sensing. In other work, we have shown that the ruthenium (Ru) mediates

the catalytic oxidation of NO. In this work, we tried to achieve improved sensitivity by combining both Ru nanoparticles and PEDOT using the layer-by-layer (LBL) modification method. Further, to eliminate interferences the Ru-PEDOT-Ru modified carbon fiber was coated with a nafion layer, which acts as an anionic filter. We used our NO-sensor to accurately monitor NO release from mouse embryonic fibroblast cells as well as isolated single human umbilical vein endothelial cells.

A second part of this work focused on testing the performance of our sensors in characterizing NO release from liposomes with confined NOS enzyme. Liposomes are spherical, closed, self-assembled phospholipids, which enclose part of the surrounding solvent in their interior. Liposomes can enclose an aqueous medium separate from the external aqueous medium. Therefore, liposomes can be used as carriers of enzymes (NOS in this case) without negative impact on the molecular function of the encapsulated biomolecule and can be considered as a promising way to transport and deliver NO to targets. We prepared NOS-loaded liposomes and characterized encapsulation efficiency of various procedures. We also tested the performance of our NO-sensors to monitor and quantify NO release from NOS-loaded liposomes as potential vehicles for on-site NO delivery.

TABLE OF CONTENTS

Page

ACKNOWLEDMENTS ……..iii

DEDICATION……v

ABSTRACT ……..…….. .vi

LIST OF TABLES .……. …xiii

LIST OF SCHEMES…….xiv

LIST OF FIGURES ..…….…...xv

CHAPTER I: NITRIC OXIDE MEASUREMENT IN NOS CONFINED ENVIRONMENT USING AN IMPROVED SENSOR PLATFORM

1.1 Introduction ……..…… 1

1.2 Properties of NO……..……4

1.3 Nitric oxide production in biological systems ……7

1.4 Nitric oxide synthase ……..……..……9

1.5 Biological function of NO ……..11

1.5.1 NO in the vascular system ……..…..……..12

1.5.2 Neuronal NO..…….13

1.5.3 NO in the immune system ……..13

1.6 NO detection in live cells …….. …….14

1.7 Detection of NO……..15

1.8 Electrochemical NO Sensors ……..18

1.9 NO and Sulfur Interactions……..20

1.10 NOS encapsulation in liposomes…….....24

1.11 References……....29

CHAPTER II: DEVELOPMENT OF HIGH SENSITIVE AND SELECTIVE NO SENSOR USING A CARBON FIBER MICROELECTRODE MODIFIED WITH AN ELECTROCONDUCTIVE POLYMER (EDOT) AND THE TRANSITION METAL CATALYST RUTHENIUM

2.1. Introduction ……..……..……..41

2.2. Experimental Section……45

2.2.1. Chemicals and Reagents ……45

2.2.2. Electrochemical apparatus and electrode materials ……...46

2.2.3. Electrode preparation……..…….……47

2.2.4. Preparation of NO stock solution……48

2.2.5 Experimental procedure……49

2.3. Results and discussion……. ……49

2.3.1. Electrodeposition of EDOT on CFE ……..49

2.3.2 Characterization of modified microelectrodes……..…53

2.3.3 Electrochemical detection…….60

2.4. Summary for Chapter II…… 75

2.5. References ……77

CHAPTER III: DETECTION AND QUANTIFICATION OF NITRIC OXIDE RELEASED FROM LIVE CELLS

3.1 Introduction……..82

3.2 Experimental Section…….……. ……84

3.2.1 Chemicals and reagents……..84

3.2.2 Materials and Apparatus ….……...84

3.2.3 Cell Culture Preparation……..85

3.2.4 Cell Experiment Setup……85

3.3 Results and Discussions ……...…..……. 88

3.3.1 NO released from mouse embryonic fibroblast cells …….……...88

3.3.2 NO released from Human Umbilical Vein Endothelial cells……100

3.3.3 NO detection in an isolated single HUVEC cells…….108

Appendix: Calculation of the amount of NO released from single cell……..…110

3.4. Summery for Chapter II…….……. .….112

3.5. References ……..…….. …113

CHAPTER IV: THE NOS-LOADED LIPOSOME AS A PLATFORM FOR THE TREATMENT OF NO/NOS DEFICIENT TARGETS

4.1 Introduction ……..…….…...118

4.2 Experimental Section……...……..122

4.2.1 Materials ……..…… …….. 122

4.2.2 Apparatus ……... 122

4.2.3 Liposome Preparation …….123

4.2.4 NOS encapsulation in liposomes ……....124

4.2.5 Size determination and the stability of NOS-loaded liposome ..…..……124

4.2.6 Visualization of NOS inside the liposome……125

4.2.6.1 Formation of Ni-NTA-Gold tag NOS……...125

4.2.6.2 Gold enhanced (EM) Ni-NTA-Gold labeled NOS…….125

4.2.7 Bradford Assay procedure…….…..126

4.2.8 Griess Assay procedure……..126

4.2.9 Measuring of the NOS activity in liposomes……..126

4.3 Results and Discussion …….…….....127

4.3.1 Characterization of Liposomes ……127

4.3.1.1 AFM images of Liposomes……..…127

4.3.1.2 Microscopic images of Liposomes…….130

4.3.2 Size determination and the stability of NOS-loaded liposome …….……. 131

4.3.3 Visualization of NOS inside the liposome …….……..134

4.3.4 Protein content inside the liposome ..……..……137

4.3.5 Quantification of NO production (NOS activity) using the Griess Assay….139

4.3.6 Measurement of NO released by NOS-loaded liposomes using the NO sensor……141

4.4 Summary for Chapter IV……...…….145

4.5. References…….……..……146

CHAPTER V: FUTURE DIRECTIONS - THE INTRACELLULAR DELIVERY OF LIPOSOME-ENCAPSULATED NOS IN CULTURED HUMAN EMBROYONIC KIDNEY CELLS

5.1 Introduction ……..……..…….……150

5.2. Experimental Section ……..153

5.2.1 Materials and Apparatus……...….153

5.2.2 Liposome preparation……...…….153

5.2.3 Cell Culture Preparation ……..…….154

5.2.4. *In vitro* liposome-cell interaction……..154

5.2.5. Electrochemical Experiments……155

5.3 Preliminary Results and Discussion……..155

5.4 References……..164

LIST OF TABLES

1.1 Pathologic effects of NO……..……..11

2.1 Comparison of sensitivities and detection limits of modified CFEs ..…… 65

2.2 Comparison of sensitivities and detection limits of published NO sensors……69

2.3 Interferences of various compounds with the three layers modified sensor……..75

4.1 The values obtained from Bradford assay…….……139

4.2 The values obtain from the Griess assay…… ..140

LIST OF SCHEMES

1.1 The overall reaction is catalyzed and the cofactors of NOS electrons ……..….8

1.2 Interconversion of different redox forms of NO …….21

2.1 Polymerization of EDOT on the electrode surface …….52

3.1 Schematic diagram showing the NO diffusion from a cell surface ……...…….110

4.1 The diagram of His-tagged protein and Ni-NTA-Nanogold complex ……..…135

LIST OF FIGURES

1.1 Reaction of NO-related compounds in a biological environment.…….5

1.2 The reaction of NO production by means of NOS enzyme ……..7

1.3 Schematic diagram of Nitric Oxide Synthase ……..11

1.4 Resonance structures of *S*-nitrosothiols ……..……..23

1.5 Schematic diagram of different kinds of liposomes. ……..25

1.6 Representation diagram of the mechanism drug delivery…….27

2.1 Cyclic voltammograms showing electro-deposition of EDOT ……51

2.2 FESEM images of unmodified and PEDOT modified CFEs ……...54

2.3 FESEM images of layer-by-layer modified CFEs…….55

2.4 AFM images of PEDOT and layer-by-layer modified HOPG surface ……57

2.5 EDS spectra of unmodified and modified CFEs …….…….59

2.6 Amperometric responses for 7-μm unmodified CFE and modified CFEs……62

2.7 Amperometric responses for 30-μm unmodified CFE and modified CFEs…..64

2.8 Current/NO dose plot for 7-μm unmodified and modified CFEs……..……67

2.9 Typical Amperometric responses of modified CFE for addition of 250 pM of NO……68

2.10 Flow injection analysis response of unmodified and modified CFEs …….71

2.11 Amperometric response of modified CFE for 50 μM NO_2^- in different potential……73

2.12 Amperometric responses of Nafion coated modified CFE to addition of NO and other interferences…….74

3.1 The experimental setup used for cell analysis…….86

3.2 Representative showing the fate of NO released from cells……...87

3.3 The structure of Lipopolysaccharide (LPS)……89

3.4 Schematic diagram of iNOS expression cascade by stimulation with LPS……91

3.5 Amperometric response of the modified electrode for addition of LPS to the fibroblast cell culture……93

3.6 Structure of nitric oxide synthase (NOS) inhibitor, L-NAME……...93

3.7 Amperometric response of the modified electrode for addition of LPS to the fibroblast cell culture after L-NAME inhibition……95

3.8 Amperometric response of the modified electrode for addition of LPS to the PBS solution……96

3.9 Amperometric response of the modified electrode for addition of LPS to the cell culture (summary)…….97

3.10 Calibration plot for modified CFE in cell experiment conditions…….99

3.11 The structure of Bradykinin…….101

3.12 Substrate and cofactor requirements for NOS activation……102

3.13 Current-response for NO released from HUVEC with different amounts of bradykinin stimulation…….103

3.14 Change in concentration of NO released with the varying amount of bradykinin……104

3.15 Amperometric response of the modified electrode for NO released from bradykinin stimulated HUVEC……105

3.16 Amperometric response of the modified electrode for addition of bradykinin to the buffer solution……106

3.17 Amperometric response of the modified electrode for addition of Bradykinin to the HUVEC culture before and after L-NAME inhibition……...107

3.18 Amperometric response of the modified electrode for addition of Bradykinin to an isolated single cell……..109

4.1 Representative AFM images of liposomes on mica surfaces..…….….129

4.2 Three-dimensional images of the typical aggregated vesicle formed from multiple liposome …….129

4.3 Inverted microscopic images of large liposomes……130

4.4 Size distribution for vesicles in suspension measured in DLS……..131

4.5 Mean size variation of liposomal suspension as a function of time……..133

4.6 Microscopic image of NOS-Ni-NTA-Gold loaded liposome……..136

4.7 The absorbance Vs wave length curve for the standard for Bradford protein assay ……..138

4.8 The calibration plot for Bradford protein assay…….138

4.9 The calibration plot for the Griess assay……140

4.10 Amperometric response of the modified electrode for addition of NADPH and PBS buffer solution to the NOS-encapsulated liposome……142

4.11 Amperometric response of the modified electrode for the addition of NADPH close to the NOS-encapsulated liposomes and to the bulk solution…….143

4.12 Amperometric response of the modified electrode for the addition of NADPH to the NOS-encapsulated liposome after the L-NAME treatment……144

5.1 Schematic representation of the possible mechanism by which the liposomes can interact with cells *in vitro* and deliver their content ……..152

5.2 Amperometric response of the modified electrode for addition of L-Arginine to the HEK cell culture……156

5.3 Amperometric response of the modified electrode for addition of L-Arginine to the cell culture that treated with L-NAME ……157

5.4 Amperometric response of the modified electrode for addition of L-Arginine to the PBS solution……..158

5.5 Amperometric response of the modified electrode for addition of L-Arginine to the HEK cell culture incubated with NOS-loaded liposome…..160

5.6 Schematic representation of immobilized Biotin-tag NOS-loaded liposome on solid carrier…….162

5.7 Solution phase AFM image of biotin-tag NOS-loaded liposome on mica surface……163

CHAPTER I

NITRIC OXIDE MEASUREMENT IN NOS CONFINED ENVIRONMENT USING AN IMPROVED SENSOR PLATFORM

1.1 Introduction

It was long thought that NO is just a poisonous, unpleasant, and dangerous gas and is far from having any physiological implications in living organisms. The discovery of NO as the vasodilatory messenger spurred a significant increase in research interest in NO and its roles in biological systems. In fact, NO was named "Molecule of the Year" by Science magazine [1], and the 1998 Nobel Prize in Physiology and Medicine was awarded to three scientists: Ferid Murad, Robert F. Furchgott, and Louis Ignarro [2, 3], for pioneering work discovering the biological roles of NO. Bio-synthesis of this extremely important molecule involves nitric oxide synthase (NOS), which contains several cofactors [5]. NO is produce from the terminal nitrogen atom of the substrate L-arginine in the presence of NADPH and dioxygen (O_2) catalyzed by NOS enzyme.

Nitric oxide plays a role in a variety of biological processes including neurotransmission [6-8], vasodilation [9], immune defense, associated dysfunction [10], inhibition of platelet aggregation [11], and the regulation of cell death (apoptosis) and cell motility. Due to the wide spectrum of activity of NO, a fluctuation of physiological NO concentration contributes to a number of pathogeneses of several diseases. A deficiency of NO production plays a key role in atherosclerosis, hypertension, hyperglycemia, stroke, myocardial infarction, and ischemia [12-16]. Conversely, an overproduction of NO is associated with arthritis, septic shock, hypotension, reperfusion injury and cancer [17]. Thus, for medical and pharmacological approaches, it is important to identify the change of NO production in biological systems by analyzing NO concentration.

The analysis of NO release at the single cell level provides a great advantage in understanding many physiological functions associated with NO. Since NO is a free radical with a short half-life (<10s), it is react fast with superoxide and other radicals and with many biological species, such as transition metal ions and molecular oxygen [18, 19]. A sensitive and selective method therefore is required to measure NO in biological systems. Many indirect and direct approaches for NO detection have been reported [20-29], but electrochemical techniques are the most promising methods because they can be applied for real-time *in vivo* and *in vitro* detection of NO with satisfactory temporal and spatial resolution.

However, NO can oxidize at various electrode surfaces when sufficiently positive potentials are applied, in which case a number of other biological intereferents can also oxidize. Thus, to achieve high sensitivity, as well as high selectivity for NO, the surface of the electrode needs to be modified in a way that gives high signal priority to NO over other interfering analytes.

NO can interact with transition metals (such as iron), thiol groups, other free radicals, oxygen, superoxide anion, unsaturated fatty acids, and other molecules. Some of these reactions result in the oxidation of nitric oxide to nitrite and nitrate in order to terminate its effect, while other reactions can lead to altered protein structures, function, and/or catalytic capacity. For example, NO reacts with S-nitrosylation and converts thiol groups (including cystein residues) in proteins, to form S-nitrosothiols (RSNOs), which corroborate the known interaction of NO and sulfur-containing groups [30]. Our first aim here is to develop an ultra-sensitive electrochemical sensor that takes advantage of NO-sulfur chemistry for accurate quantification of NO in biological systems. Considering the catalytic electro-oxidation of NO on the surface of transition metals [31-34], incorporation of metal catalyst with sulfur compounds would be an ideal approach to achieve required sensitivity for NO detection.

Accurate and reliable quantification of NO in biological systems provides a great advantage to identifing and understanding the pathogenises diseases that can open up correct avenues to treat disease states. The transpotation of the NO/NOS enzyme, which can supply NO flux, is one of the approaches to treat disease states that are associated

with the deficiency of NO. Liposomes have been considered as effective carriers of protein because of their ability to trap an aqueous solution separated from the external aqueous medium. Thus, our goal in the second part of this work is to development of NOS loaded liposomes as a platform for NO delivery to targets.

1.2 Properties of NO

Nitric oxide is a colorless gas that contains 46.68 % nitrogen and 53.32 % oxygen at typical conditions. The molecular weight of NO is 30.01 g/mol, while the boiling point and melting point are -151.7 ^{o}C and -163.6 ^{o}C respectively. The nitrogen and oxygen atoms are bound by a double bond with the bond order of 2.5, leaving two pairs of non-bonding electrons on the oxygen atom and one pair of non-bonding electrons and one unpaired electron on the nitrogen atom as shown in the following Lewis structure.

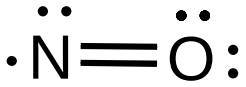

Due to the free radical on the nitrogen atom, NO is very reactive and thus extremely unstable. NO cannot maintain its original form for very long in a biological environment. The hydrophobic nature of NO makes it diffusible through the biological membrane. As a result, NO undergoes complex changes immediately after being

released. The possible reactions of NO in physiological conditions are shown in Figure 1.1.

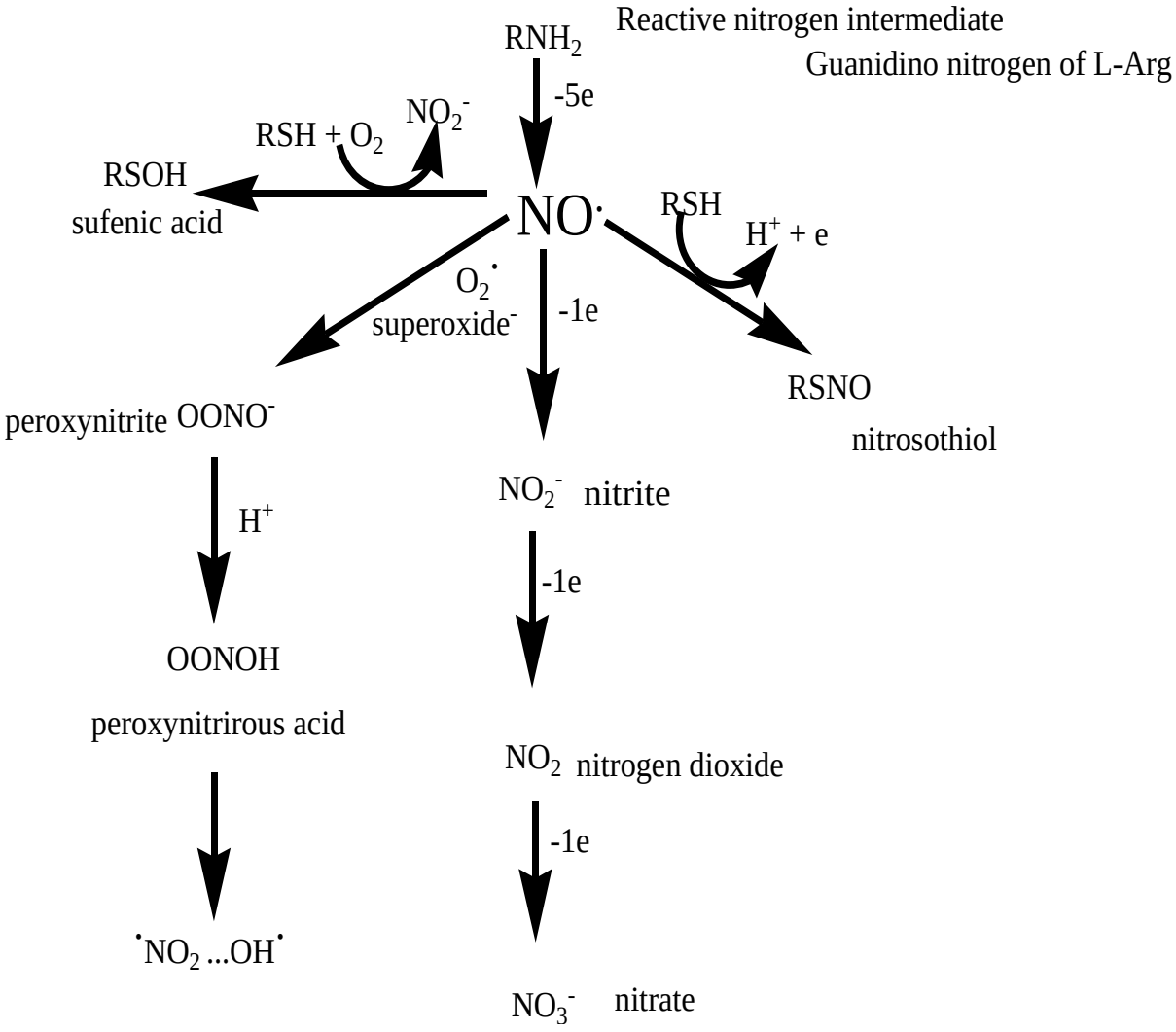

Figure 1.1. Reaction of NO-related compounds in a biological environment. Adapted from reference [35].

NO readily reacts with molecules with unpaired electrons that are classified as free radicals ($O_2^{\cdot}$ -superoxide, $OH^{\cdot}$ -hydroxyl ion) or transition metals like heme iron (myoglobin, hemoglobin, cytochromes). Therefore, the above radicals reduce the bioavailability of NO. The final products of NO reactions vary depending on the system within which the reactions occur. The main oxidative product of NO in i*n vitro* systems, is NO_2^- (nitrite), but, *in vivo,* NO undergo sequence of reactions with hemoglobin and other biological compounds and end up with NO_3^- (nitrate) as the main degradation product [35]. In biological systems NO reacts with oxy-myoglobin to form nitrate and methemoglobin (MetHb) or metmyoglobin (equation 1.1) [36]. This reaction is identified as the NO regulatory mechanism for control NO concentration *in vivo*. Therefore, the specificity of NO towards transition metals allows the target tissue to receive the information based on the NO concentration.

$$Hb(Fe\text{-}O_2) + NO \longrightarrow MetHb(Fe(III)) + NO_3^- \qquad \text{Equation 1.1}$$

1.3 Nitric oxide production in biological systems

Nitric oxide (NO) is produced from the guanidino group of L-arginine in an NADPH-dependent reaction catalyzed by a family of NO synthase (NOS) enzymes [37]. Arginine and oxygen are converted to NO and citrulline by the enzyme NOS. The chemical reaction in Figure 1.2 illustrates the NO production by NOS enzymes and the scheme 1.1 shows the participation of cofactors of NOS in NO production.

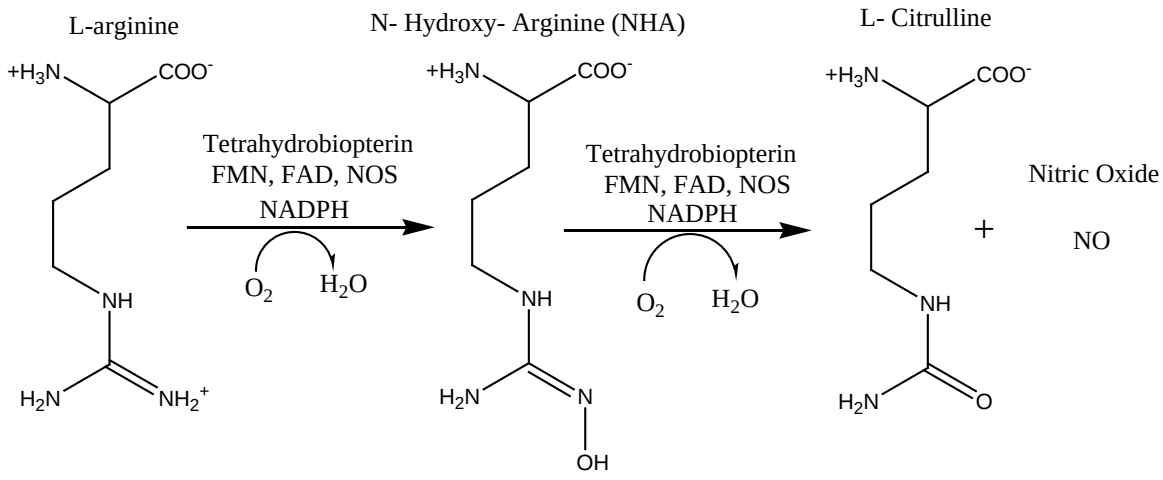

Figure 1.2. The reaction of NO production by means of NOS enzyme.

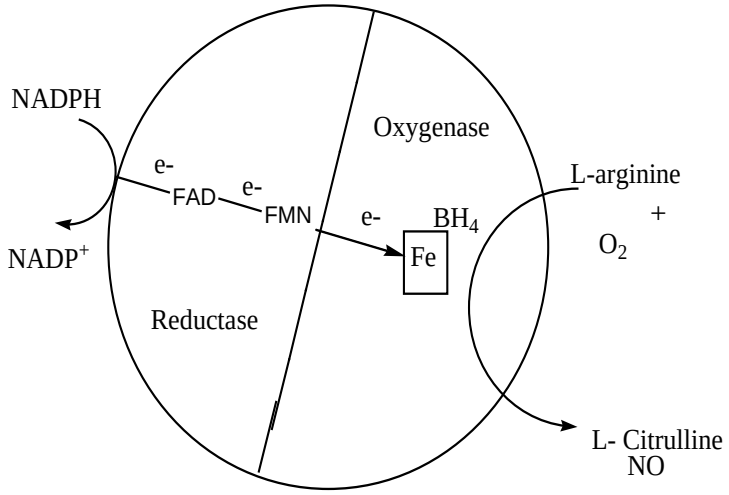

Scheme. 1.1 The overall reaction is catalyzed and the cofactors of NOS electrons (e-) are donated by NADPH to the reductase domain of the enzyme and proceed via FAD and FMN redox carriers to the oxygenase domain where they are used in the activation of oxygen in the presence of L-arginine. Citrulline and NO are generated as products. Adapted from [38].

1.4 Nitric oxide synthase

The NOS enzymes belong to the heme-containing family of enzymes called monooxygenases [39]. Depending on the expression, activity, and the structure, there are three distinct isoforms of NOS that exhibit multiple physiological and pathological functions. The three NOS groups are neuronal NOS (nNOS), inducible NOS (iNOS), and endothelial NOS (eNOS) [40].

The iNOS is expressed in many cell types mostly in response to inflammatory cytokines. In a majority of cell types, iNOS level is either very low or undetectable. Since production of NO by iNOS can be controlled through transcription, stimulation of the cells can lead to increased transcription of the iNOS gene, with the subsequent production of NO. The nNOS is expressed in neuronal cells and skeletal muscles. On the other hand the eNOS protein is identified in endothelial cells. NO produced by eNOS has an important role in the regulation of vasodilation and antithrombotic actions [40].

Increases in intracellular calcium levels lead to an ephemeral increase in NO production by binding eNOS and nNOS to the increased level of calmodulin. In contrast, iNOS activity is not able to respond to changes in calcium levels in cells because iNOS can bind so strongly to calmodulin even at very low levels of cellular calcium [41]. The nNOS and eNOS isoforms are constitutively expressed and regulated by calcium levels, which are associated with calmodulin interactions. The calcium-calmodulin complex stabilizes the NOS dimer and BH_4 is essential for NOS dimer formation.

NOS exhibit a bidomain structure in which an N-terminal oxygenase domain containing binding sites for heme, tetrahydrobiopterin (BH_4) and L-arginine is linked by a CaM-recognition site to a C-terminal reductase domain that contains binding sites for FAD, FMN and NADPH [42-45]. Both domains are catalytically active. Reconstitution of the second step of NO synthesis has been achieved by combining the reductase and oxygenase domains of human eNOS and murine iNOS [46]. The general structure that shows both domains of NOS enzymes is illustrated in Figure 1.3.

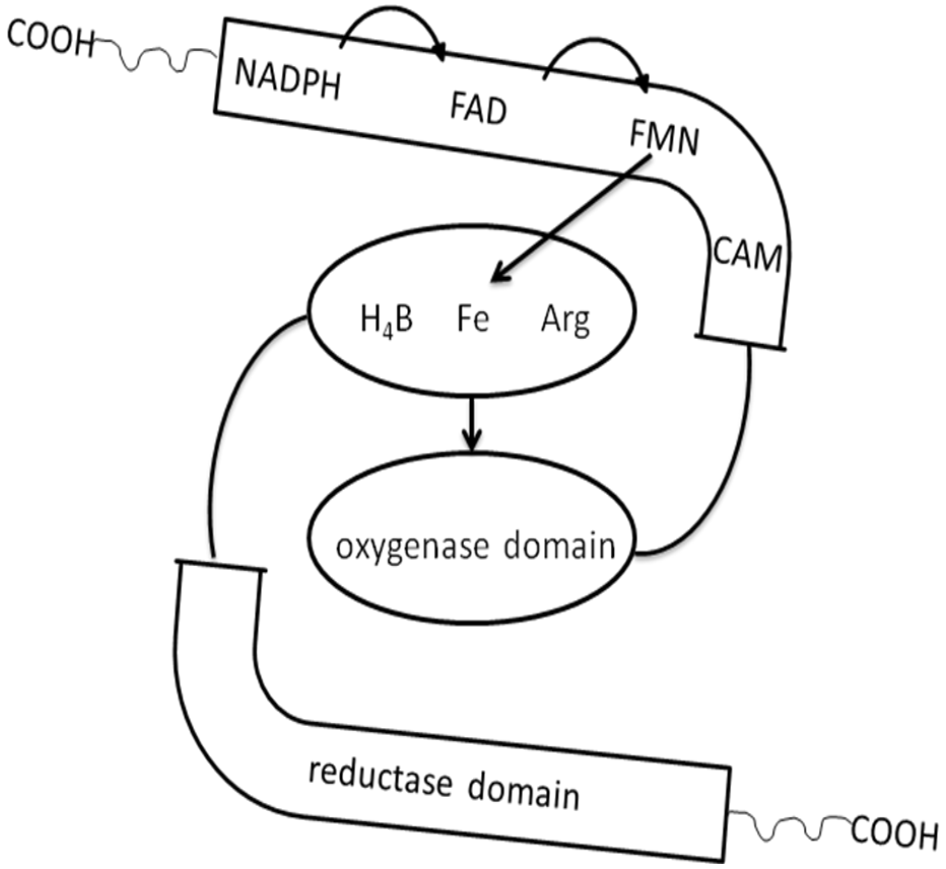

Figure 1.3. Schematic diagram of Nitric Oxide Synthase adapted from [42].

1.5 Biological function of NO

As explained earlier, NO is an extreamely important and versatile messenger in the biological system. At first, it was recognized as an endothelium-derived relaxing factor in the vascular system [47]. It has also been identified as a neurotransmitter or neuromodulator in the neuronal system [41] and a cytotoxic factor in the immune system [33, 47-54]. In addition, it is believed that NO is related to some tissue damage, such as ischemia/reperfusion tissue damage [55, 56] and excitatory neuronal death [57-59].

1.5.1 NO in the vascular system

The endothelium (inner lining) of blood vessels use NO to signal the surrounding smooth muscles to relax, thus dilating the arteries and increasing blood flow. NO produced by eNOS diffuses into the vascular smooth muscle cells adjacent to the endothelium and activates guanylyl cyclase by binding to it. The guanylyl cyclase enzyme catalyzes the dephosphorylation of guanylyl triphosphate (GTP) to cyclic guanylyl monophosphate (cGMP), which serves as a secondary messenger for carring out important cellular functions, especially for signaling smooth muscle relaxation.

The production and hence the concentration of NO is elevated for humans at high-altitudes, which helps people avoid hypoxia. In such situations, nitroglycerin and amyl nitrite act as vasodilators because they are converted to nitric oxide in the body. Nitric oxide contributes to vessel homeostasis by inhibiting vascular smooth muscle contraction and growth, platelet aggregation, and leukocyte adhesion to the endothelium.

1.5.2 Neuronal NO

NO is also generated in neuron cells in the central or peripheral nervous systems [60]. The nNOS is activated with an intracellular calcium increase through agonist-receptor interactions. In the peripheral nerve system, the main function of NO is vasoregulation [36]. In addition to its direct action, renal blood flow is regulated indirectly with NO through the reduction of sympathetic neuronal activity [61, 62]. Nerve cells tend to die from over-stimulation of excitatory neurotransmitters or agonists. NO or the NO donor leads to marked neurotoxicity [63], by the production of toxic compounds, such as peroxynitrite ($ONOO^-$), which form in the reaction of NO and superoxide (the reduced form of oxygen).

1.5.3 NO in the immune system

Immune cells (Macrophage, nuclephile, monocyte, and kuppfer cells) release a greater amount of NO than endothelium or nerve cells by activating inducible NOS (iNOS). The iNOS can be induced with the stimulation of cytokines or lipopolysaccharide (LPS) [64]. The NO produced from iNOS has cytostatic and cytotoxic effects on invading microorganisms or tumor cells [65]. The effect of the cytotoxicity is found in two categories. First is the inhibition of the respiration of mitochondria [66]. The enzymes that have an Iron-sulfur center in their catalytic site can strongly interact with NO and ultimately inhibit and terminate the electron transfer system. Second is the direct modulation to the DNA synthesis, which can inhibit some enzymes [67].

Lipopolysaccharide (LPS), which is a constituent of the bacterial outer membrane, may cause a decrease in blood pressure, cardiovascular and kidney damage, and bleeding in some organs. In such environments, NO production and concentration increase, and, hence, a drop in blood pressure occurs immediately [68].

1.6 NO detection in live cells

The cell is the smallest structural unit of biological life. These microscopic systems have many functions such as energy metabolism, intra and intercellular signaling by chemical and electrical means, and self-reproduction. Due to the ultra-small size of single cells (diameter 7–200μm, volume fL–nL), ultra-trace amount of component (zmol–fmol), and ultra-rapid biochemical reaction (ms), highly efficient, highly sensitive, and highly selective detection methods are necessary for single cell analysis.

Combining capillary electrophoresis (CE) with the detection of laser-induced fluorescence (LIF), electrochemical detection (ED), and mass spectrometry (MS) enable direct intrinsic studies of single cells [69]. These systems are based on conventional technologies and instrumentation. They give only limited information about the cell content and do not present a general method for single cell analysis. Electrochemical methods such as amperometry and voltammetry are suitable methods to measure sub-nanomolar levels of oxidizable chemicals such as NO, which are secreted from a single cell.

As described in section 1.1, NO is involved in many important physiological processes. Therefore NO level in biological systems is under intense investigation as a therapeutic target for variety of conditions. A deficiency in NO plays a role in hypertension, hyperglycaemia, arteriosclerosis, Parkinson's disease, and Alzheimer's disease [51-53]. Conversely, increased NO levels contribute to arthritis, reperfusion injury, and cancer [48-50]. Thus, it is important to measure and quantify the amount of NO production in biological matrices to elucidate the physiological and pathological processes related to NO production and release.

1.7 Detection of NO

The field of NO detection techniques has grown rapidly due to the need of understanding the physiological and pathological functions of NO. With the high reactivity and short half-life of NO, direct detection of NO in biological systems is a demanding task.

There are number of methods available for NO measurement, including mass spectrometry, spectrophotometry, chemiluminescence and electron paramagnetic resonance [70, 71]. Most of these approaches rely on the measurement of secondary reaction products (e.g., nitrites and nitrates, Hemoglobin-Fe^{3+} and L -citrulline) and formation of stable adducts (e.g., hemoglobin–Fe^{2+} –NO and other NO–iron complexes) that require sample processing. They do not allow real time measurements of endogenous

NO production; they also provide complementary information that is difficult to translate into the NO concentration dynamics in tissues.

Spectrophotometry measurements of NO are based on the measurement of absorbance of colored compounds, which are complex with NO or its secondary reaction products. There are two main spectrophotometry methods: Griess assay [22] and hemoglobin-dioxy assay. In Griess assay, nitrite and nitrate, the biological metabolites of NO, produce the diazonium ion with sulfanilic acid, which couple with N-(naphthyl) ethylenediamine to form a colored complex of chromophoric azo-derivative [72]. On the other hand, in hemoglobin dioxy assay, the shift of the Soret band (due to reaction of hemoglobin-dioxy with NO to form methemoglobin) accounts for the quantification of NO. These methods are inapplicable in biological samples due to the lack of sensitivity and a deprived detection limit.

The chemiluminescence technique [25, 73] is a direct method to measure NO and is based on the reaction of NO with ozone (O_3). The reaction forms the excited state NO_2 and can emit photon when it reverts to the lower energy states, which is proportional to the NO concentration. However, bulk instrumentation and time and reagents are not compatible with real time measurement of NO. A number of methods of NO-trapping techniques have been developed for the detection of NO. The spin-trapping approach is widely used, where the additional reactions of NO with other compounds form EPR-active and stable adducts [74, 75]. This strategy has also drawbacks, such as high cost,

large equipment size, and need of specialized operators and special ion trap, and therefore, does not allow real time analysis of NO.

From this angle, electrochemical methods are very attractive alternatives for monitoring NO concentration *in situ*. The use of microelectrodes for the electrochemical detection of NO in tissues makes real time measurements possible due to the high temporal resolution. The small size of these microelectrodes (0.5–35 μm diameter) allows a high spatial resolution and makes them excellent sensors for direct placement into biological preparations, without causing extensive damage to tissues [54, 76-78].

Electrochemical detection of NO involves the oxidation of NO on the surface of the working electrode, which produces a Faradaic redox current. (Equation 1.2).

$$NO \rightleftharpoons NO^{+} + e^{-} \qquad \text{Equation 1.2}$$

1.8 Electrochemical NO Sensors

The first electrochemical electrode for detecting NO in biological samples was published by Shibuki [77], where a platinum wire was used as the working electrode and a silver wire was used as the counter/ reference electrode in the Clark-type probe. The current is generated by oxidation of NO measured at a constant potential of +0.9 V vs. Ag wire.

One of the commercially available NO sensor was developed by World Precision Instruments, (WPI) [29] . This sensor called the “ISO-NOP” and the modified platinum wire disk covered with the NO-selective membrane was used as the working electrode, and the Ag/AgCl electrode was used as the reference electrode. Although the sensor has advantages in measurement of NO, due to the fragility of the membrane and the difficulty in calibration, the real time analysis is complicated.

Due to the high reactivity of NO and the low concentration of NO in biological systems, the direct electro-oxidation of NO on the electrode surface does not produce a significantly high response. Therefore, to achieve high sensitivity, the surface of the electrode needs to be modified with a supportive compound to amplify the NO signal. There are two major types of surface-modified electrodes that are suitable for the oxidative determination of NO. The first type works by direct oxidation of NO at sufficiently high electrode potential using gas permeable membranes to enhance

selectivity. The second type is based on the coating of the electrode surface with suitable modifiers.

Different types of sensors have been developed to detect NO by modifying the surface of the electrode, for example: metal compounds [79, 80], organometallic compounds (such as Fe, Ni, Mn, Cu) [28, 29, 79, 81, 82], enzymes [83], and polymers [31, 84-87]. The performances of these sensors vary depending on the materials and the method used to modify the surface, the potential used to NO oxidation, and other experimental conditions. Despite the advantages of such sensor designs their application in biological systems is limited due to low sensitivity, low selectivity, and slow response time, the application of these sensors in the biological systems is limited.

The layers of the deposited polymer films have better analytical properties, such as selectivity, sensitivity or stability. In fact, most of the described microelectrodes are based on a conventional two or three-polymer films design with each film performing specific tasks [32, 33]. In a general case, applications of chemically modified electrodes to solve analytical problems require reproducible preparation procedure of the modified surfaces and an accurate control of the permeability characteristics of the electrode coatings. Electro-polymerization of suitable monomers is ome method of electrode modification use to achieve controlled layer [32, 33, 54]. The additional advantage of the electro-polymerization design is the ability to coat very small or narrow-sized electrode surfaces.

1.9 NO and Sulfur Interactions

In living bodies, nitric oxide tends to react rapidly with oxygen and superoxide, as explained in section 1.2, and forms other oxides of nitrogen, some of which are toxic. However, the lifetime of NO is extended, and the concentration of the free NO is regulated through its binding with several acceptors, such as metals (binding of NO with the heam in hemoglobin) and thiols.

Iron nitrosyls and nitrosothiols are the most important agents that account for the storage and transport of the NO and related compounds. Most of the target receptors of NO also contain an iron center and thiol groups. Nitrosothiols and metal nitrosyl complexes belong to important external sources of nitric oxide (NO-donors), and complex interactions are observed in ternary iron–sulfur–nitrosyl systems [30].

Biological functions of nitric oxide and its redox forms are essentially related to the chemistry of thiol groups [88] and transition metal centers [89] present in various biomolecules. Regulatory properties of nitric oxide are based on interactions with iron and sulfur moieties. Redox properties of iron centers are considerably modulated with protein-bound thiols and nitric oxide. They can interact mutually with each other, and these interactions may account for important physiological and pathophysiological processes.

S-Nitrosothiols (thionitrites) have very important physiological roles and considered as the principal stores of NO. [30]. They participate in NO redox changes as illustrated in scheme 1.2, which are the source of thiyl radicals; they are also involved in other regulatory processes.

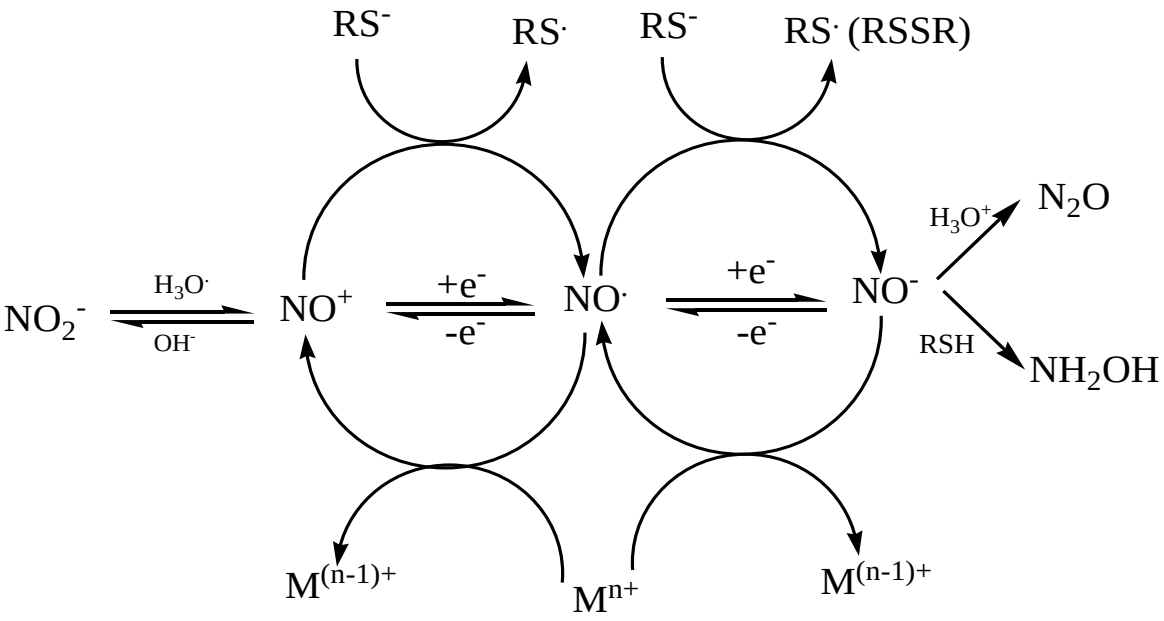

Scheme 1.2. Interconversion of different redox forms of nitric oxide in reaction with biologically relevant reducers and oxidants (M = Fe, Cu, Co). Adapted from [90].

Nitrosothiols are usually formed in reactions between thiols and various nitrosation agents, including nitric oxide in the presence of electron acceptors, nitrosonium salts, nitrous acid and inorganic nitrites, metal nitrosyl complexes and many others [91]. *S*-Nitrosothiols are typically unstable and undergo spontaneous decomposition via homolytic cleavage of the S-N bond according to the Equations (1.3) and (1.4) [30]:

$$RSNO \rightarrow RS\bullet + NO\bullet \qquad \text{Equation 1.3}$$

$$2RS\bullet \rightarrow RSSR \qquad \text{Equation 1.4}$$

The strength of the S-N bond is controlled by the RSNO thermal stability. Typically, the *S*-nitrosothiols bonds become more stable as the contribution of the resonance structure (II) becomes higher (Figure 1.4), which is affected by the electron releasing substituents.

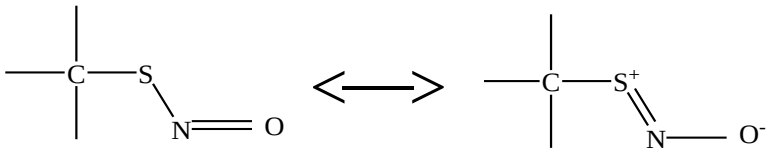

Structure (I) Structure (II)

Figure 1.4. Resonance structures of *S*-nitrosothiols.

Because of the generally favorable S-NO interactions, the development of a sulfur based NO sensor is an ideal approach to achieve required sensitivity towards NO oxidation. As a sulfur-containing compound we used a conductive polymer, poly 3,4-ethylenedioxythiophene (PEDOT), to modify the electrode surface. The combination of deposited polymer film brings better analytical properties, such as selectivity, sensitivity or stability. Prior work in overlab show advantageous catalytic properties of transition metal ruthenium, therefore we used the ruthenium with combination of PEDOT to achieve the synergetic performances. In this work we report the development and the performances of sulfur based NO sensor in measuring NO released from live single cells and cell collection as well as from modified liposomes.

1.10 NOS encapsulation in liposomes

Liposomes are spherical, closed, self-assembled phospholipids, which enclose part of the surrounding solvent in their interior. Liposome and micelles, considered as precursors of a protocell [92, 93], served to provide the compartment that functions like a minimal cell where biological activities take place [94-96]. The lipid bilayers that liposomes made up have been considered as models of biomembranes. Because liposomes are closed vesicles with no exposed hydrophobic edges, they are energetically more favorable structures than open membranes. The most important quality of liposomes is their ability to enclose an aqueous medium separate from the external medium. Thus, it is considered as a simple-model system to study cellular properties.

Depending on the number of bilayers, liposomes can be named as multilamellar vesicles (MLV) and unilamellar (ULV) vesicles (Figure1.5). Multilamellar vesicles do not represent a well-defined system and are not often used in scientific experiments. Vesicles with a size of 1-300 μm are considered giant vesicles (GV), and vesicles in the nanometer size are considered small vesicles (SV)[4].

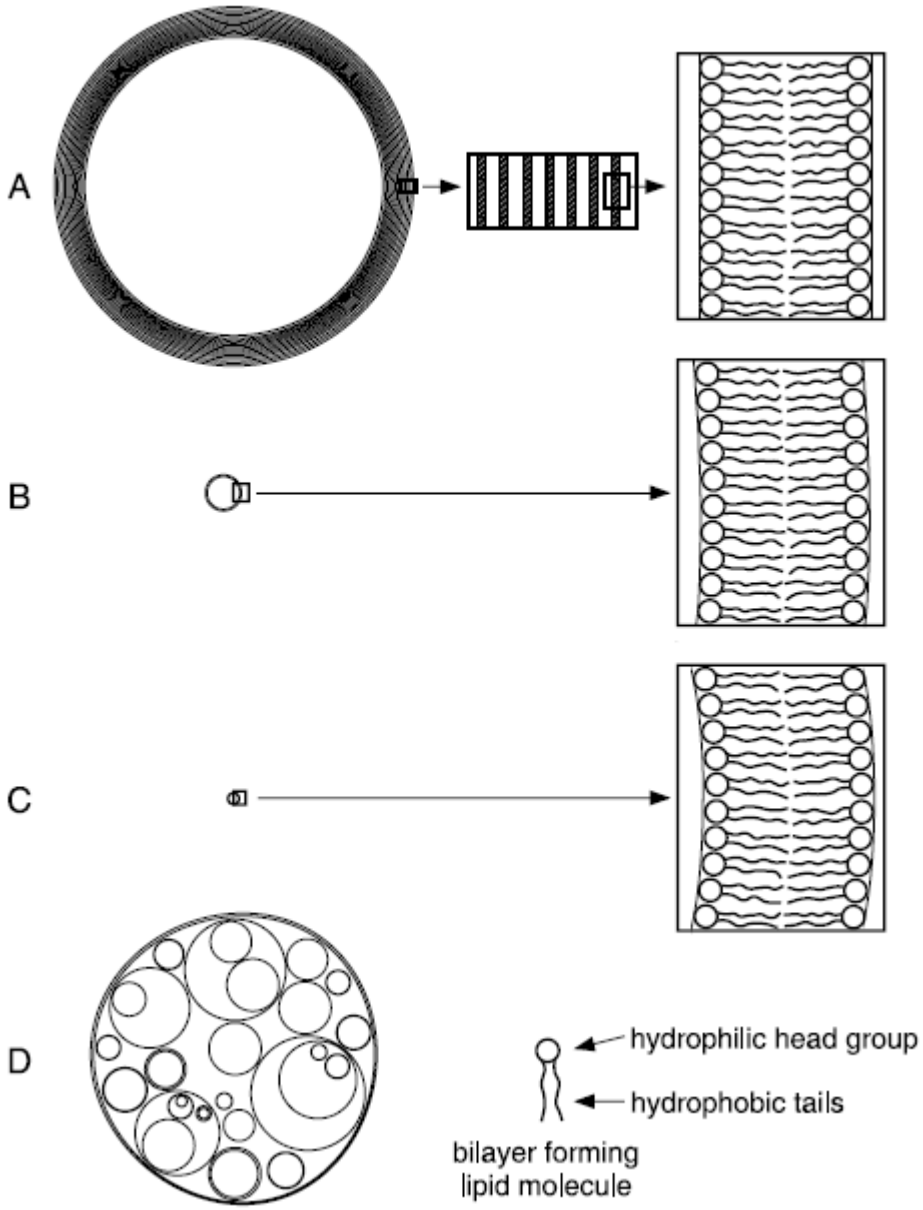

Figure 1.5. Schematic diagram of different kinds of liposomes. (A) Multi lamellar vesicles (B) Large unilamellar vesicles (C) Small unilamellar liposome (D) Multivesicular vesicles. (Reprinted from reference [4])

Due to their unique properties, liposomes are used for drug delivery. Hydrophobic chemicals can be dissolved into the membrane and the hydrophilic compounds can entrap in their hollow microenvironment. Therefore, liposomes can carry both hydrophobic molecules as well as hydrophilic molecules. To deliver the molecules to sites of action, the lipid bilayer fuses with other bilayers, such as cell membranes. Figure 1.6 shows the schematic diagram of one of the liposomal drug delivery mechanisms to the target cells.

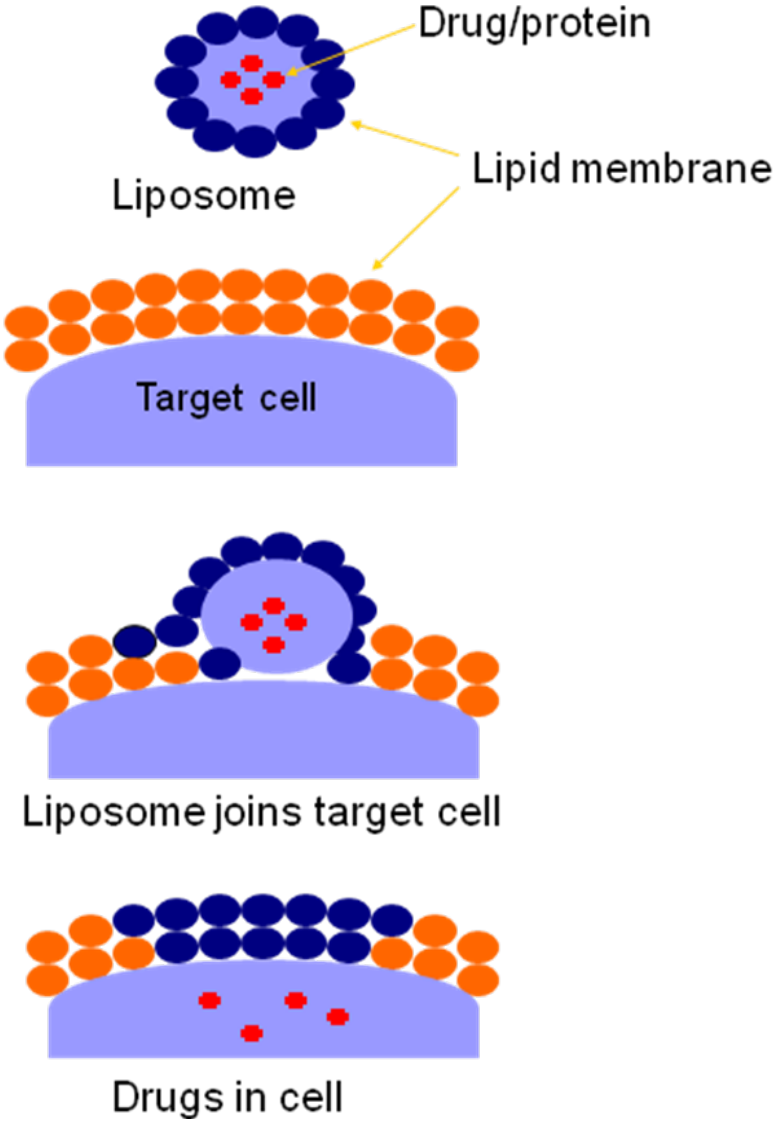

Figure 1.6. Representation diagram to show the drug delivery mechanism (fusion) to target cells by liposome.

The investigation of the use of liposomes as protein carriers has gained great interest for a number of potential applications in pharmaceutical formulations. Concerning the liposomes in genomic and medical applications, a large measure of proteins, notably enzymes, has been used. The attractiveness of liposomes as a enzyme/protein delivery system is due in part to the fact that the encapsulated proteins remain in their preferred aqueous environment within the vesicles, while the liposomal membrane protects them against destabilizing exterior agents such as proteases [97, 98] and protects the enzyme from self-denaturation and dilution effects. In addition to its stabilizing effect, the usefulness of liposomes is extended as enzyme carrier systems in biotechnological applications. The undemanding ability of entraping of substances inside liposomes and the possibility to regulate entrance of substance or exit of product from the membrane of liposome gained considarable interest of drug delivery innovation. Protein encapsulation in liposomes would be a great success in vaccine development, in protein absorption enhancement, and in drug delivery. In this study we investigate the encapsulation of nitric oxide synthase (NOS) enzyme inside liposomes for possible delivery to deficient target sites.

1.11 References

1. Koshland DE, Jr. The molecule of the year Science 1992;258: 1861.
2. Derentowicz P, Markiewicz K, Wawrzyniak M, Czerwinska-Kartowicz I, Bulawa E, and Siwinska-Golebiowska H. [Nitric oxide (NO)--Nobel prize in medicine and physiology for 1998] Med Wieku Rozwoj 2000;4: 209-217.
3. Raju TN. The Nobel chronicles. 1998: Robert Francis Furchgott (b 1911), Louis J Ignarro (b 1941), and Ferid Murad (b 1936) Lancet 2000;356: 346.
4. Walde P, and Ichikawa S. Enzymes inside lipid vesicles: Preparation, reactivity and applications Biomolecular Engineering 2001;18: 143-177.
5. Nathan C, and Xia Q. Nitric oxide synthases: roles, tolls, and controls. Cell 1994;78: 915-918.
6. Snyder SH. Neuroscience. Vehicles of inactivation Nature 1991;354: 187.
7. Bredt DS, Hwang PM, Glatt CE, Lowenstein C, Reed RR, and Snyder SH. Cloned and expressed nitric oxide synthase structurally resembles cytochrome P-450 reductase Nature 1991;351: 714-718.
8. Feldman PL, Griffith OW, and Stuehr DJ. The surprising life of nitric oxide. Chemical Engineering News 1993;20: 26-37.
9. Ignarro LJ, Buga GM, Wood KS, Byrns RE, and Chaudhuri G. Endothelium-derived relaxing factor produced and released from artery and vein is nitric oxide Proc Natl Acad Sci U S A 1987;84: 9265-9269.
10. Ignarro LJ. Nitric oxide. A novel signal transduction mechanism for transcellular communication Hypertension 1990;16: 477-483.

11. Rodomski MW, Palmer RMJ, and Moncada S. An L-arginine/nitric oxide pathway present in human platelets regulates aggregation Proc Natl Acad Sci USA 1990;87: 5193- 5197.

12. Ignarro LJ, Napoli C, and Loscalzo J. Nitric oxide donors and cardiovascular agents modulating the bioactivity of nitric oxide: an overview Circ Res 2002;90: 21-28.

13. Leopold JA, and Loscalzo J. Clinical importance of understanding vascular biology Cardiol Rev 2000;8: 115-123.

14. Forgione MA, Leopold JA, and Loscalzo J. Roles of endothelial dysfunction in coronary artery disease Curr Opin Cardiol 2000;15: 409-415.

15. Loscalzo J, Freedman J, Inbal A, Keaney JF, Jr., Michelson AD, and Vita JA. Nitric oxide insufficiency and arterial thrombosis Trans Am Clin Climatol Assoc 2000;111: 158-163.

16. Eberhardt RT, Forgione MA, Cap A, Leopold JA, Rudd MA, Trolliet M, Heydrick S, Stark R, Klings ES, Moldovan NI, Yaghoubi M, Goldschmidt-Clermont PJ, Farber HW, Cohen R, and Loscalzo J. Endothelial dysfunction in a murine model of mild hyperhomocyst(e)inemia J Clin Invest 2000;106: 483-491.

17. Malinski T. Understanding nitric oxide physiology in the heart: a nanomedical approach Am J Cardiol 2005;96: 13i-24i.

18. Beckman JS, Chen J, Ischiropoulos H, and Crow JP. Oxidative chemistry of peroxynitrite Methods Enzymol 1994;233: 229-240.

19. Stamler JS. Redox signaling: nitrosylation and related target interactions of nitric oxide Cell 1994;78: 931-936.

20. Taha ZH. Nitric oxide measurements in biological samples Talanta 2003;61: 3-10.

21. Guthohrlein G, and Knappe J. Modified determination of citrulline Anal Biochem 1968;26: 188-191.

22. Griess JP. Coloring matters Ber. Dtsch. Chem. Ges 1879;12: 426-429.

23. Marzinzig M, Nussler AK, Stadler J, Marzinzig E, Barthlen W, Nussler NC, Beger HG, Morris SM, Jr., and Bruckner UB. Improved methods to measure end products of nitric oxide in biological fluids: nitrite, nitrate, and S-nitrosothiols Nitric Oxide 1997;1: 177-189.

24. Hevel JM, and Marletta MA. Nitric-oxide synthase assays Methods Enzymol 1994;233: 250-258.

25. Archer S. Measurement of nitric oxide in biological models Faseb J 1993;7: 349-360.

26. Lim MH, and Lippard SJ. Metal-based turn-on fluorescent probes for sensing nitric oxide Acc Chem Res 2007;40: 41-51.

27. Brunet A, Pailleret A, Devynck MA, Devynck J, and Bedioui F. Electrochemical sensing of nitric oxide for biological systems: methodological approach and new insights in examining interfering compounds Talanta 2003;61: 53-59.

28. Ciszewski A, and Milczarek G. Electrochemical detection of nitric oxide using polymer modified electrodes Talanta 2003;61: 11-26.

29. Zhang X. Real time and in vivo monitoring of nitric oxide by electrochemical sensors--from dream to reality Front Biosci 2004;9: 3434-3446.

30. Szacilowski K, Chmura A, and Stasicka Z. Interplay between iron complexes, nitric oxide and sulfur ligands: Structure, (photo)reactivity and biological importance Coordination Chemistry Reviews 2005;249: 2408.

31. Malinski T, and Taha Z. Nitric oxide release from a single cell measured in situ by a porphyrinic-based microsensor Nature 1992;358: 676-678.

32. Prakash R, Srivastava RC, and Seth PK. Polycarbazole modified electrode; nitric oxide sensor Polym.Bull. 2001;46: 487-490.

33. Lee Y, Oh BK, and Meyerhoff ME. Improved planar amperometric nitric oxide sensor based on platinized platinum anode. 1. Experimental results and theory when applied for monitoring NO release from diazeniumdiolate-doped polymeric films Anal Chem 2004;76: 536-544.

34. Lee Y, and Kim J. Simultaneous electrochemical detection of nitric oxide and carbon monoxide generated from mouse kidney organ tissues Anal Chem 2007;79: 7669-7675.

35. Nathan C, and Shiloh MU. Reactive oxygen and nitrogen intermediates in the relationship between mammalian hosts and microbial pathogens Proc Natl Acad Sci U S A 2000;97: 8841-8848.

36. Toda N, Kitamura Y, and Okamura T. Role of nitroxidergic nerve in dog retinal arterioles in vivo and arteries in vitro Am J Physiol 1994;266: H1985-1992.

37. Beckman JS. The physiological and pathological chemistry of nitric oxide-Nitric Oxide-Principles and Actions 1996: 1-83.

38. Alderton WK, C.E. C, and R.G. K. Biochem. J. 2001;357: 593-615.

39. Rosen GM, Tsai P, and Pou S. Chem. Rev 2002;102: 1191.

40. Forstermann U, Closs EI, Pollock JS, Nakane M, Schwarz P, Gath I, and Kleinert H. Nitric oxide synthase isozymes. Characterization, purification, molecular cloning, and functions Hypertension 1994;23: 1121-1131.

41. Nathan C. Nitric oxide as a secretory product of mammalian cells Faseb J 1992;6: 3051-3064.

42. Cho HJ, Xie QW, Calaycay J, Mumford RA, Swiderek KM, Lee TD, and Nathan C. Calmodulin is a subunit of nitric oxide synthase from macrophages J Exp Med 1992;176: 599-604.

43. Salerno JC, Frey C, McMillan K, Williams RF, Masters BS, and Griffith OW. Characterization by electron paramagnetic resonance of the interactions of L-arginine and L-thiocitrulline with the heme cofactor region of nitric oxide synthase J Biol Chem 1995;270: 27423-27428.

44. Persechini A, McMillan K, and Masters BS. Inhibition of nitric oxide synthase activity by Zn2+ ion Biochemistry 1995;34: 15091-15095.

45. Richards MK, and Marletta MA. Characterization of neuronal nitric oxide synthase and a C415H mutant, purified from a baculovirus overexpression system Biochemistry 1994;33: 14723-14732.

46. Ghosh DK, Abu-Soud HM, and Stuehr DJ. Reconstitution of the second step in NO synthesis using the isolated oxygenase and reductase domains of macrophage NO synthase Biochemistry 1995;34: 11316-11320.

47. Palmer RM, Ferrige AG, and Moncada S. Nitric oxide release accounts for the biological activity of endothelium-derived relaxing factor Nature 1987;327: 524-526.

48. Moncada S, and Higgs EA. Molecular mechanisms and therapeutic strategies related to nitric oxide Faseb J 1995;9: 1319-1330.

49. Rees DD, Cellek S, Palmer RM, and Moncada S. Dexamethasone prevents the induction by endotoxin of a nitric oxide synthase and the associated effects on vascular tone: an insight into endotoxin shock Biochem Biophys Res Commun 1990;173: 541-547.

50. Dawson TM, and Dawson VL. Nitric oxide synthase: role as a transmitter/mediator in the brain and endocrine system Annu Rev Med 1996;47: 219-227.

51. Moncada S, Palmer RM, and Higgs EA. Biosynthesis of nitric oxide from L-arginine. A pathway for the regulation of cell function and communication Biochem Pharmacol 1989;38: 1709-1715.

52. Schmidt HH, Warner TD, Ishii K, Sheng H, and Murad F. Insulin secretion from pancreatic B cells caused by L-arginine-derived nitrogen oxides Science 1992;255: 721-723.

53. Linder L, Kiowski W, Buhler FR, and Luscher TF. Indirect evidence for release of endothelium-derived relaxing factor in human forearm circulation in vivo. Blunted response in essential hypertension Circulation 1990;81: 1762-1767.

54. Kitamura Y, Uzawa T, Oka K, Komai Y, Ogawa H, Takizawa N, Kobayashi H, and Tanishita K. Microcoaxial electrode for in vivo nitric oxide measurement Anal Chem 2000;72: 2957-2962.

55. Moncada C, Lekieffre D, Arvin B, and Meldrum B. Effect of No Synthase Inhibition on Nmda-Induced and Ischemia-Induced Hippocampal-Lesions Neuroreport 1992;3: 530-532.

56. Jaeschke H, Schini VB, and Farhood A. Role of Nitric-Oxide in the Oxidant Stress during Ischemia Reperfusion Injury of the Liver Life Sciences 1992;50: 1797-1804.

57. Manchester KS, Jensen FE, Warach S, and Lipton SA. Chronic Administration of Nitroglycerin Decreases Cerebral Infarct Size Neurology 1993;43: A365-A365.

58. Dawson TM, Dawson VL, and Snyder SH. A Novel Neuronal Messenger Molecule in Brain - the Free-Radical, Nitric-Oxide Annals of Neurology 1992;32: 297-311.

59. Lipton SA, Choi YB, Pan ZH, Lei SZZ, Chen HSV, Sucher NJ, Loscalzo J, Singel DJ, and Stamler JS. A Redox-Based Mechanism for the Neuroprotective and Neurodestructive Effects of Nitric-Oxide and Related Nitroso-Compounds Nature 1993;364: 626-632.

60. Grozdanovic Z, Bruning G, and Baumgarten HG. Nitric-Oxide - a Novel Autonomic Neurotransmitter Acta Anatomica 1994;150: 16-24.

61. Togashi H, Sakuma I, Yoshioka M, Kobayashi T, Yasuda H, Kitabatake A, Saito H, Gross SS, and Levi R. A Central-Nervous-System Action of Nitric-Oxide in

Blood-Pressure Regulation Journal of Pharmacology and Experimental Therapeutics 1992;262: 343-347.

62. Sakuma I, Togashi H, Yoshioka M, Saito H, Yanagida M, Tamura M, Kobayashi T, Yasuda H, Gross SS, and Levi R. Ng-Methyl-L-Arginine, an Inhibitor of L-Arginine-Derived Nitric-Oxide Synthesis, Stimulates Renal Sympathetic-Nerve Activity Invivo - a Role for Nitric-Oxide in the Central Regulation of Sympathetic Tone Circulation Research 1992;70: 607-611.

63. Dawson V, Dawson T, M., London E, D., Bredt D, S. , and Snyder S, H. Nitric oxide mediates glutamate neurotoxicity in primary cortical cultures Neurobiology 1991;88: 6368-6371.

64. Baek KJ, Thiel BA, Lucas S, and Stuehr DJ. Macrophage nitric oxide synthase subunits. Purification, characterization, and role of prosthetic groups and substrate in regulating their association into a dimeric enzyme J Biol Chem 1993;268: 21120-21129.

65. Farias-Eisner R, Sherman MP, Aeberhard E, and Chaudhuri G. Nitric oxide is an important mediator for tumoricidal activity in vivo Proc Natl Acad Sci U S A 1994;91: 9407-9411.

66. Stadler J, Billiar TR, Curran RD, Stuehr DJ, Ochoa JB, and Simmons RL. Effect of exogenous and endogenous nitric oxide on mitochondrial respiration of rat hepatocytes Am J Physiol 1991;260: C910-916.

67. Maragos CM, Wang JM, Hrabie JA, Oppenheim JJ, and Keefer LK. Nitric oxide/nucleophile complexes inhibit the in vitro proliferation of A375 melanoma cells via nitric oxide release Cancer Res 1993;53: 564-568.

68. Lai CS, and Komarov AM. Spin trapping of nitric oxide produced in vivo in septic-shock mice FEBS Lett 1994;345: 120-124.

69. Stuart JN, and Sweedler JV. Single-cell analysis by capillary electrophoresis Anal Bioanal Chem 2003;375: 28-29.

70. Ichimori K, Ishida H, Fukahori M, Nakazawa H, Murakami Brunet AE, Privat C, Stepien O, David-Dufilho M, Devynck J, and Devynck MA. Analusis 2000;28: 469-474.

71. Pallini M, Curulli A, Amine A, and Palleschi G. Electroanalysis 1998;10: 1010-1016.

72. Miles AM, Wink DA, Cook JC, and Grisham MB. Determination of nitric oxide using fluorescence spectroscopy Methods Enzymol 1996;268: 105-120.

73. Gorimar TS (1985). Total nitrogen determination by chemiluminescence. In Bioluminescence and Chemiluminescence: Instruments and applications, Van Dyke Ke, ed. (Boca Raton, FL: CRC Press), pp. 43-78.

74. Buettner GR. Spin trapping: ESR parameters of spin adducts Free Radic Biol Med 1987;3: 259-303.

75. Wang QZ, Jacobs J, DeLeo J, Kruszyna H, Kruszyna R, Smith R, and Wilcox D. Nitric oxide hemoglobin in mice and rats in endotoxic shock Life Sci 1991;49: PL55-60.

76. Cserey A, and Gratzl M. Stationary-state oxidized platinum microsensor for selective and on-line monitoring of nitric oxide in biological preparations Anal Chem 2001;73: 3965-3974.

77. Shibuki K. An electrochemical microprobe for detecting nitric oxide release in brain tissue Neurosci Res 1990;9: 69-76.

78. Saxena V, Shirodkar V, and Prakash R. Copper(II) ion-selective microelectrochemical transistor Appl Biochem Biotechnol 2001;96: 63-69.

79. Bedioui F, and Villeneuve N. Electrochemical nitric oxide sensors for biological samples - Principle, selected examples and applications Electroanalysis 2003;15: 5-18.

80. Privat C, Stepien O, David-Dufilho M, Brunet A, Bedioui F, Marche P, Devynck J, and Devynck MA. Superoxide release from interleukin-1B-stimulated human vascular cells: in situ electrochemical measurement Free Radic Biol Med 1999;27: 554-559.

81. Jin J, Miwa T, Mao L, Tu H, and Jin L. Determination of nitric oxide with ultramicrosensors based on electropolymerized films of metal tetraaminophthalocyanines Talanta 1999;48: 1005-1011.

82. Pei JJ, Braak E, Braak H, Grundke-Iqbal I, Iqbal K, Winblad B, and Cowburn RF. Distribution of active glycogen synthase kinase 3beta (GSK-3beta) in brains staged for Alzheimer disease neurofibrillary changes J Neuropathol Exp Neurol 1999;58: 1010-1019.

83. Kroning S, Scheller FW, Wollenberger U, Lisdat F, and Myoglobin-clay electrode for nitric oxide(NO) detection in solution Electroanalysis 2004;16: 253-259.

84. Pontie M, Gobin C, T. P, Bedioui F, and J. D. Electrochemical nitric oxide microsensors: sensitivity and selectivity characterisation Analytica Chimica Acta 2000;411: 175-185.

85. Diab N, Oni J, and Schuhmann W. Electrochemical nitric oxide sensor preparation: A comparison of two electrochemical methods of electrode surface modification Bioelectrochemistry 2005;66: 105-110.

86. Schuhmann W. Conducting Polymer Based Amperometric Enzyme Electrodes Mikrochim. Acta 1995;121: 1-29.

87. Fabre B, Burlet S, Cespuglio R, and Bidan G. Voltammetric detection of NO in the rat brain with an electronic conducting polymer and Nafion® bilayer-coated carbon fibre electrode Journal of electroanalytical chemistry 1997;426: 75-83.

88. Gaston B. Nitric oxide and thiol groups Biochim Biophys Acta 1999;1411: 323-333.

89. Cooper CE. Nitric oxide and iron proteins Biochim Biophys Acta 1999;1411: 290-309.

90. Stamler JS, Singel DJ, and Loscalzo J. Biochemistry of nitric oxide and its redox-activated forms Science 1992;258: 1898-1902.

91. Szaciłowski K, and Stasicka Z. Progr. React. Kin. Mech 2001;1: 26.

92. Deamer DW. The first living systems: a bioenergetic perspective Microbiol Mol Biol Rev 1997;61: 239-261.

93. Oro J, Miller SL, and Lazcano A. The origin and early evolution of life on Earth Annu Rev Earth Planet Sci 1990;18: 317-356.

94. Oberholzer T, Albrizio M, and Luisi PL. Polymerase chain reaction in liposomes Chem Biol 1995;2: 677-682.

95. Oberholzer T, Wick R, Luisi PL, and Biebricher CK. Enzymatic RNA replication in self-reproducing vesicles: an approach to a minimal cell Biochem Biophys Res Commun 1995;207: 250-257.

96. Wick R, and Luisi PL. Enzyme-containing liposomes can endogenously produce membrane-constituting lipids Chem Biol 1996;3: 277-285.

97. Meyenburg S, Lilie H, Panzner S, and Rudolph R. Fibrin encapsulated liposomes as protein delivery system. Studies on the in vitro release behavior J Control Release 2000;69: 159-168.

98. Corvo ML, Boerman OC, Oyen WJ, Jorge JC, Cruz ME, Crommelin DJ, and Storm G. Subcutaneous administration of superoxide dismutase entrapped in long circulating liposomes: in vivo fate and therapeutic activity in an inflammation model Pharm Res 2000;17: 600-606.

CHAPTER II

DEVELOPMENT OF HIGH SENSITIVE AND SELECTIVE NO SENSOR USING A CARBON FIBER MICROELECTRODE MODIFIED WITH AN ELECTROCONDUCTIVE POLYMER (EDOT) AND THE TRANSITION METAL CATALYST RUTHENIUM (Ru)

2.1 Introduction

Nitric oxide (NO) is a freely diffusible, gaseous free radical associated with many physiological and pathological processes. Biologically relative processes include neuronal signaling, immune response, inflammatory response, modulation of ion channels, platelet adhesion and activation, and cardiovascular homeostasis as well as antitumor activities [1, 2]. Nitric oxide is produced from one of the terminal guanidino nitrogens of L-arginine in an NADPH-dependent reaction, which is catalyzed by nitric oxide synthase (NOS) enzyme. Understanding its biological role requires the measurement of NO *in situ* and in real time in a selective, sensitive, and quantitative manner. Due to the short lifetime and the lower levels of NO released by biological systems, its direct determination has been a challenging task [3]. Different approaches for

NO quantification were reported, including spectrophotometry, mass spectrometry, chemiluminescence, and electron paramagnetic resonance [4, 5]. These methods rely on the measurement of the products (e.g., nitrites and nitrates, hemoglobin-Fe^{3+}, and L-citrulline) of NO reactions with oxygen, hemoglobin, and other biological complexes (e.g., Hemoglobin–Fe^{2+}–NO). Real time measurement of endogenously produced NO is difficult for these techniques, because they require sample processing prior to the analysis and provide indirect information that has to be converted to NO concentration.

Electrochemical approaches are promising techniques for direct monitoring of NO concentration *in situ;* in fact, studies on various types of electrode materials that are sensitive for NO have been published [6, 7]. Electrochemical techniques using carbon fiber electrodes (CFEs) have demonstrated several advantages such as simplicity, fast response and ease of handling. Electrochemical detection of NO using CFE involves the oxidation of NO on the surface of the electrode, which produces a Faradaic redox current.

The design of the microelectrodes for electrochemical detection of NO allows real time measurements *in vivo* due to the high temporal and spatial resolution. The appropriate dimensions allow the direct implantation of the microelectrodes into micro-sliced tissues and even single cells without consequential damage. Nitric oxide molecule can be oxidized at various electrode surfaces if sufficient positive potentials are applied, in which case a number of other biological interferents can also oxidize. To achieve high sensitivity and high selectivity for NO, the surface of the electrode needs to be modified in a way that gives priority and a high signal to NO over other interfering analytes. Thus,

it is essential to use different materials to modify the surface, each of which performs different tasks and provides improvement to analytical properties, such as selectivity, sensitivity, or stability. Electrochemical modification of electrode surfaces with electroactive polymers led to important development in analytical measurements with a reproducible surface preparation procedures and close control of electrode coatings [8-10].

Success of NO measurement can be achieved by selecting a polymer film on the electrode surface with a high affinity for NO. Several kinds of polymer-modified electrodes have been reported, which involve metal phthalocyanines [11], metalloporphyrins [12, 13], and pyrrole and its derivatives [14, 15]. Although such sensor designs offer some advantages for NO detection. Their use in direct measurement of NO in biological system was limited, due to low sensitivity, high detection limit and slow response time.

NO can interact with transition metals such as iron, thiol groups, other free radicals, oxygen, superoxide anion, unsaturated fatty acids, and other molecules. Some of these reactions result in the oxidation of nitric oxide to nitrite and nitrate, while other reactions can lead to altered protein structure, function, and/or catalytic capacity. For example, NO reacts with S-nitrosylation and converts thiol groups, including cysteine residues in proteins, to form S-nitrosothiols (RSNOs) [16-19]. Nitrosothiols and iron nitrosyls are the most important agents that account for the storage and transport of NO and related compounds. Most target receptors of nitric oxide also contain the iron center

and thiol groups [16]. Therefore, it is obvious that sulfur and NO have unique affinity to each other. Thus, to improve electrochemical detection of NO electrode modification with sulfur compounds may provide a beneficial approach. This approach may lower the oxidation potential of NO due to sulfur-NO interactions.

One goal of this work was to develop an ultra-sensitive and selective NO electrochemical sensor taking advantage of NO-sulfur chemistry for accurate quantification of NO in biological systems. In particular, PEDOT was used by electropolymerizing EDOT (3,4-ethylenedioxythiophene) monomers to modify the electrode to increase the sensitivity of the sensor towards NO. The amount of redox current typically generated by the oxidation of NO released by biological systems is extremely small. Thus, the design of an electrode for NO detection requires enormously sensitive electronic and ultra-low noise amplification circuitry. Our previous studies showed that the transition metal Ru mediates the catalytic oxidation of NO. This enhancement is the result of the electrocatalytic response of Ru oxide nanoparticles in the presence of NO. Therefore, we tried to achieve the improved sensitivity of a PEDOT modified electrode by combining both Ruthenium nanoparticles and PEDOT using the layer-by-layer (LBL) modification method. The CFE was modified first with ruthenium nanoparticles as described in literature; [20] then, EDOT was polymerized on top of the Ru particles and again a Ru-layer is deposited on top of the PEDOT layer. Further, to eliminate the other interferences the Ru/PEDOT modified carbon fiber was coated with a Nafion layer, which acts as an anionic filter [21, 22].

Surface morphology of modified fibers was characterized using Field Emission Scanning Electron Microscope (FESEM). Atomic Force Microscopy (AFM) was used to analyze the surface morphology as well as film thickness of the PEDOT thin layer deposited on the surface of Ru film. Energy dispersive X-ray spectroscopy (EDS) was used to further study the more detailed surface composition of the Ru and PEDOT film coated on the electrode.

2.2 Experimental Section

2.2.1 Chemicals and reagents

3,4-ethylenedioxythiophene, acetonitrile (99.93% HPLC grade), NaH_2PO_4, $NaHPO_4$, pyrogallol, KOH, hemoglobin, $RuCl_3.xH_2O$ and sodium hydrosulfite were purchased from Sigma-Aldrich (St Louis, MO). Carbon fibers (7-μm and 30-μm) were obtained from Goodfellow (Devon, PA) and World Precision Instrumentation (Sarasota, FL), respectively. Highly Oriented Pyrolytic Graphite (HOPG) surfaces (SPI-1 Grade) were purchased from SPI suppliers (West Chester, PA). Silver conductive epoxy was purchased from Chemtronics (Santa Ana, CA). All stock solutions were prepared with nanopure-deionized water from a Barnstead water purification system model D8961 (specific resistance >18.2 Ω cm). All other chemicals were analytical grade and were used as received.

2.2.2 Electrochemical apparatus and electrode materials

Amperometric measurements were performed using a CHI-440 electrochemical workstation. All potentials reported here are versus a Ag/AgCl reference electrode. A platinum wire was used as the auxiliary electrode and modified or unmodified carbon fibers (7- and 30-μm) were used as working electrodes. UV-visible absorbance spectra were recorded on Agilent 8453 spectrophotometer using 1-cm path UV-visible cells.

The morphology of the unmodified and modified CFEs was imaged using the field emission scanning electron microscope (FESEM) Hitachi S-4500 equipped with energy dispersive X-ray (EDX) elemental analysis capability. Atomic force microscope (AFM) (Molecular Imaging Corp, Tampe, AZ) was used in high resolution surface characterization.

A homemade flow-cell was fabricated with transparent plexiglass to insert a carbon fiber microelectrode, an Ag/AgCl reference electrode, and a stainless steel auxiliary electrode tube that was also used as the outlet. A Masterflex peristaltic pump and a Rheodyne 5020 manual injector (Sigma-Aldrich Corp, St. Louis, MO) with a 500-μL-injection loop were used to inject NO solution into the buffer stream in flow-cell.

2.2.3 Electrode Preparation

The 7-μm and 30-μm diameter carbon fiber microelectrodes were prepared using published methods described elsewhere [23]. Briefly, fibers were isolated and sonicated in acetone, then in nitric acid (1:1), and finally in distilled water. A single dried fiber was mounted on the end of a copper wire using conductive epoxy compound. After the tip of the manually pulled glass capillary was cut to obtain a smooth blunt opening (25-35 μm diameter), each carbon fiber was inserted into the glass capillary and sealed with non-conductive epoxy. The copper wire was fixed to the stem of the glass tube with epoxy glue and dried prior to use. After the epoxy had cured, the tip portion of carbon fiber was cut, leaving 3 mm of the fiber protruding.

All electro-deposition and electro-polymerization experiments were performed in a three-electrode cell on a BAS electrochemical workstation that stood at room temperature. EDOT polymerization was done by using 0.05 M EDOT in the presence of 0.1 M tetrabutylammonium tetrafluoroborate in acetonitrile solution at a potential range from +1.5 V to -1.5 V and at a scan rate of 250 mV/s. For Ruthenium nanoparticle modification, 0.02 M $RuCl_3$ in 10 mM perchloric acid solution was used and electrodeposited in the potential range of -0.85 and +0.65 V at 100 V/s over 20 minutes. A silver chloride (Ag/AgCl) electrode was used as the reference electrode, unless otherwise indicated. Platinum wire and unmodified or modified carbon fiber electrodes were used as auxiliary and working electrodes. After each modification, the electrode was

gently washed with nanopure-deionised water to remove excess material and allowed to dry prior to use.

2.2.4 Preparation of NO stock solution

NO stock solution was prepared by bubbling purified NO gas through nanopure-deionized water [24]. A small glass vial containing 10 ml deionized water and capped with a rubber septum was treated with purified nitrogen passing through an alkaline pyrogallol (5% w/v) solution for 30 minutes. Then purified NO gas was bubbled through the treated water for another 30 minutes in a fume hood. The purified NO gas was prepared by passing the gas through a 5% pyrogallol solution in saturated potassium hydroxide to remove oxygen and then through 10% (w/v) potassium hydroxide to remove other nitrogen oxides. The concentration of the NO saturated water was 2 mM, which was confirmed by a photometric method based on the conversion of NO by oxyhemoglobin to methemoglobin [25]. The NO standard solution was freshly prepared by serial dilution of the NO saturated solution prior to each experiment.

2.2.5 Experimental procedure

The amperometric measurements were performed using CHI electrochemical station. The pH 7.0 phosphate buffer was purged with purified nitrogen gas for at least 20 minutes prior to the experiments to remove dioxygen; a nitrogen blanket was kept on the electrochemical cell throughout the experiment. Amperometric experiments were performed by applying +0.5 V potential at the working NO-sensing electrode. A moderate stirring of the solution was maintained at about 250 rpm, which allowed the transient background current to decay to a steady-state value in the absence of NO. An airtight Hamilton syringe was used to inject the different concentrations of NO into the buffer solution.

2.3 Results and Discussion

2.3.1 Electrodeposition of EDOT on CFE

The polymerization of EDOT on the electrode surface was performed electrochemically using multiple scan cyclic voltammetry on the carbon fiber electrode. A regular growth was observed for PEDOT in the potential window from +1.5 V to -1.5 V and at a scan rate of 250 mV/s. An increase in both anodic and cathodic current was observed during the electropolymerization process. Typical cyclic voltammograms recorded during the film formation are shown in Figure 2.1. The mechanism of the polymerization of water insoluble monomers on conductive surfaces has been addressed in the literature [26]. This process ultimately led to the formation of the polymer PEDOT

on the surface of the electrode as illustrated in scheme 2.1. Scan rate dependence experiments for the current response during redox cycling of EDOT between +1.5 V and -1.5 V were also conducted and results were in line with the deposition of a conductive polymer on the surface. For the polymerization process, we adopted the use of 10 continuous cyclic scans and the scan rate of 250 mV/s as optimum conditions. Large number of scans (above 12) and or higher scan rates led to very unstable film and affected the reproducibility of NO measurements.

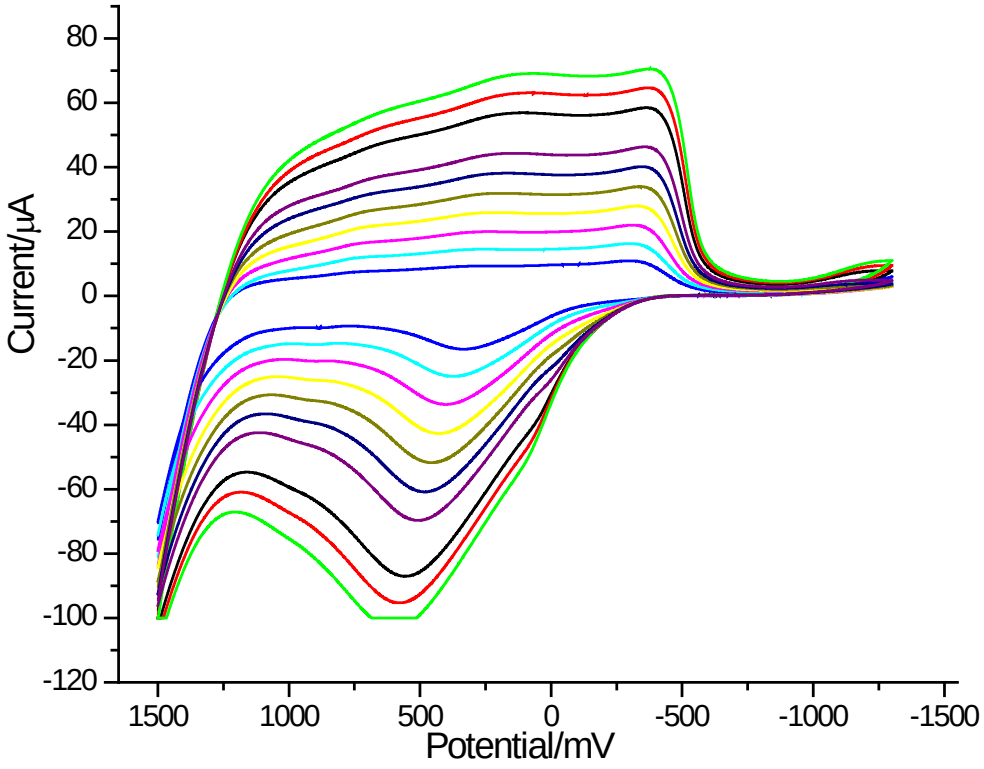

Figure 2.1. Cyclic voltammograms showing electro-deposition of EDOT by continuous cyclic scaning between +1.5 V and –1.5 V in a solution containing 0.05 M EDOT in the presence of 0.1 M tetrabulyl ammonium tetrafluoroborate in acetonitrile solution. Scan rate: 250 mV/s.

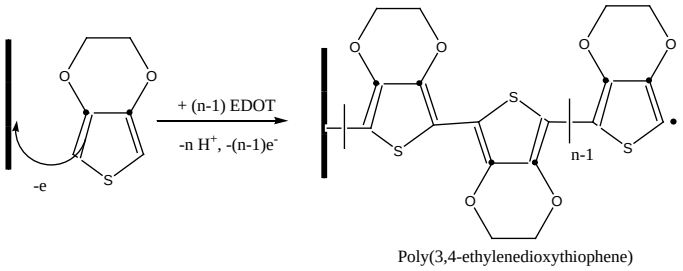

Scheme 2.1. Polymerization of EDOT on the electrode surface.

In order to enhance the sensitivity of a PEDOT modified electrode, Ru nanoparticles were electrodeposited on the electrode in alternate layers with PEDOT layers. In this case, ruthenium nanoparticles were deposited on the CFE electrochemically from a $RuCl_3$ solution. Then, the PEDOT layer was polymerized on the top of the Ru particles; subsequently, Ru particles were again deposited on top of the PEDOT layer to get three successive layers (Ru-PEDOT-Ru).

2.3.2 Characterization of modified microelectrodes

The FESEM micrographs of PEDOT polymerized fiber samples (Figure 2 B, D) showed thicker morphology, resembling a “cauliflower” type of coating, compared to uncoated carbon fibers (Figure 2.2 A, C). This coating apparently increases the surface area of the electrode. Due to the grooves present on the surface of 7-μm fiber (Figure 2.2 C, D), it was found that the deposition of PEDOT on the 7-μm fiber was higher than that of 30-μm fiber (Figure 2.2 A, B). The surface morphology of electrodeposited ruthenium oxide on the carbon fiber surface appears as the characteristic granular-type structures (Figure 2.3 A, B). In the sequential deposition modification, the surface morphology of the Ru film was changed from a small granular type to cauliflower type with many recesses after the polymerization of PEDOT on the Ru surface as shown in Figure 2.3 C, D [27]. FESEM images of the Ru-PEDOT-Ru modified fiber showed small Ru granules on the top of PEDOT layer (Figure 2.3 E, F), as expected for the sequential electrodeposition.

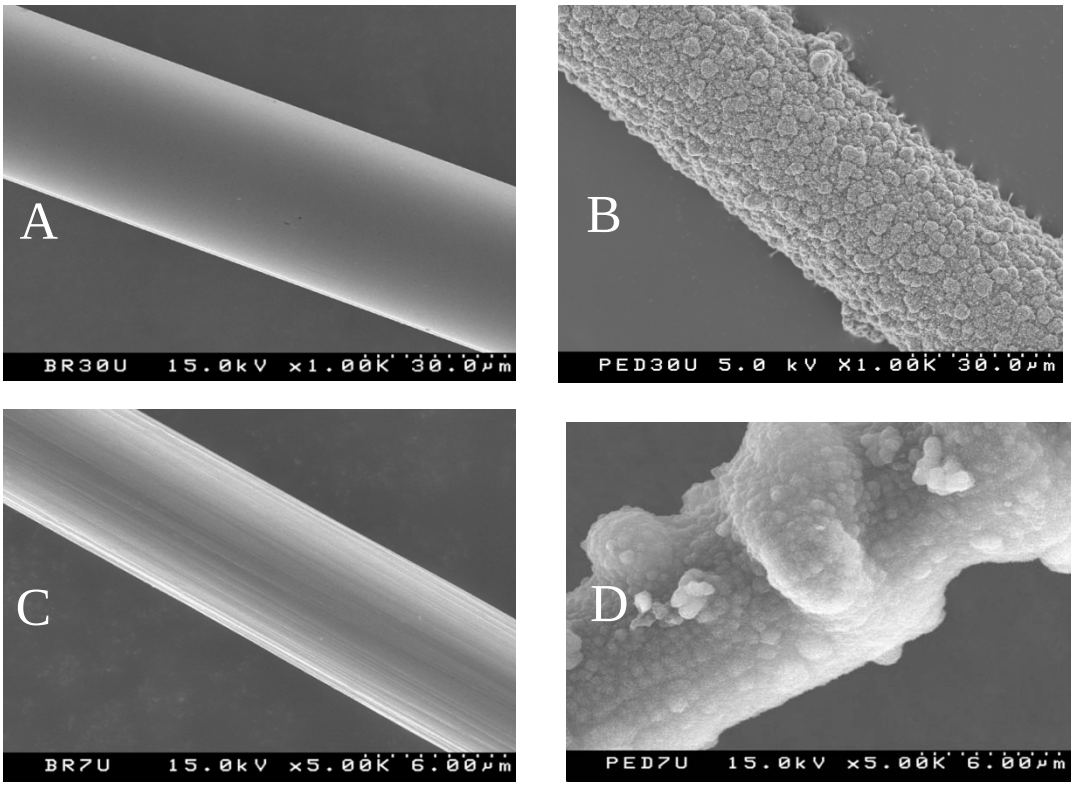

Figure 2.2. FESEM images of CFEs- unmodified 30-µm (A); PEDOT modified 30-µm (B); unmodified 7-µm (C); PEDOT modified 7-µm(D);

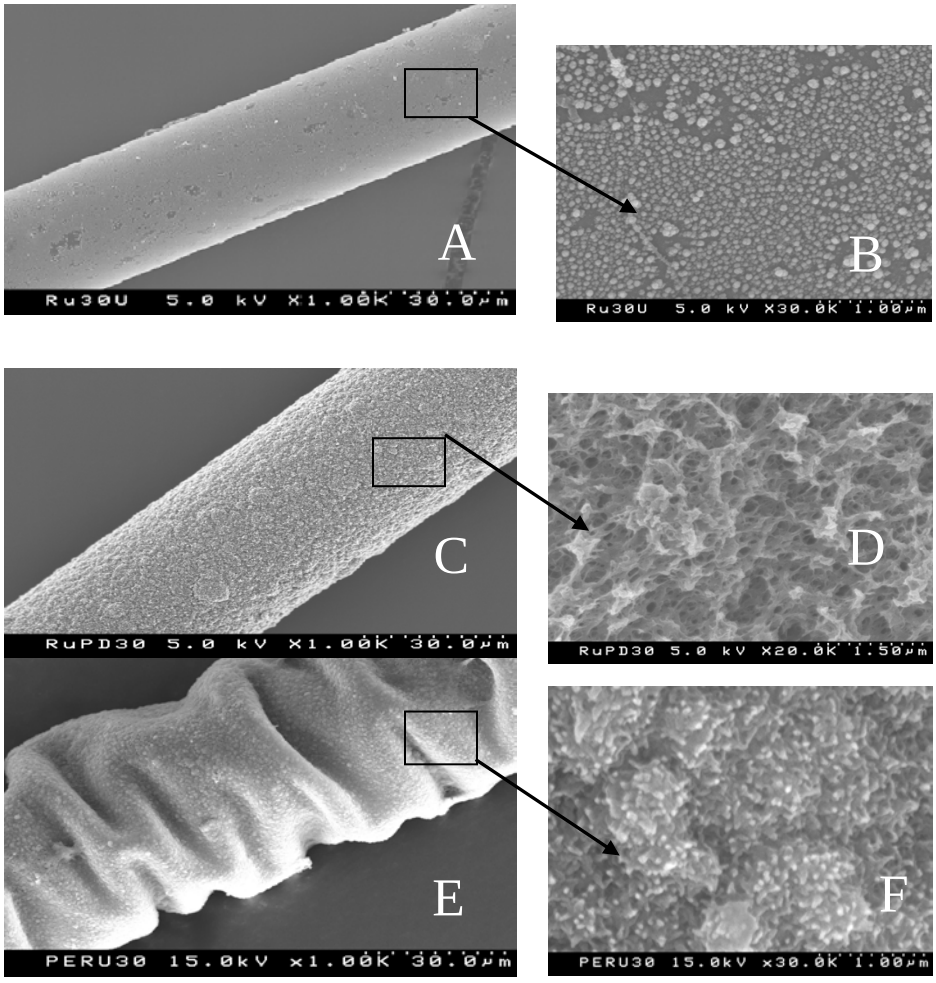

Figure 2.3. FESEM images of CFEs- Ru Modified CFE 1000x (A); Ru Modified CFE 30000x (B); Ru-PEDOT 1000x (C); Ru-PEDOT 20000x. (D); Ru-PEDOT-Ru modified CFE 1000x and (E); Ru-PEDOT-Ru modified CFE 30000x (F).

The same modification procedures for Ru deposition and PEDOT polymerization were applied to modify the highly oriented pyrolytic graphite (HOPG) surface for AFM analysis. AFM images shows that the thickness of the modified surface or the PEDOT film is ~200 nm (z height) (Figure 2.4 B). The AFM image of the PEDOT-Ru layer-by-layer modified surface shows the full coverage of Ru nanoparticles on the top of the PEDOT film. The z height of Ru nanostructures alone was found to be around 2 nm, which is very small compared to that of the PEDOT layer. Therefore, sequential deposition of Ru on the PEDOT surface did not adversely affect the thickness of the PEDOT film (Figure 2.4 C).

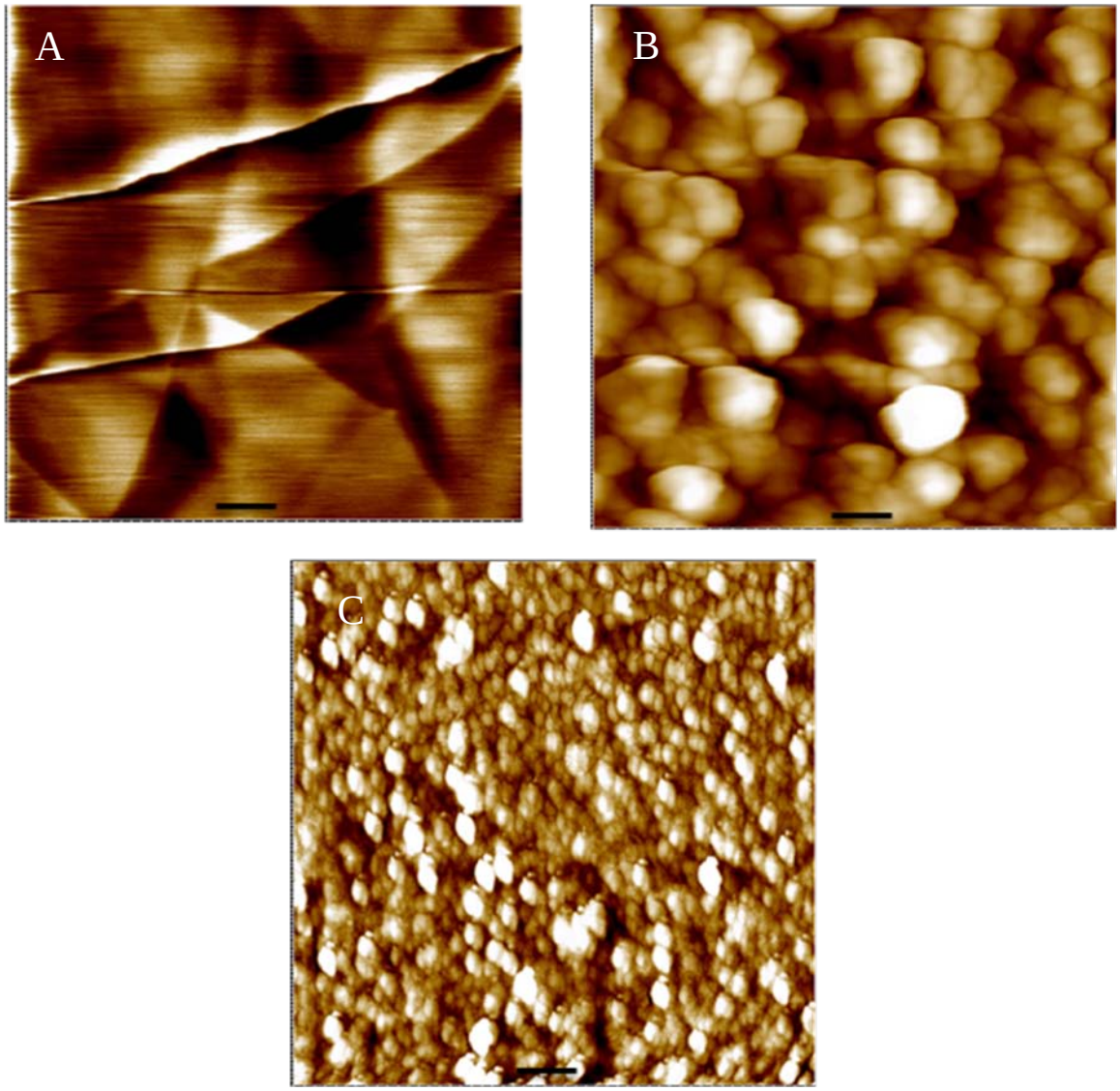

Figure 2.4. Contact AFM topological images for (A) unmodified HOPG surface (B) PEDOT modified HOPG surface (C) Ru on the top of the PEDOT surface. Scale bar is 500 nm.

The FESEM and AFM images of unmodified and modified CFE showed distinct morphological differences on their surfaces. The EDS analysis demonstrated the actual composition of each compound (Ru and PEDOT) on the surface. As expected EDS analysis plots (Figure 2.5) indicated a high percentage of sulfur content in the composition of PEDOT modified electrodes (4000 counts in Figure 2.5 plot C, D) compared to the unmodified (Figure 2.5 plot a) and Ru-modified electrodes (<500 counts, Figure 2.5 plot B). Moreover, expected Ru peaks were observed in Ru modified electrodes as shown in Figure 2.5, plot B and D. Thus, EDS analysis confirmed that the modified electrodes contained both sulfur from PEDOT and Ru on its surface.

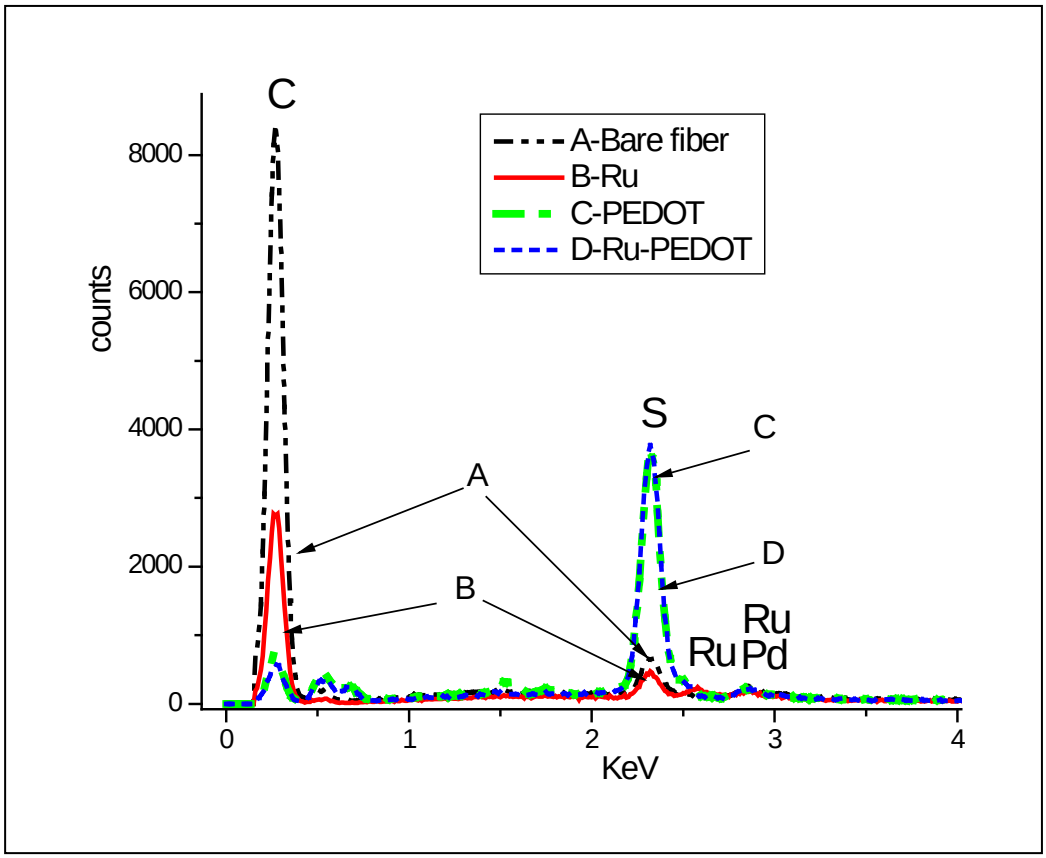

Figure 2.5. EDS spectra for the (A) unmodified CFE (B) Ru modified CFE (C) PEDOT modified CFE (D) Ru-PEDOT modified CFE.

2.3.3 Electrochemical detection

Constant potential amperometry was used to measure NO in a standing solution using our Ru-PEDOT modified NO sensor. Amperometric detection of NO involves the oxidation of NO on the surface of the electrode and the measurement of the subsequent (redox) current generated. Thus, the amount of NO oxidized is proportional to the current flow at the working electrode. The electrochemical detection of NO in solution occurs at a positive potential and the process typically involves both electrochemical and chemical reactions [28].

Figure 6 A illustrates the typical amperometric response of a 7-μm unmodified CFE and the PEDOT modified CFE upon successive additions of NO in the range of 100 nM - 12.8 μM NO into a stirred, deoxygenated 0.1 M PBS buffer solution at +0.5 V (vs. Ag/AgCl reference electrode). In this relatively low potential, the modified CFE responds rapidly to the added aliquots of NO, reaching a steady state current within a few seconds. A plot of the steady state current vs. the NO concentration for both 7-μm electrodes is shown in the inset of Figure 2.6 A. The PEDOT modified CFE exhibits significantly enhanced electrochemical response compared to the unmodified CFE. The sensitivity of PEDOT modified CFE is ~6.3 pA/nM, compared to the sensitivity of ~0.1 pA/nM for unmodified CFE.

The increased sensitivity for the PEDOT modified electrode highlights the importance of sulfur-NO favorable interactions during the NO oxidation process. The

amperometric response for Ru-PEDOT-Ru modified and unmodified 7-μm CFEs at +0.5 V vs. Ag/AgCl is shown in Figure 2.6 B. The calibration plot shown in the inset (Figure 2.6 B) shows that observed sensitivity for Ru-PEDOT-Ru modified 7-μm CFE is improved to 15 pA/ nM. When the electrodes were modified with three sequential layers, the sensitivity increased ~2.5 times compared to the PEDOT modified CFE.

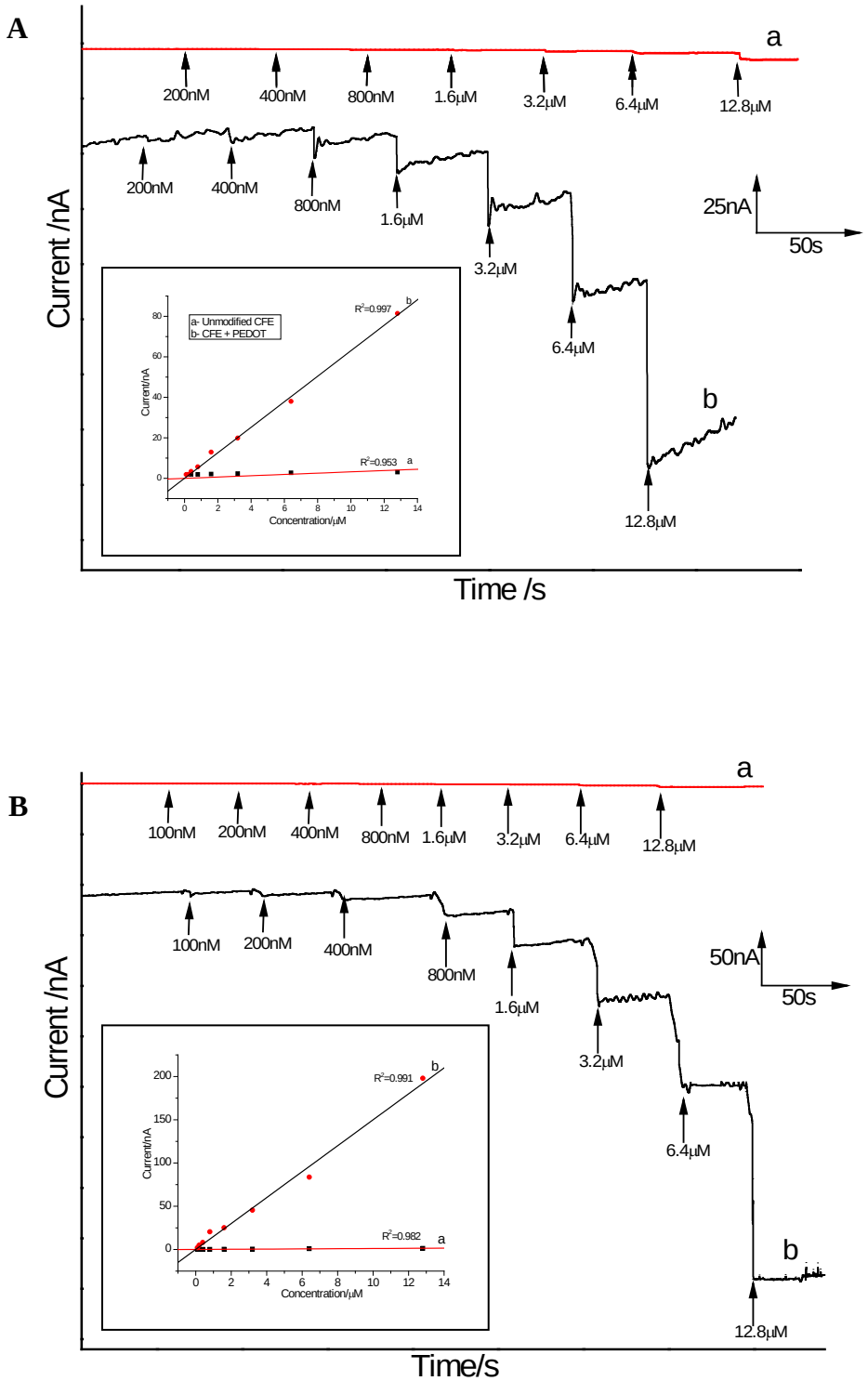

Figure 2.6. (A) Amperometric responses for 7-μm unmodified CFE (a) and PEDOT modified CFE (b). (B) Amperometric responses for 7-μm unmodified CFE (a) and Ru-PEDOT-Ru layers modified CFE (b). The insets are the resulting calibration plot.

We also investigate the response of NO using 30-μm modified CFEs in the same manner. The electrode responses for NO modified with PEDOT and Ru-PEDOT-Ru layers are shown in Figure 2.7 A, B. The sensitivities of PEDOT and Ru-PEDOT-Ru modified 30-μm are 2.5 pA/nM and 5.7 pA/ nM respectively. As in 7-μm CFE, the sensitivity for 30-μm LBL modified CFE is improved by ~2.3 fold compared to the PEDOT modified CFE. The enhanced sensitivity observed at electrodes modified with three successive layers (Ru-PEDOT-Ru) demonstrates the synergetic effect of conductive polymer PEDOT as a matrix and electrocatalytic activity of Ru catalyst particles.

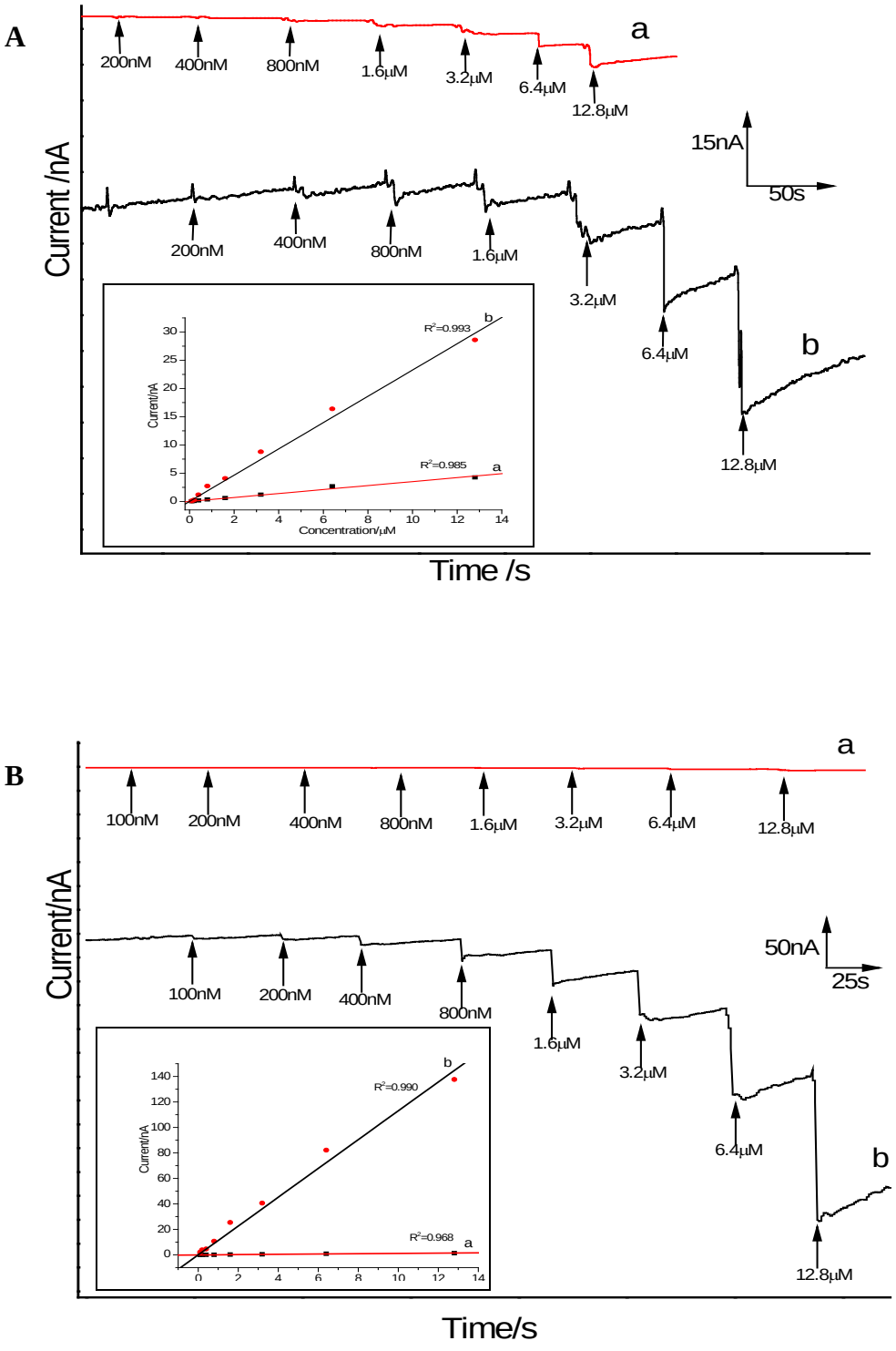

Figure 2.7. (A) Amperometric responses for 30-μm unmodified CFE (a) and PEDOT modified CFE (b). (B) Amperometric responses for 30-μm unmodified CFE (a) and Ru-PEDOT-Ru layers modified CFE (b). The insets are the resulting calibration plot.

The higher sensitivity of both PEDOT and Ru-PEDOT-Ru modified 7-μm CFE, compared to the 30-μm CFE can be attributed to a better modification process of the smaller fiber due to faster establishment of radial diffusion profiles during the electrochemical modification process. Thus, 7-μm CFE modified with Ru-PEDOT-Ru was used for further characterization and analysis as discussed later. The comparison of sensitivities and detection limits obtained from modified 7- and 30-μm CFEs are reported in the Table 2.1. Normalized sensitivities of 7- and 30-μm CFEs are calculated for comparison purposes. Both PEDOT and Ru-PEDOT-Ru modified 7-μm CFEs showed ~10 fold enhanced normalized-sensitivities than the modified 30-μm CFEs.

Table 2.1. Comparison of sensitivities and detection limits of 7- or 30- μm modified CFE.

Diameter of the Sensor (μm)	Sensitivity		Normalized Sensitivity		Limit of Detection
	PEDOT (pA/nM)	Ru-PEDOT-Ru (pA/nM)	PEDOT (pA/nM/μm^2)	Ru-PEDOT-Ru (pA/nM/μm^2)	Ru-PEDOT-Ru
7	6.3	14.99	1.43×10^{-4}	3.40×10^{-4}	250pM
30	2.5	5.7	1.32×10^{-5}	3.01×10^{-5}	6nM

The detection limit is important when analyzing biological samples and depends highly on the detection system (chemistry of sensor) employed and the resulting

sensitivity of the sensor. The sensitivity achieved by our 7-μm CFE modified with Ru-PEDOT-Ru sensor for lower the concentration range (100-800nM) of NO (Figure 2.8 A) is 24.46 pA/nM, which is much higher than the sensitivity (14.96 pA/nM) observed in the higher concentration range (1.0-12.5 μM) (Figure 2.8 B). The high performance of sensitivity in the low NO concentrations can be explained from the electrocatalytic behavior of the NO determination and available electrocatalytic sites relative to amounts of NO. At low doses (low concentration range) saturation of sites is unlikely and the response is maximum. When the NO concentration is increased, pre-saturation occurs and the catalytic sites and starts to limit the sensitivity of the electrode.

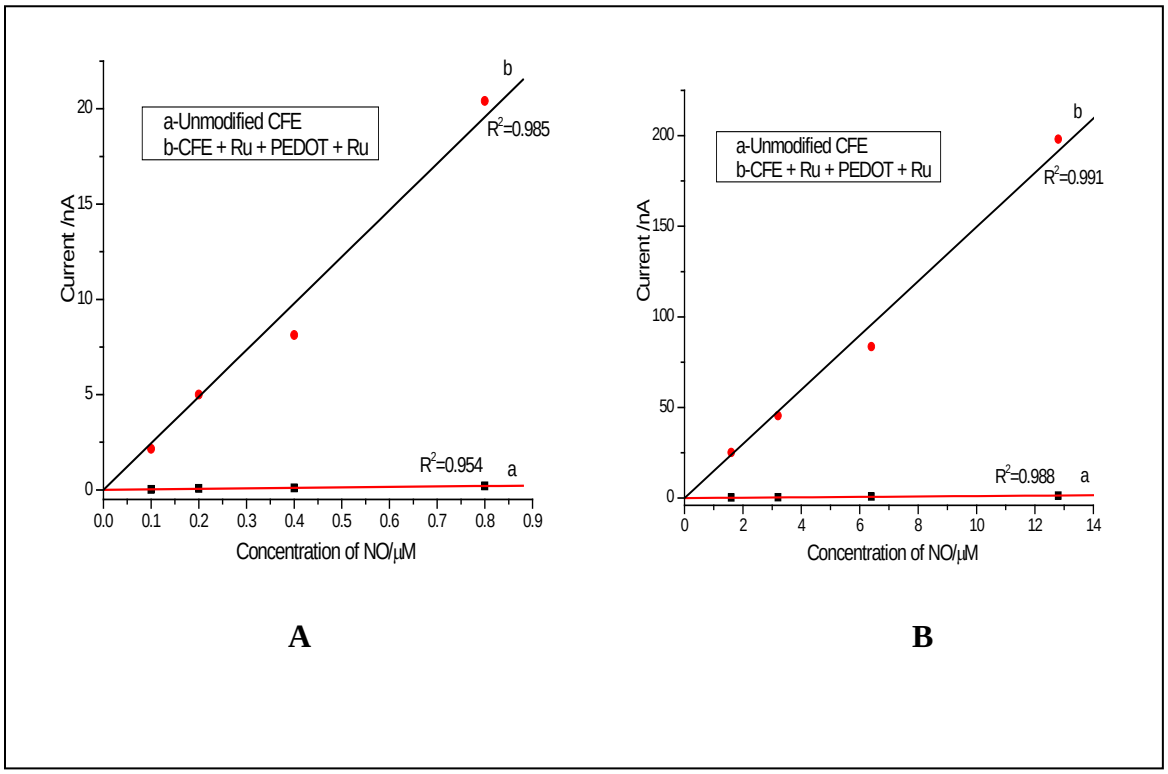

Figure 2.8. Current/NO dose plot for 7-µm unmodified CFE and Ru-PEDOT-Ru layers modified CFE. (A) low NO concentration (B) high NO concentration. Applied potential is +0.5 V *vs* Ag/AgCl.

The limit of detection (LOD) is the lowest concentration of analyte that can be analyzed by the sensor with a significantly low background noise (signal/noise = 3). We were able to measure NO concentration as low as 250 pM for Ru-PEDOT-Ru modified CFE as shown in Figure 2.9 with a signal-to-noise ratio of 3. The sensitivity and the limit of detection obtained with our Ru-PEDOT no sensor show high performance compared to other reported values in the literature using CFE sensors (we are comparing only surfaces

of similar geometries to ours). The comparison of sensitivities and detection limits of similar NO sensors that used polymeric matrices to modify the surface and our sensor are shown in Table.2.2.

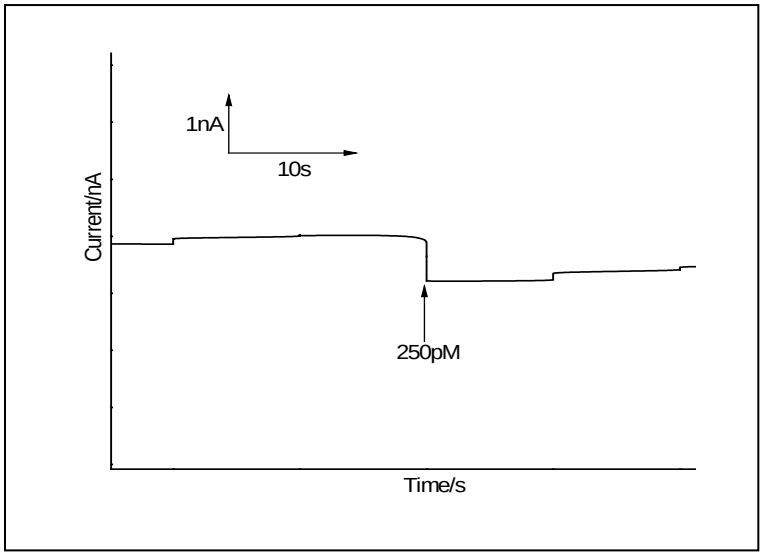

Figure 2.9. Amperometric response of Ru-PEDOT-Ru layers modified CFE to 250 pM NO under stirring (250 RPM) pH 7 PBS. Applied potential is +0.5 V *vs* Ag/AgCl.

Table 2.2. Comparison of sensitivities and detection limits of few published NO sensors.

Sensor assembly		NO response characterizing			Ref.
Support	Membrane	Potential at which NO is determined (reference electrode)	Sensitivity	Limit of detection	
Carbon (fiber (cylindrical; diameter = 7μm length = 2 mm)	Nafion |WPI membrane	0.86 V/Ag-AgCl	1.03 pA/ nM	5 nM	[29]
Carbon (fiber (cylindrical; diameter = 8μm length = 2 mm)	Ni-THMPP [a]|Nafion	0.79 V/Ag-AgCl	6.28 pA/ nM	1 nM	[30]
Carbon (fiber (cylindrical; diameter = 7μm length = 2 mm)	Ni-THMPP|Nafion|AAO [b]| poly-lysin	0.7 V/Ag-AgCl	1.34 pC/nM	0.5 nM	[31]
Carbon (fiber (cylindrical; diameter = 30μm length = 2-3 cm)	Nafion| o-PD [c]	+0.9 V/Ag-AgCl	31 pC/μM	35nM	[7]
Carbon (fiber (cylindrical; diameter = 7.8μm length = 0.5 mm	PBPB [d]|Nafion	0.80 V/Ag-AgCl	1.04 pA/ nM	3.6nM	[32]
Carbon (fiber (cylindrical; diameter = 7μm length = 2 mm	Ru| PEDOT| Ru| Nafion	0.50 V/Ag-AgCl	15 pA/ nM	250 pM	This work

[a] THMPP = tetrakis-4-hydroxy-3-3methoxyphenylporphyrin,
[b] AAO = Ascorbic acid oxidase;
[c] o-PD = o-Phenylenediamine
[d] PBPB = Poly bromophenol blue

We also investigated the response of our Ru-PEDOT-RU sensor in flow injection analysis (FIA) method that leads itself to automated analysis (especially in the clinical field). The buffer solution was used as the carrier stream in which different NO concentrations were injected. Our NO sensor (Ru-PEDOT-Ru modified 7-μm CFE) was used as the working electrode in the FIA system. Short analysis times enabled quick sample analysis. The significant increase in the peak current observed with modified CFE clearly confirms the improved sensitivity of the modified electrode (Figure 2.10). The resulting charge/NO dose response plot (Figure 2.10, inset) shows high sensitivity (0.9 μC/nM) compared to the unmodified CFE (sensitivity is 0.007 μC/nM).

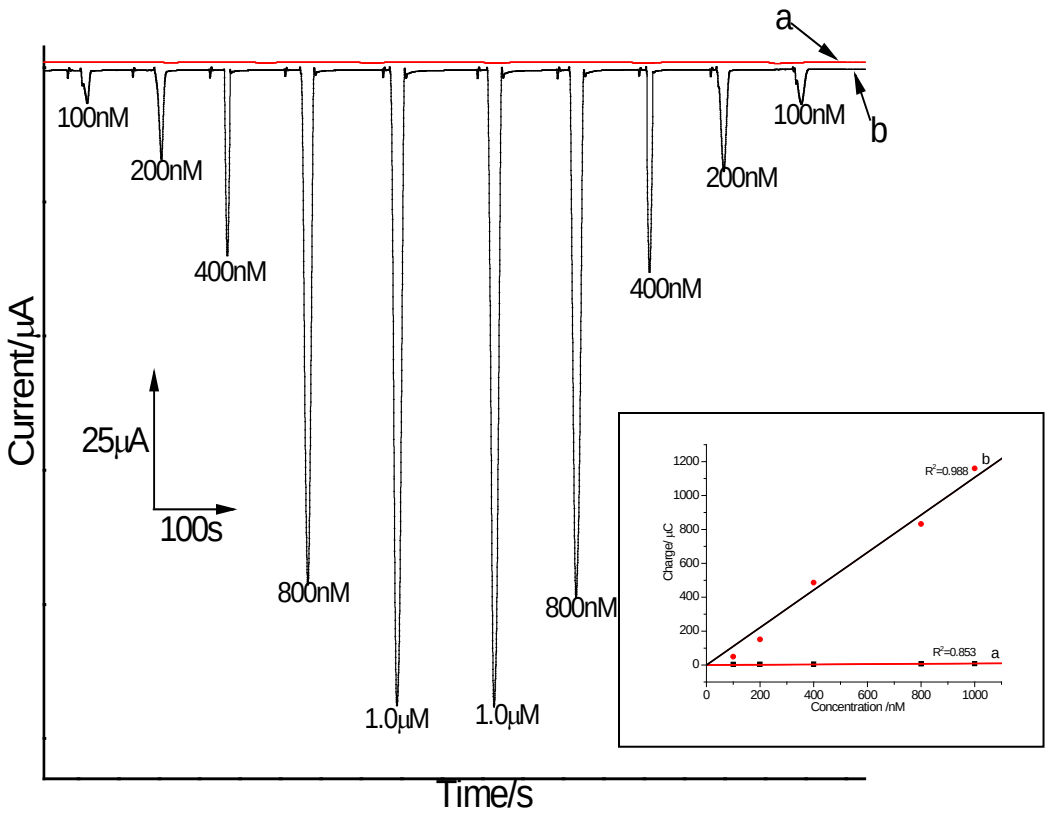

Figure 2.10. Flow injection analysis response of unmodified (a) and modified (b) CFE. The inset is the resulting calibration plot. Applied potential +0.5V *vs* Ag/AgCl.

We also focused on improving the selectivity of the sensor towards NO for further applications in biological systems. In fact, NO sensors are practically useless unless they are immune to interference from other species present in the measured environment. Selectivity can be achieved by carefully choosing the applied voltage and by using selective membranes. Since the applied voltage in our case was +0.5 V, which is less positive than most potentials used for available NO sensors (e.g. compare this to +0.85 V used for WPI sensors), it was selective for NO in the presence of other species requiring more positive potentials. By applying such a low potential we could eliminate interfering nitrite ions from NO detection (Figure 2.11). In addition, with regard to sensor application in biological systems, using a permeable membrane can provide more selectivity. Nafion has been extensively employed in the design of many chemical sensors and biosensors for *in vitro* as well as *in vivo* applications [7, 15, 21]. Nafion, a negatively charged polymer, can be used on the surface of the electrode to prevent anionic electroactive species from interfering with the oxidation of NO. Figure 2.12 clearly shows the protective action of Nafion coated Ru-PEDOT-Ru modified CFE against interferences such as L-ascorbic acid, arginine, and nitrite. High concentrations of interferences were tested and the sensitivities of each compound and the NO: interference ratios are reported in the Table 2.3.

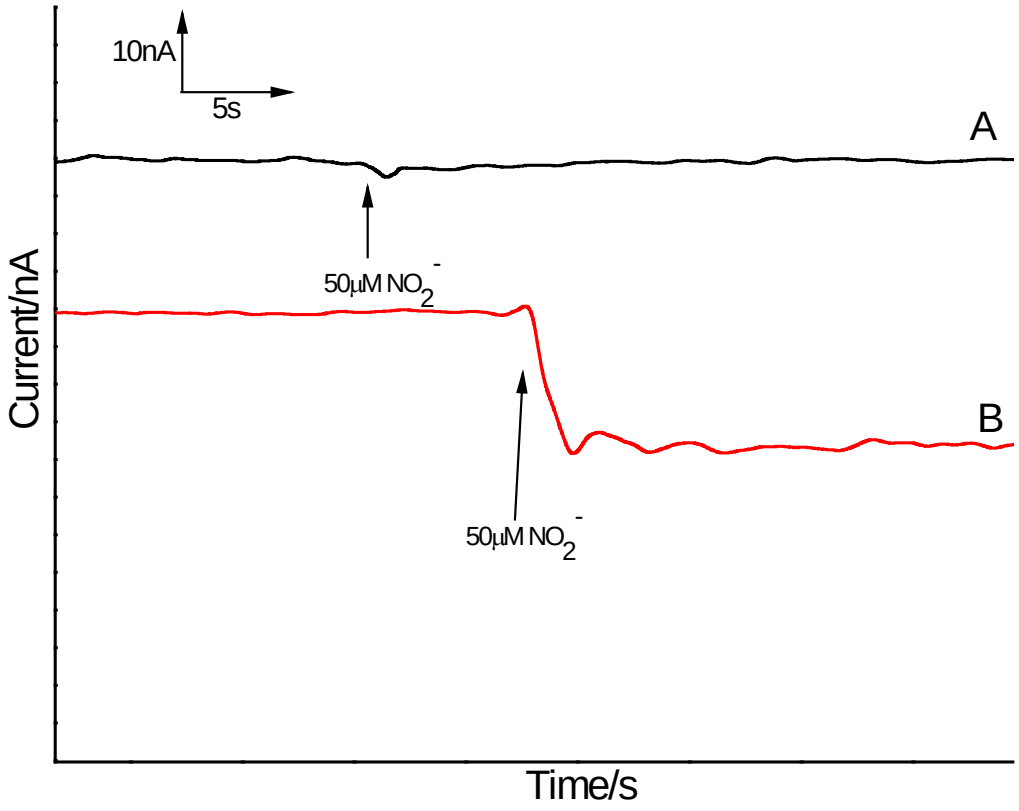

Figure 2.11. (A) Amperometric response of 7-μm Ru-PEDOT-Ru layers modified CFE for 50 μM NO_2^- at the potential of +0.5 V *vs.* Ag/AgCl (B) Amperometric response of 7-μm Ru-PEDOT-Ru layers modified CFE for 50 μM NO_2^- at the potential of +0.8 V *vs.* Ag/AgCl.

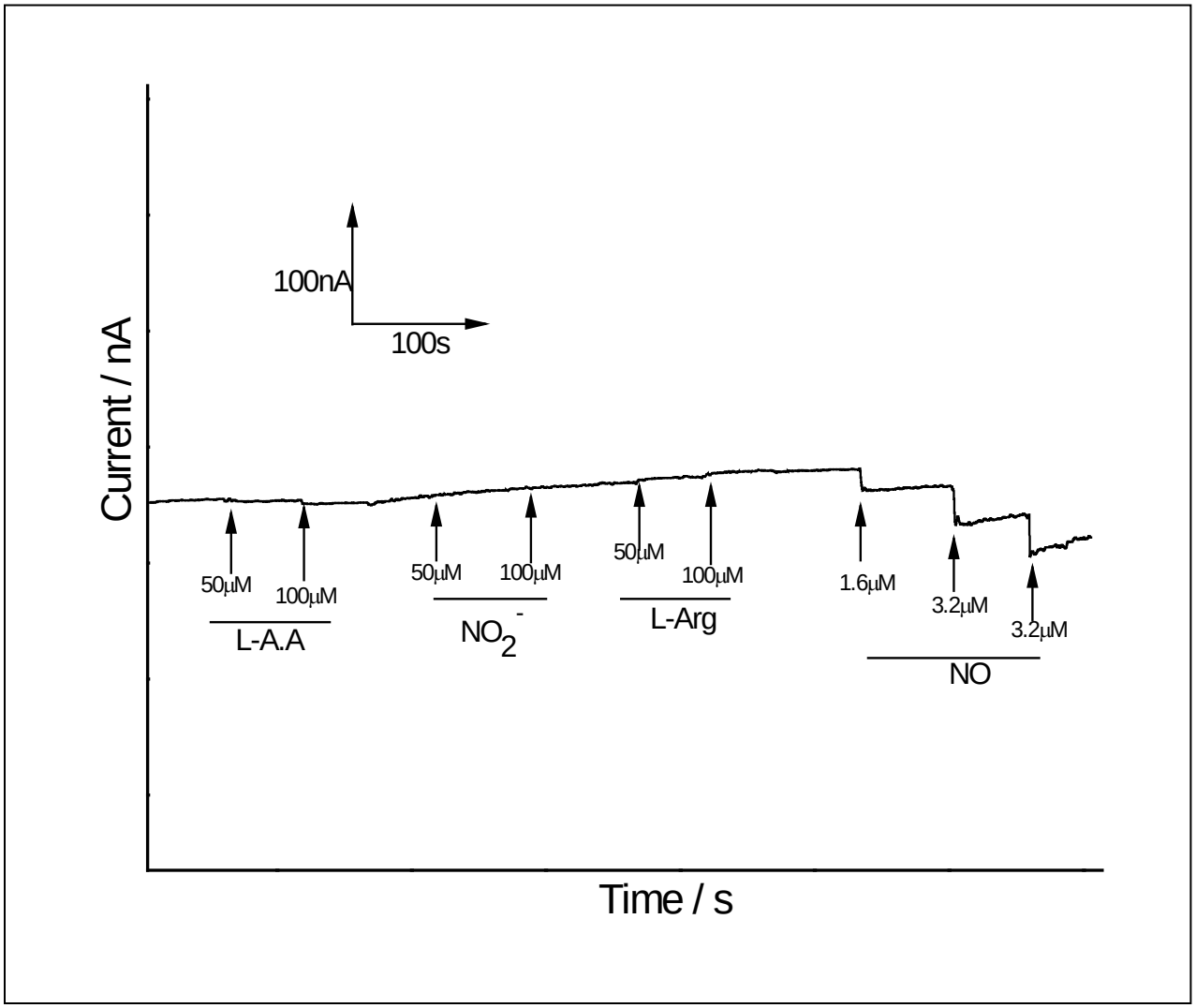

Figure. 2.12. Amperometric responses of nafion coated Ru-PEDOT-Ru modified CFE to addition of NO and other interferences (L-Ascorbic acid (L-A.A), Nitrite (NO_2^-) and L-Arginine (L-Arg)). Applied potential is +0.5 V *vs* Ag/AgCl.

Table 2.3. Interferences of various compounds with the three layers modified sensor.

Compound	Tested Concentration (μM)	Sensitivity (pA/ nM)	NO : Interference ratio
Ascorbic acid (AA)	100	1.899×10^{-2}	531:1
NO_3^-	100	1.98×10^{-5}	1400:1
NO_2^-	100	4.19×10^{-3}	1204:1
L-Arginine	100	5.2×10^{-5}	970:1

2.4 Summary of Chapter II

In this study, we have developed a highly sensitive and selective NO sensor based on a composite combination of conductive polymer and catalytic transition metal on CFE. The PEDOT modified 7-μm carbon fiber microelectrode shows high sensitivity of 6.3 pA/nM, which is ~60 times higher value compared to the unmodified CFE (0.1 pA/nM). On the other hand PEDOT modified 30-μm carbon fiber microelectrode shows sensitivity of ~3 pA/nM. The modified electrodes give rapid and reproducible response for NO concentrations at a relatively low applied potential (+0.5 V as compared to +0.8 V or higher for all current commercial probes). The lower oxidation potential is a result of favorable sulfur-NO interactions.

Further, the three consecutive layers modification of CFE with the combination of transition metal catalyst Ru results in higher sensitivity for NO detection (about 6 pA/nM for 30 μm CFE and 15 pA/nM for 7-μm CFE) with excellent linearity (a wide linear range from nM to μM). The sensitivity of Ru-PEDOT-Ru modified 7-μm CFEs is enhanced to about 150 times compared to unmodified CFE. In the low range of NO concentrations, Ru-PEDOT-Ru modified 7-μm CFEs give superior sensitivity (~25 pA/nM) for NO than in higher ranges. As such we achieved a significantly lower value for the detection limit (250 pM). In addition to a potential-based selectivity (at +0.5 V nitrite does not interfere), we showed that Nafion membranes could also be used on our Ru-PEDOT-Ru to prevent anionic electroactive interferents from being oxidized with NO. Our high sensitive and selective sensor offers great promise for measurement of NO in biological systems, such as live cells.

2.5 References.

1. Ignarro LJ. Nitric oxide as a unique signaling molecule in the vascular system: a historical overview J Physiol Pharmacol 2002;53: 503-514.
2. Palmer RM, Ashton DS, and Moncada S. Vascular endothelial cells synthesize nitric oxide from L-arginine Nature 1988;333: 664-666.
3. Voegtle HL, Sono M, Adak S, Pond AE, Tomita T, Perera R, Goodin DB, Ikeda-Saito M, Stuehr DJ, and Dawson JH. Spectroscopic characterization of five- and six-coordinate ferrous-NO heme complexes. Evidence for heme Fe-proximal cysteinate bond cleavage in the ferrous-NO adducts of the Trp-409Tyr/Phe proximal environment mutants of neuronal nitric oxide synthase Biochemistry 2003;42: 2475-2484.
4. Menzel L, Kosterev AA, Curl RF, Tittel FK, Gmachl C, Capasso F, Sivco DL, Baillargeon JN, Hutchinson AL, Cho AY, and Urban W. Spectroscopic detection of biological NO with a quantum cascade laser Appl Phys B 2001;72: 859-863.
5. Zweier JL, Wang P, and Kuppusamy P. Direct measurement of nitric oxide generation in the ischemic heart using electron paramagnetic resonance spectroscopy J Biol Chem 1995;270: 304-307.
6. Trevin S, Bedioui F, and Devynck J. Electrochemical and spectrophotometric study of the behavior of electropolymerized nickel porphyrin films in the determination of nitric oxide in solution Talanta 1996;43: 303-311.

7. Friedemann MN, Robinson SW, and Gerhardt GA. o-Phenylenediamine-modified carbon fiber electrodes for the detection of nitric oxide Anal Chem 1996;68: 2621-2628.

8. Lee Y, Oh BK, and Meyerhoff ME. Improved planar amperometric nitric oxide sensor based on platinized platinum anode. 1. Experimental results and theory when applied for monitoring NO release from diazeniumdiolate-doped polymeric films Anal Chem 2004;76: 536-544.

9. Prakash R, Srivastava RC, and Seth PK. Polycarbazole modified electrode; nitric oxide sensor Polym.Bull. 2001;46: 487-490.

10. Kitamura Y, Uzawa T, Oka K, Komai Y, Ogawa H, Takizawa N, Kobayashi H, and Tanishita K. Microcoaxial electrode for in vivo nitric oxide measurement Anal Chem 2000;72: 2957-2962.

11. Pontie M, Gobin C, T. P, Bedioui F, and J. D. Electrochemical nitric oxide microsensors: sensitivity and selectivity characterisation Analytica Chimica Acta 2000;411: 175-185.

12. Malinski T, and Taha Z. Nitric oxide release from a single cell measured in situ by a porphyrinic-based microsensor Nature 1992;358: 676-678.

13. Diab N, Oni J, and Schuhmann W. Electrochemical nitric oxide sensor preparation: A comparison of two electrochemical methods of electrode surface modification Bioelectrochemistry 2005;66: 105-110.

14. Schuhmann W. Conducting Polymer Based Amperometric Enzyme Electrodes Mikrochim. Acta 1995;121: 1-29.

15. Fabre B, Burlet S, Cespuglio R, and Bidan G. Voltammetric detection of NO in the rat brain with an electronic conducting polymer and Nafion® bilayer-coated carbon fibre electrode Journal of electroanalytical chemistry 1997;426: 75-83.

16. Szacilowski K, Chmura A, and Stasicka Z. Interplay between iron complexes, nitric oxide and sulfur ligands: Structure, (photo)reactivity and biological importance Coordination Chemistry Reviews 2005;249: 2408.

17. Stasko NA, Fischer TH, and Schoenfisch MH. S-nitrosothiol-modified dendrimers as nitric oxide delivery vehicles Biomacromolecules 2008;9: 834-841.

18. Lopez-Sanchez LM, Corrales FJ, Gonzalez R, Ferrin G, Munoz-Castaneda JR, Ranchal I, Hidalgo AB, Briceno J, Lopez-Cillero P, Gomez MA, De La Mata M, Muntane J, and Rodriguez-Ariza A. Alteration of S-nitrosothiol homeostasis and targets for protein S-nitrosation in human hepatocytes Proteomics 2008;8: 4709-4720.

19. Gow A, Doctor A, Mannick J, and Gaston B. S-Nitrosothiol measurements in biological systems J Chromatogr B Analyt Technol Biomed Life Sci 2007;851: 140-151.

20. Bayachou M, and Peiris P. Nitric Oxide Sensor WIPO Patent 2008:

21. Santos RM, Lourenco CF, Piedade AP, Andrews R, Pomerleau F, Huettl P, Gerhardt GA, Laranjinha J, and Barbosa RM. A comparative study of carbon fiber-based microelectrodes for the measurement of nitric oxide in brain tissue Biosens Bioelectron 2008;24: 704-709.

22. Hrbac J, Gregor C, Machova M, Kralova J, Bystron T, Ciz M, and Lojek A. Nitric oxide sensor based on carbon fiber covered with nickel porphyrin layer deposited using optimized electropolymerization procedure Bioelectrochemistry 2007;71: 46-53.

23. Koh DS, and Hille B. Rapid fabrication of plastic-insulated carbon-fiber electrodes for micro-amperometry J Neurosci Methods 1999;88: 83-91.

24. Zhang X, and Broderick M. Mod. Aspects Immunobiol. 2000;1: 160.

25. Murphy ME, and Noack E. Nitric oxide assay using hemoglobin method Methods Enzymol 1994;233: 240-250.

26. Asami R, Fuchigami T, and Atobe M. Development of a novel environmentally friendly electropolymerization of water-insoluble monomers in aqueous electrolytes using acoustic emulsification Langmuir 2006;22: 10258-10263.

27. Yinghong X, Xinyan C, and David CM. Electrochemical polymerization and properties of PEDOT/S-EDOT on neural microelectrode arrays Journal of Electroanalytical Chemistry 2004;573: 43.

28. Zhang X. Real time and in vivo monitoring of nitric oxide by electrochemical sensors--from dream to reality Front Biosci 2004;9: 3434-3446.

29. Zhang X, Cardosa L, Broderick M, Fein H, and Lin J. An integrated nitric oxide sensor based on carbon fiber coated with selective membranes Electroanalysis 2000;12: 1113-1117.

30. Lantoine F, Trevin S, Bedioui F, and Devynck J. Selective and Sensitive Electrochemical Measurement of Nitric-Oxide in Aqueous-Solution - Discussion and New Results Journal of Electroanalytical Chemistry 1995;392: 85-89.

31. Mitchell KM, and Michaelis EK. Multimembrane carbon fiber electrodes for physiological measurements of nitric oxide Electroanalysis 1998;10: 81-88.

32. Peng Y, Hua C, Zhenga D, and Hu S. A sensitive nitric oxide microsensor based on PBPB composite film-modified carbon fiber microelectrode Sensors and Actuators B: Chemical 2008;133: 571-576.

CHAPTER III

DETECTION AND QUANTIFICATION OF NITRIC OXIDE RELEASED FROM LIVE CELLS

3.1 Introduction

NO is produced by various cell types through activation of the different isoforms of nitric oxide synthase enzyme in an NADPH dependant pathway. As explained in chapter I and II, NO plays key roles in various biological systems in a concentration-dependant manner. The fluctuation of NO concentration in biological systems can yield to a range of disorders. Lower production of NO plays a role in hypertension [1, 2], impotence [3, 4], hyperglycemia, arteriosclerosis [5, 6], Parkinson's disease, and Alzheimer's disease [9]. On the other hand, excessive production of NO contributes to rheumatoid arthritis [10], reperfusion injury [11, 12], septic shock [13], immune type diabetes [14], neurotoxicity (associated with aneurysm) [15], and hypotention [16]. Understanding of many biological processes, which are associated with NO function,

would greatly benefit from the ability to analyze NO release from cells or tissues. Measurement of NO in intact live cells provides more relevant knowledge of their physiological function than biochemical assays carried out with purified molecules in test tubes. Thus, measuring and quantifying the amount of NO production in biological systems and matrices may be vital in elucidating physiological and pathological processes related to NO production and release. However, due to low NO concentration produced *in vivo* and its high reactivity, the direct detection of NO in biological systems is a challenging task [17, 18].

Currently available analytical techniques for analyzing NO include chemiluminescence, electron paramagnetic resonance (EPR) spectroscopy, combining capillary electrophoresis (CE) with the detection of laser-induced fluorescence (LIF), and electrochemisty. As described in chapter I, in the chemiluminescence technique, NO needs to react with ozone or hydrogen peroxide, which are toxic to cells [19]. Due to the low special resolution, the EPR method also tends to be disadvantageous for real time NO measurements [20, 21]. In florescence analysis, increase in florescence inside the cells is taking account for NO measurements [22-24]. The electrochemical techniques is easily amendable to use in NO detection in live single cells in real time with sufficient special and temporal resolution.

In the recent bioscience research environment, the usefulness and versatility of cellular analysis has gained great interest. A number of indirect methods are available to detect NO at the single cell level by analyzing reactants, cofactors, and products of NOS

reaction. However, electrochemical methods provide simple and sensitive approaches that can be applied at the cellular levels. In this work we discuss the use of our Ru-PEDOT-Ru modified electrochemical sensors to monitoring NO released from mouse embryonic fibroblast cells as well as from an isolated single human umbilical vein endothelial cells.

3.2 Experimental Section

3.2.1 Chemicals and reagents

Mouse embryonic fibroblast cell culture (NIH/3T3) and human umbilical vein endothelial cells (HUVEC) were obtained from (ATCC, VA, USA). Dulbecco's modified Eagle's medium with L-glutamine, glucose, and sodium bicarbonate (DMEM), trypsin, with EDTA solution, and F-12K medium were obtained from LRI Cleveland Clinic, Cleveland. Bovine calf serum, heparin, endothelial cell growth supplement (ECGS), and fetal bovine serum were purchased from (Sigma-Aldrich, St Louis, MO).

3.2.2 Materials and Apparatus

All the materials for electrochemistry are used as indicated in section 2.2.1 and similar experimental setup and instrumentation is used as outlined in section 2.2.2. Cell experiments were carried out on the stage of Olympus IX 71 inverted microscope, Center Valley, PA.

3.2.3 Cell Culture Preparation

Mouse embryonic fibroblast cell cultures (NIH/3T3) were grown in Dulbecco's modified Eagle's medium with 4 mM L-glutamine, 4.5 g/L glucose, 90% bovine calf serum and adjusted to contain 1.5 g/L sodium bicarbonate. The medium was renewed every 2 days until confluence (4-5 days) and cell cultures were split in small dishes (35 x 10 mm). The cells were then rinsed with 0.25% (w/v) trypsin 0.53 mM EDTA solution and detached by incubating in trypsin-EDTA for 5-10 minutes at room temperature. The cell suspensions were then transferred to new cell culture dishes and allowed to grow at 37 ^{o}C in the presence of 5% CO_2 in a humidified environment. Cells were washed with PBS buffer and experiments were performed in PBS at room temperature.

Human umbilical vein endothelial cells (HUVEC) were grown in F-12K medium and 0.1 mg/ml heparin and 0.03-0.05 mg/ml endothelial cell growth supplement (ECGS) were added to the base medium and adjusted to a final concentration of 10% fetal bovine serum.

3.2.4 Cell Experiment Setup

The experimental setup for cell stimulation is shown in Figure 3.1. Prior to the experiment, the culture medium is removed and adherent cells are incubated with PBS buffer solution. Our NO microsensor (Ru-PEDOT modified carbon microfiber) is positioned 10-15 μm above the cell surface with the use of a micromanipulator attached

to the stage of an inverted microscope. A potential of +0.5 V vs. Ag/AgCl is then applied to the NO sensor. Once a steady background current is obtained, the stimulator is injected near the cells to stimulate the NO synthesis and release. Figure 3.2 shows a sketch of the setup near a cell surface and shows NO released in the microvolume above the cell and its capture at the electrode surface.

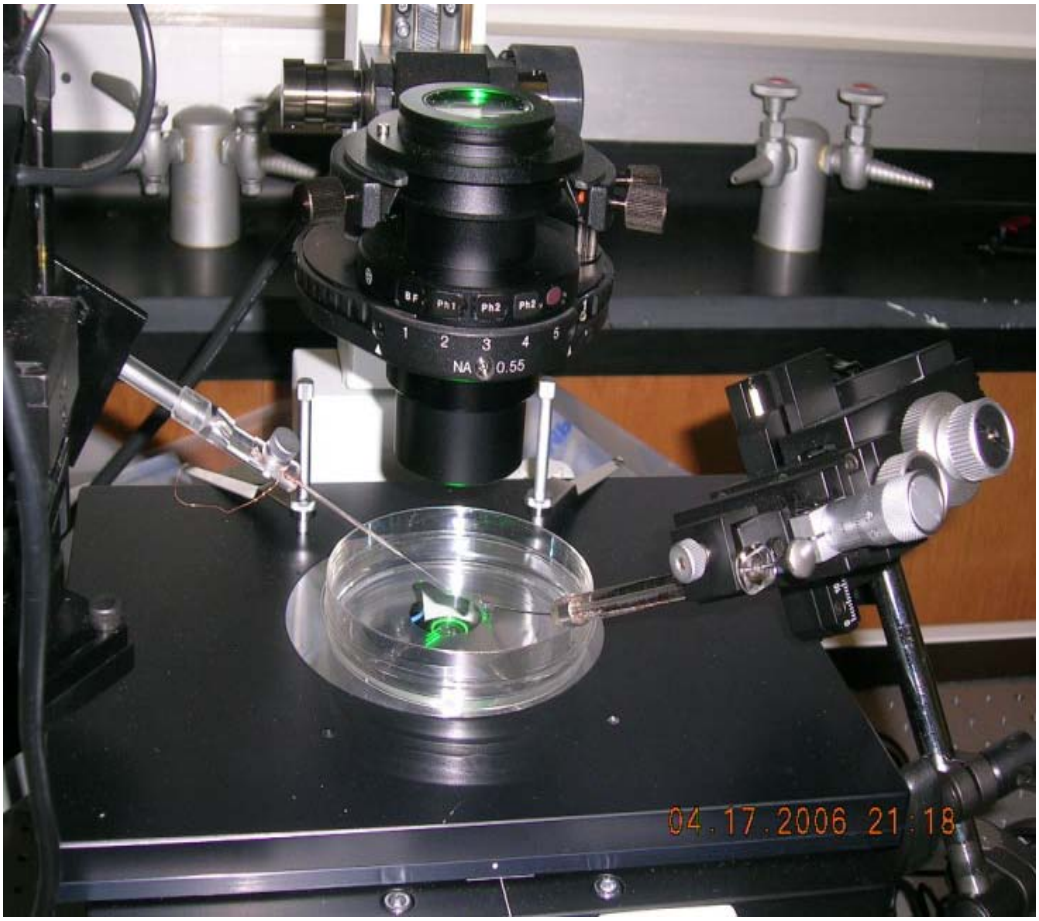

.

Figure 3.1. The experimental setup used for cell analysis.

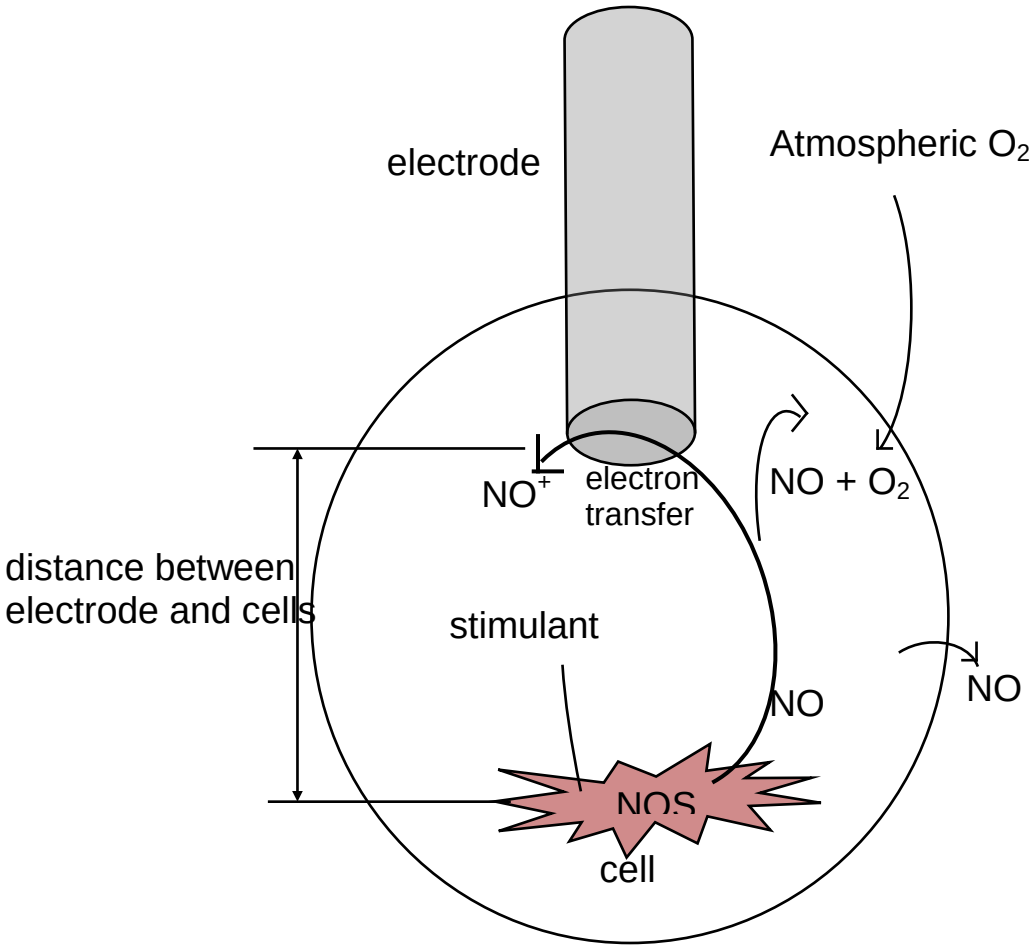

Figure 3.2. Sketch showing the fate of NO released from cells, into a micro-volume of buffer solution and its capture by oxidation at the NO-sensor. Adapted from ref. [8] .

3.3 Results and Discussion

3.3.1 NO released from mouse embryonic fibroblast cells

The potential role of mouse embryonic fibroblast cells in nonspecific host defense and inflammation can be evaluated by analyzing the pathways that regulate NO production [16]. Lipopolysaccharide (LPS) and IFN-γ are major activators of the transcription factor NF-κB, which plays a pivotal role in the regulation of the inducible NOS (iNOS) gene expression induced by inflammatory mediators [25].

Analysis of NO production in fibroblasts may provide an understanding of their potential role in host defense and inflammatory disorders. Indirect measurements of NO in mouse fibroblasts have been reported and involve mainly nitrite quantification [16]. In this work, we investigate the capability of using our sensor to detect NO released from stimulated mouse fibroblasts. The bacterial endotoxin LPS is used as the stimulant due to its ability to activate the iNOS-signaling pathway. LPS is a large molecule consisting of a lipid and a polysaccharide part (carbohydrate) bound together with covalent bond as shown in Figure 3.3.

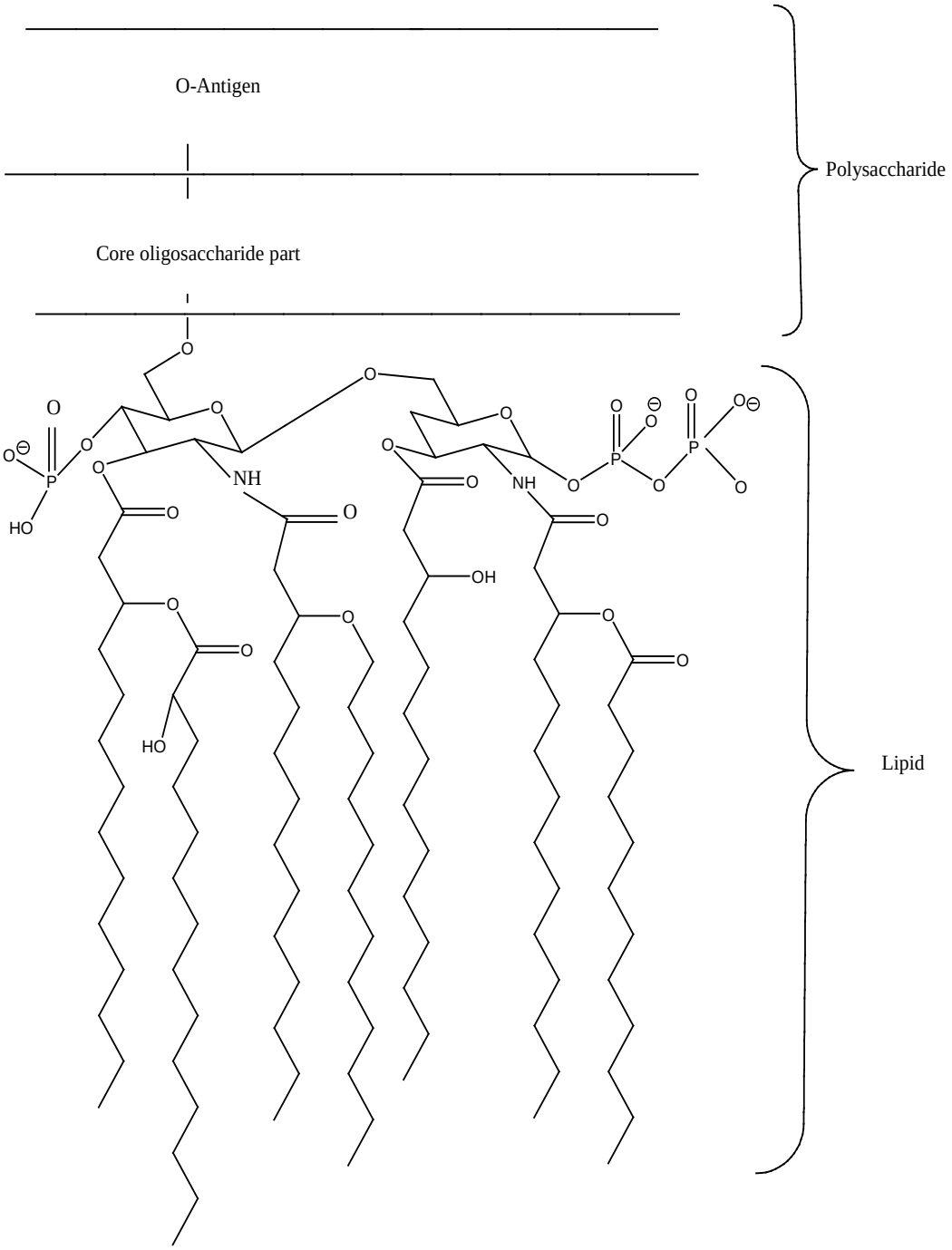

Figure 3.3 The shamatic diagram showing the structure of Lipopolysaccharide (LPS).

The iNOS expression cascade upon stimulation with LPS and IFN-γ in macrophage-like cell-lines is represented in Figure 3.4. LPS and IFN-γ have synergistic effect on iNOS expression. Onced expressed, iNOS converts L-arginine to L-citrulline and NO.

As described in section 3.2.3, the NO microsensor is positioned 5-10 μm above the surface of collection of cells. Once a steady background current is obtained, 50 μg/ml LPS is injected near the population of cells (5.0×10^5 cells/ml) to stimulate NO synthesis and release.

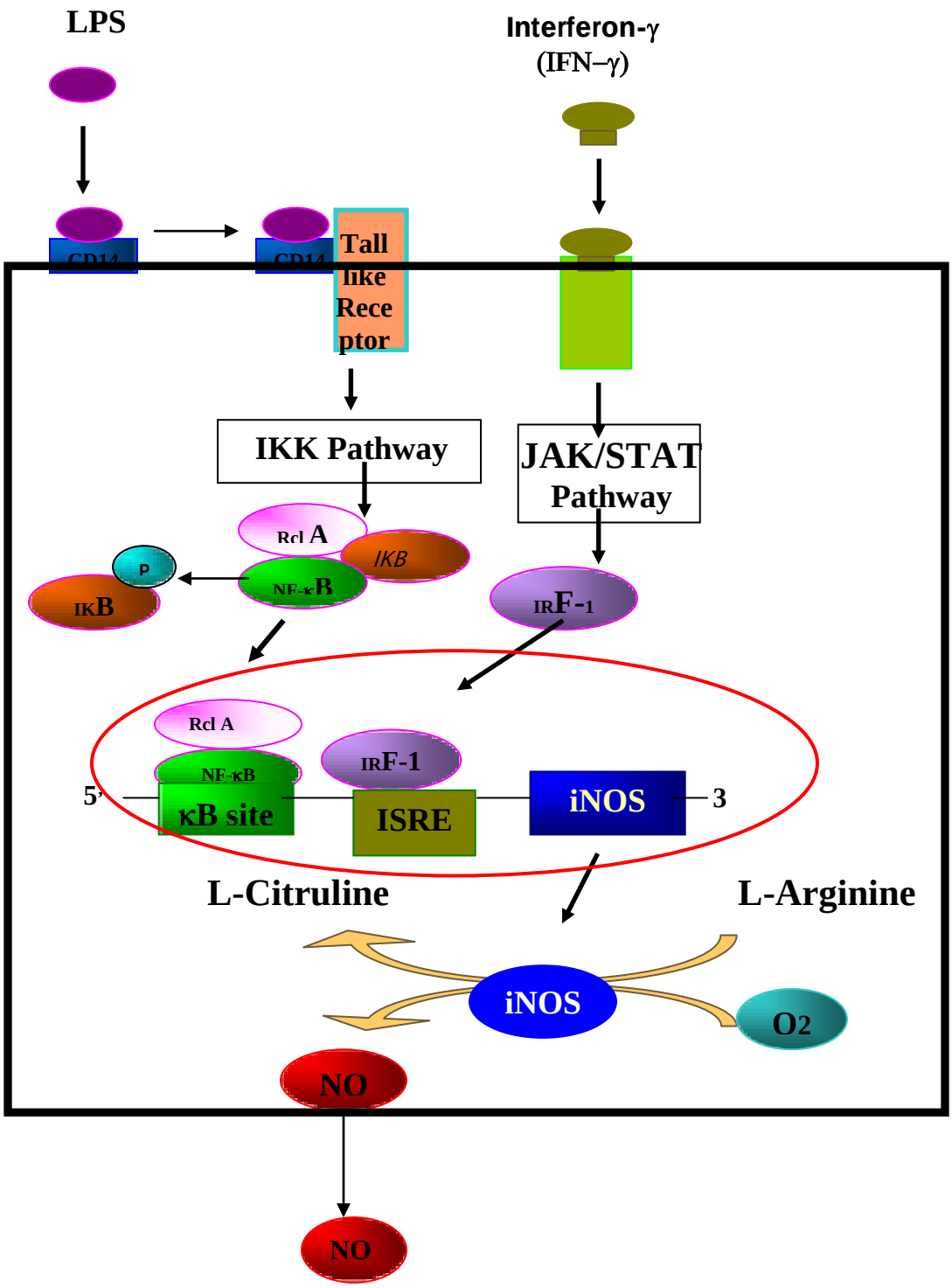

Figure 3.4. Schematic diagram of iNOS expression cascade by stimulation with lipopolysaccharide and IFN-γ. Reprinted from ref. [7].

After carefully injecting 50 μg/ml of LPS close to the cells, the changes in current signal were monitored as a function of time. A typical current-time plot obtained is shown in Figure 3.5. We observed a change in current immediately after the addition of LPS. To make sure that the NO released comes from LPS-induced iNOS cascade, the cells were treated with non-specific nitric oxide synthase (NOS) inhibitor, N^G-nitro-L-arginine methylester (L-NAME) (shown in Figure 3.6), prior to the experiment. The L-NAME inhibits the synthesis of NO by blocking the active site of iNOS.

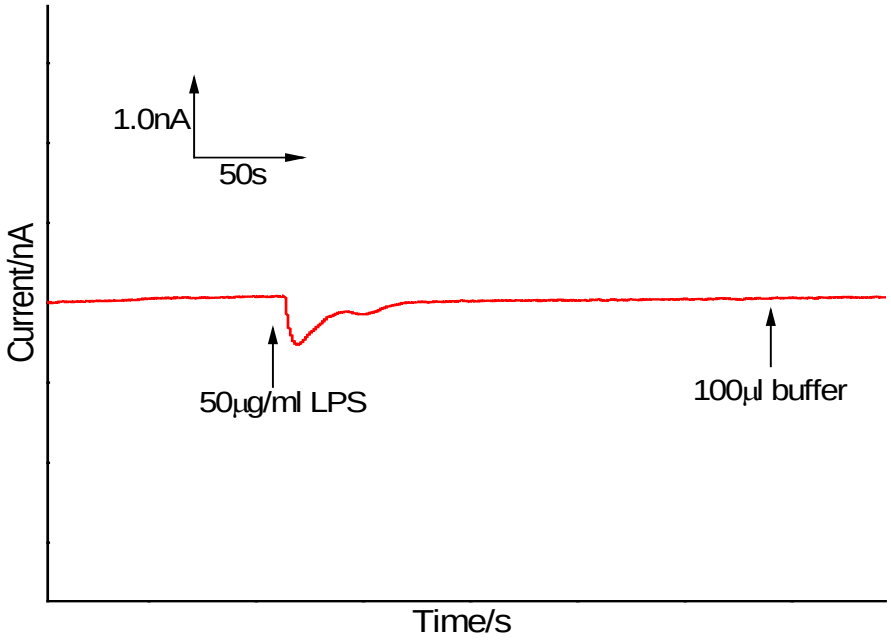

Figure 3.5. Amperometric response of our NO sensor after stimulation of NO synthesis by addition of LPS to the mouse embryonic fibroblast cell culture.

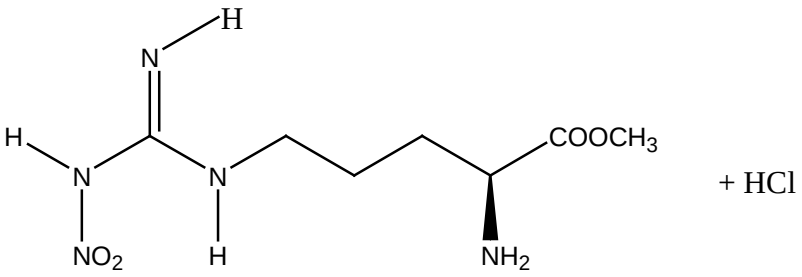

Figure 3.6. Structure of nitric oxide synthase (NOS) inhibitor, N^G-nitro-L-arginine methylester (L-NAME).

Control experiments were carried out to confirm that the response observed in Figure 3.6 is due to NO released from fibroblast cells. To check that the injection process itself does not cause the current change, an equivalent volume (100 μl) of phosphate buffer (PBS) is injected into the solution close to the cells in lieu of LPS; no significant change in the background current is observed, Figure 3.6. As such, cells were treated with L-NAME prior to LPS stimulation; as shown in Figure 3.7, no response in current was observed after LPS stimulation. Another control experiment was carried out to check whether the current observed is a result of mere redox activity of LPS. As shown in Figure 3.8, there was no response of the current when LPS is injected into buffer solution in the absence of fibroblast cells. Figure 3.9 summarizes the responses of the NO sensor after addition of LPS to the collection of cells, L-NAME treated cells, and to the buffer solution.

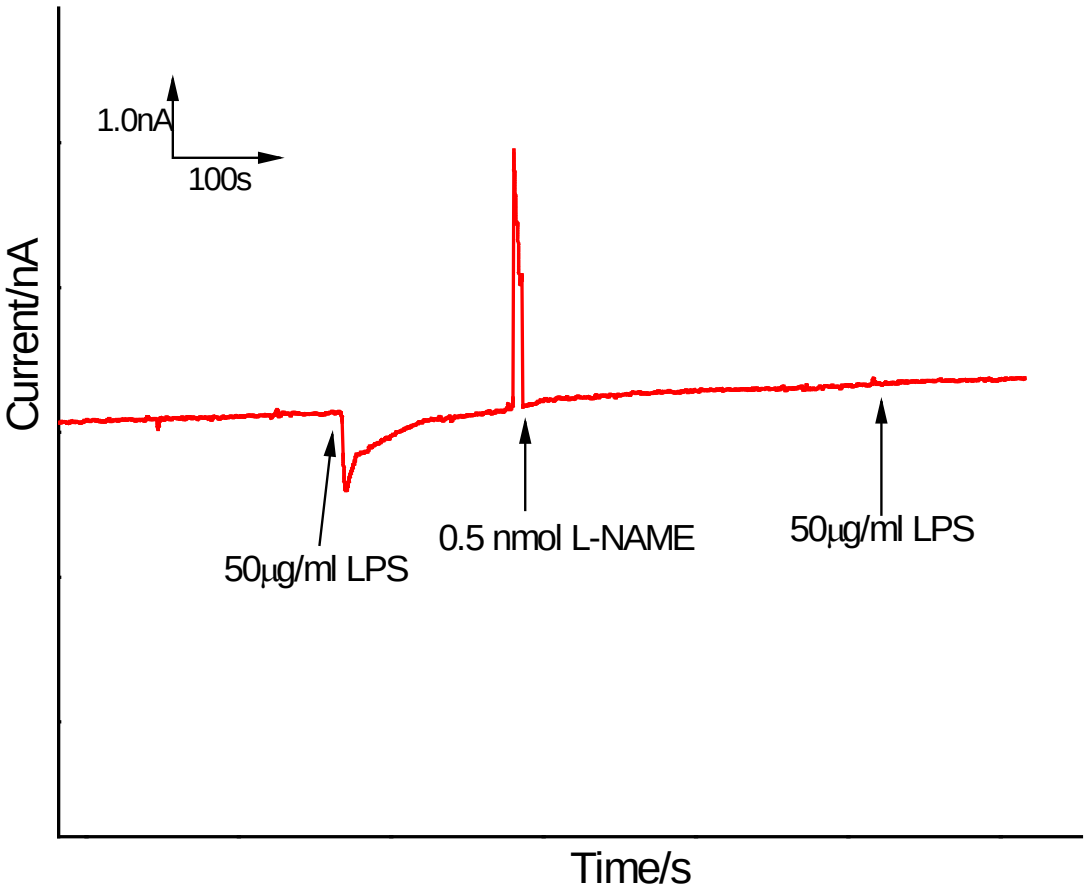

Figure 3.7. Amperometric response of our NO sensor after addition of LPS to the cell culture before and after L-NAME inhibition.

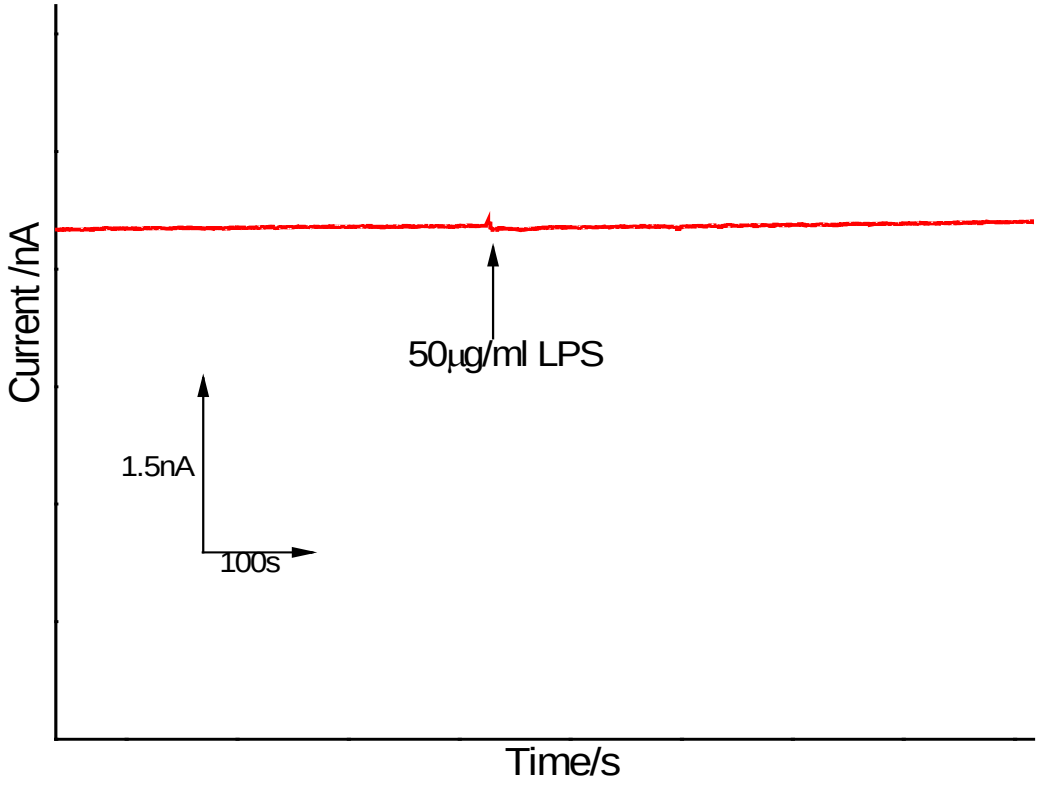

Figure 3.8 Amperometric response of our NO sensor after addition of LPS to the PBS solution.

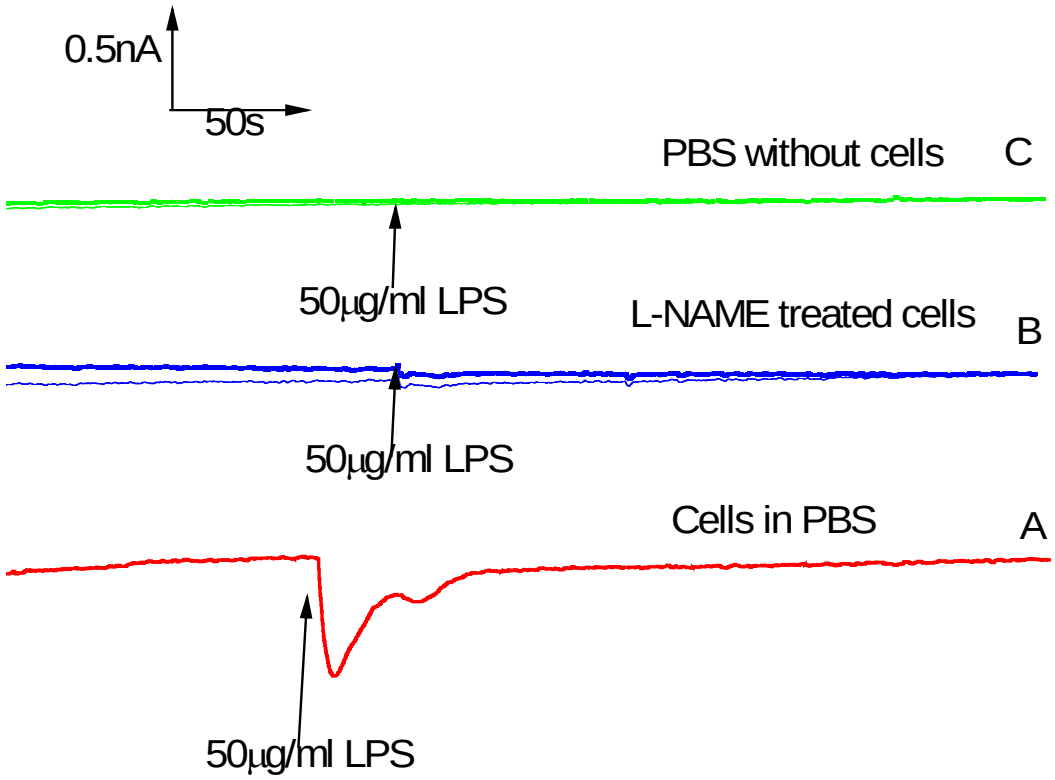

Figure 3.9. Amperometric response of our NO sensor after addition of LPS to the cell culture (A) L-NAME pretreated cells (B) and buffer solution. (C).

Together, these experiments and controls confirm that the response of the electrode observed after LPS stimulation of the fibroblast cells is due solely to the oxidation of NO released from the cells.

After cell analysis, the Ru-PEDOT-Ru NO sensor was calibrated in the same experimental conditions, by adding NO standard solutions *in situ* as detailed previously (Chapter II, section 2.3.3). The sensitivity achieved for NO concentration ranges of 0.01 μM to 0.4 μM is 17.58 pA/nM (shown in Figure 3.10). The sensitivity of electrode in open system is slightly lower compared to the closed, deoxygenated system (24.46 pA/nM) (Chapter II). The maximum current measured was equivalent to a local NO concentration of 17 ± 6.3 nM (n=5) after stimulation of fibroblast cells by LPS.

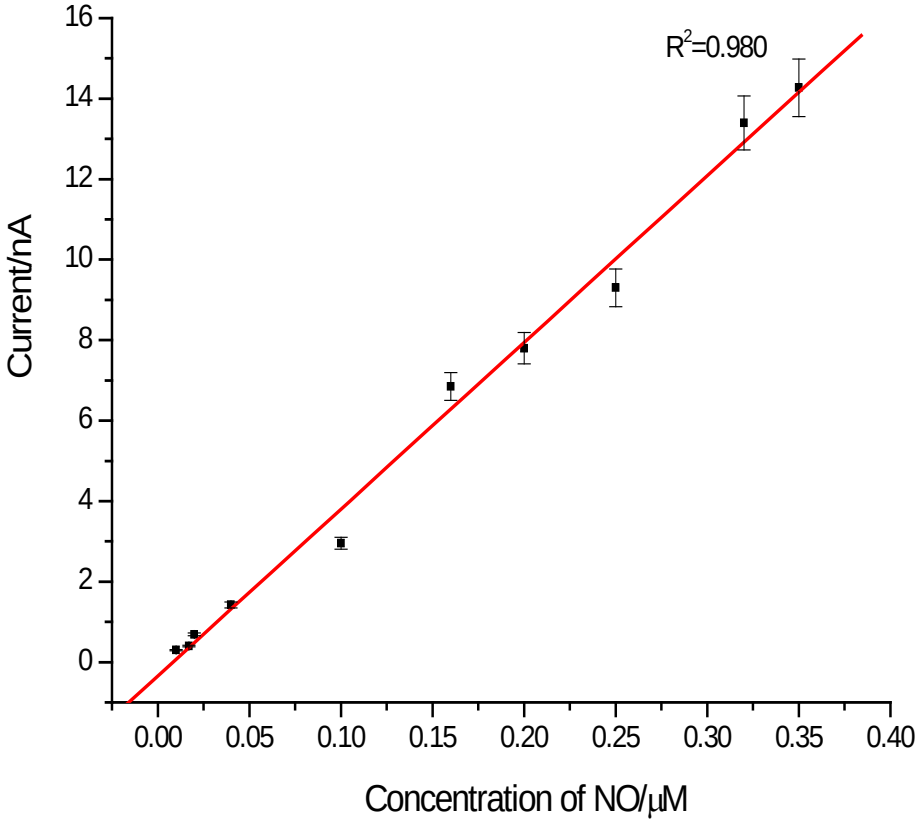

Figure 3.10. Current/NO dose plot for 7-μm Ru-PEDOT-Ru layers modified CFE in cell experiment conditions. Applied potential is +0.5 V *vs* Ag/AgCl.

3.3.2. NO released from Human Umbilical Vein Endothelial cells (HUVEC)

The endothelium that lines the interior surface of blood vessels acts as a highly specialized, metabolically active interface between blood and the underlying tissues; it also maintains vascular tone, counteract platelet adhesion, and immune response. The vascular endothelium responds to various agonists and shears flow by producing nitric oxide [26-28]. The endothelium NO production is catalyzed by a constitutive enzyme called endothelial NOS (eNOS). The change in NO production from eNOS may cause significant effects in biological functions and can signal the onset of various pathological states. Endothelial dysfunction, which is associated with deficiency of NO, occurs in hypertension, ischemia, diabetes, and stroke [29]. As pointed out earlier, high concentration of NO in biological systems is a feature of septic shock and hypotension. It is important to measure and quantify the NO production in biological matrices to elucidate the physiological and pathological processes related to NO production and release.

Our Ru-PEDOT-Ru modified NO microsensor was used to monitor NO released from HUVEC by stimulating them with bradykinin. Bradykinin, shown in Figure 3.11, is an endogenous vasodilator formed of nine amino acid residues released from plasma globulins called kininogens. It can form locally in injured tissue, act in vasodilation of small arterioles, and is considered to play a part in inflammatory processes.

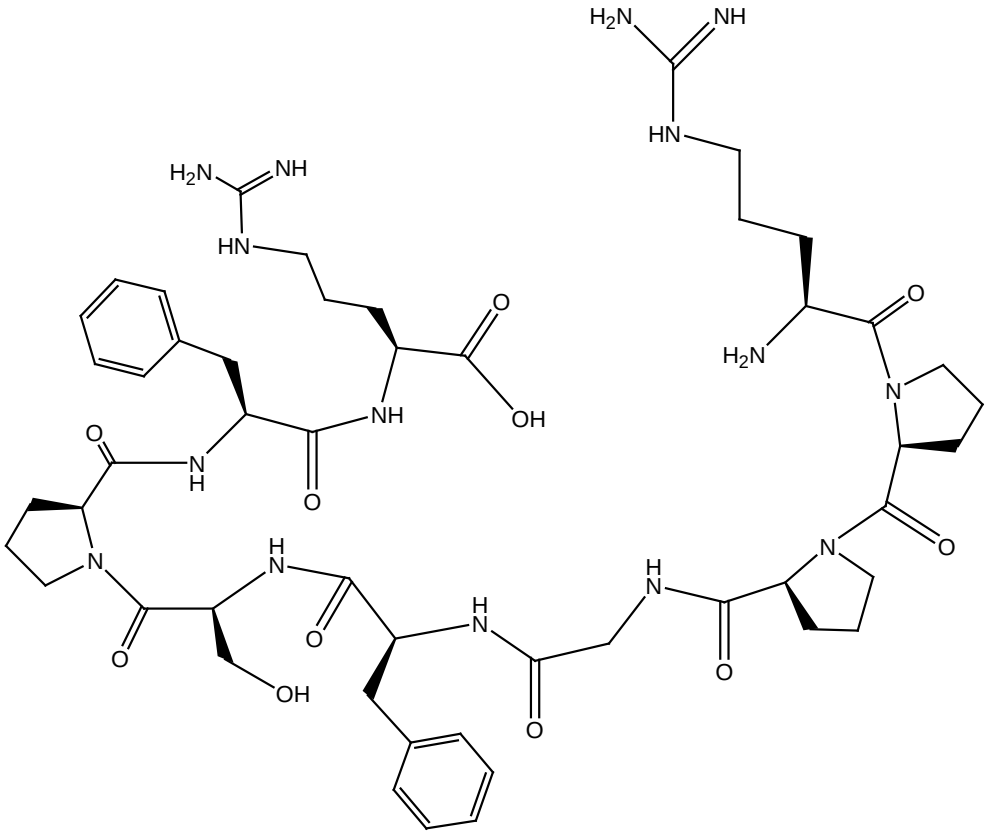

Figure 3.11. The structure of bradykinin.

Different agonist such as acetylcholine, bradykinin, and histamine can activate the endothelial NOS (eNOS) via a calmodulin-dependent pathway. The increase in intracellular Ca^{2+} concentration causes the release of NO within a second upon stimulation [30]. Endothelial NOS stimulation pathway is shown in Figure 3.12.

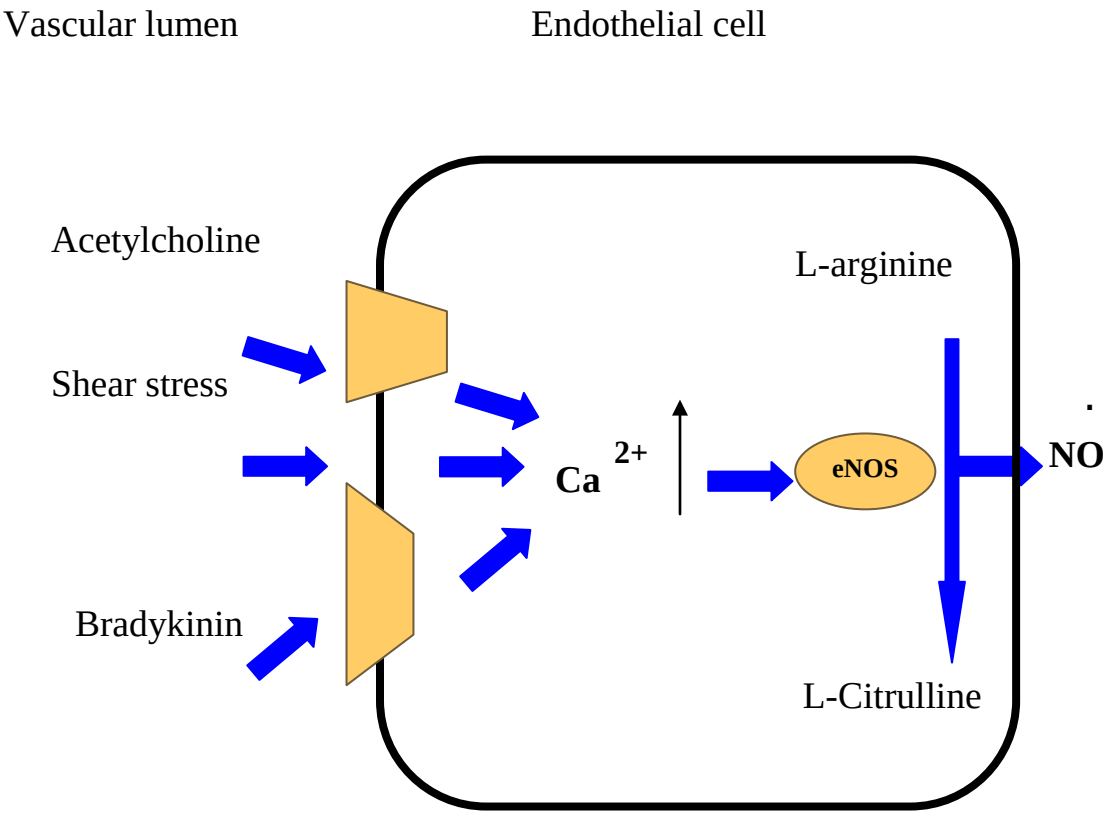

Figure 3.12. Substrate and cofactor requirements for nitric oxide (NO) synthase activation [31].

HUVEC cells (4.8 x 10^5 cells/ml) are incubated with PBS buffer solution and our NO microsensor is positioned as explained in part 3.1.4. The background current is then allowed to stabilize at an applied potential of +0.5 V vs. Ag/AgCl. NO release is stimulated using bradykinin, which is injected in the vicinity of the cell surface.

Figure 3.13 shows the amount of bradykinin-response curve of the NO release. The current response gradually increased when the amount of bradykinin increased from 0.1-0.5 μmol. A plateau was reached at the amount of bradykinin higher than 0.5 μmol.

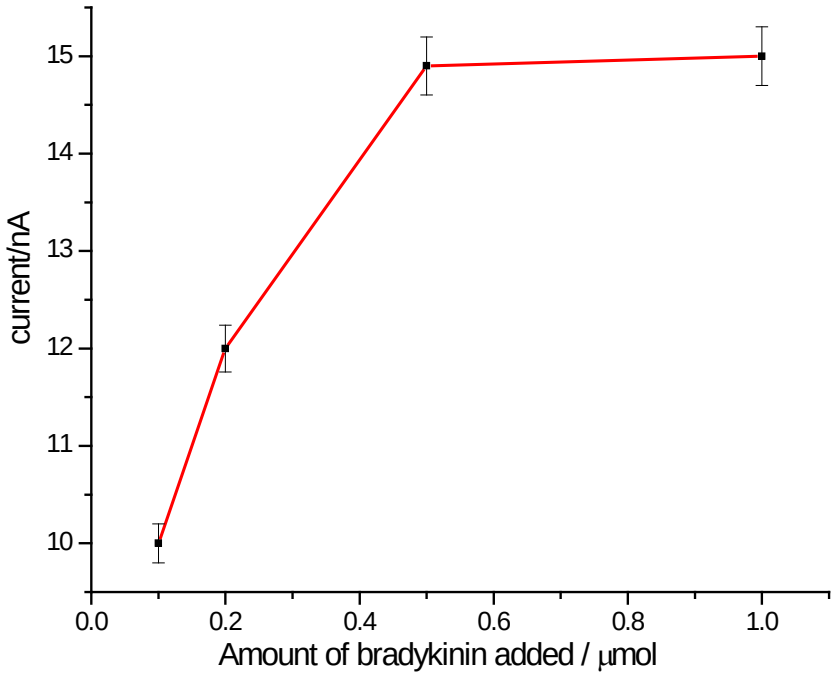

Figure 3.13. Current-response for NO released from HUVEC with different amounts of bradykinin stimulation.

The concentration of NO released by varying the bradykinin amount is shown in Figure 3.14. Since there is no change in current response (and NO release) with amounts of higher than 0.5 μmol bradykinin, this amount was used for the stimulation processes.

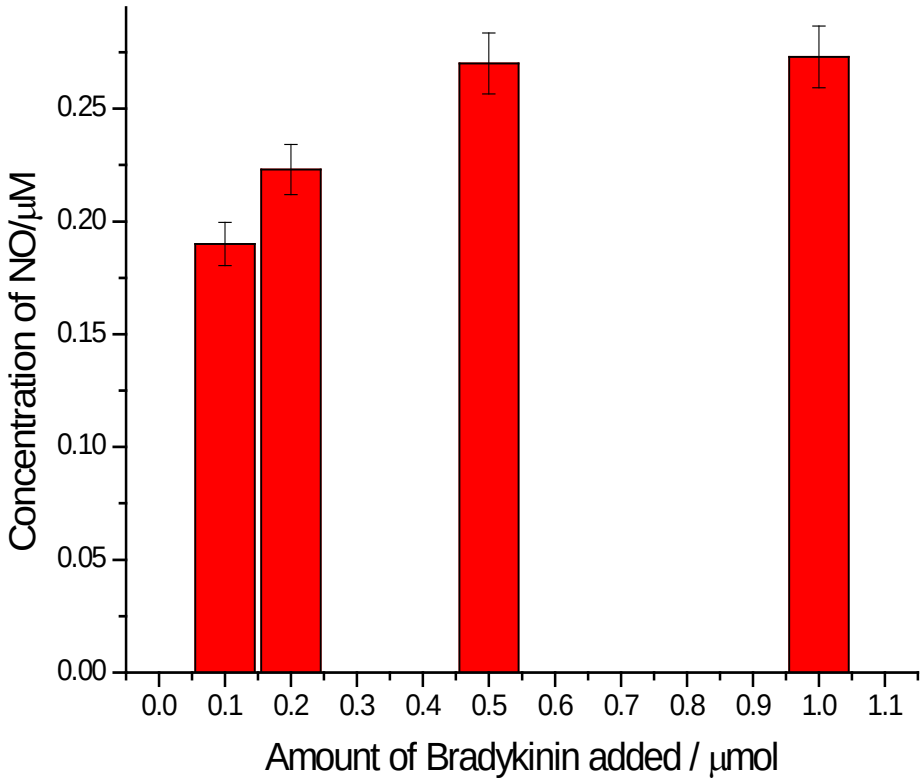

Figure 3.14. Change in concentration of NO released with the varying amount of bradykinin.

Injection of 0.5 μmol of bradykinin near the HUVEC cell surface induces a rapid and transient redox current reaching a peak within 20 s, Figure 3.15. Addition of 0.5μmol bradykinin increased the local NO concentration at the surface of collection of cells to nearly 300 nM, with maintenance of these high NO levels for ~2 min. This response is typical even when cells were repeatedly stimulated with bradykinin.

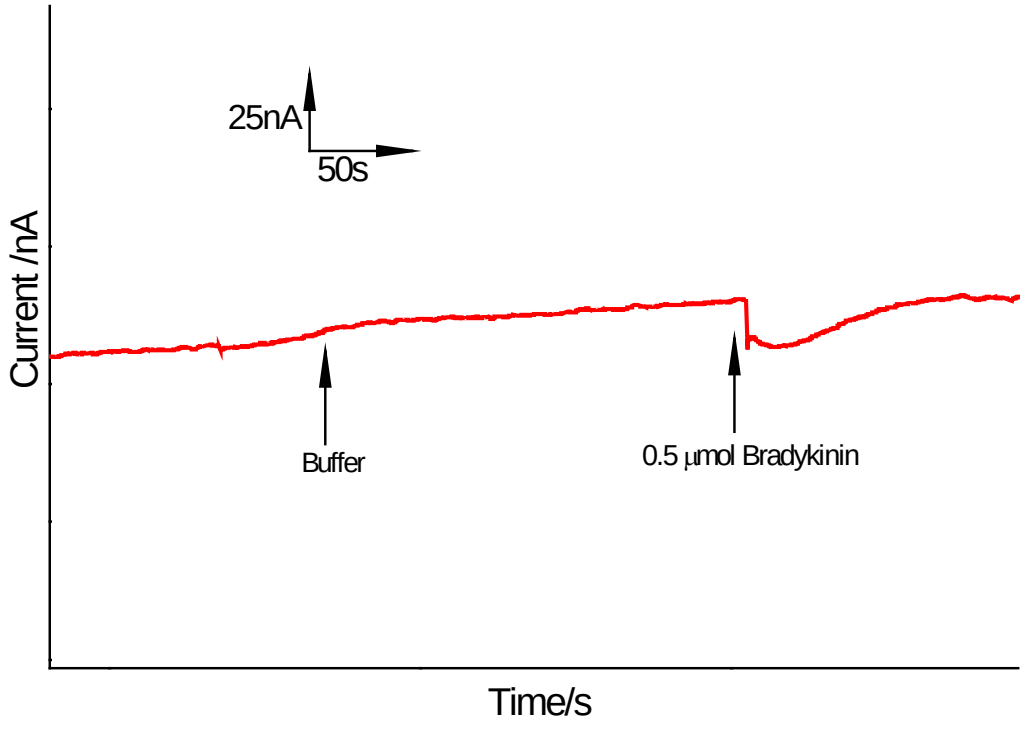

Figure 3.15. Amperometric response of our NO sensor upon addition of bradykinin to HUVEC cells.

As a control, injection of a phosphate buffer close to the cells does not result in a significant change in the background current (Figure 3.15). Similarly, the typical peak response is not observed when bradykinin is injected into buffer solution in the absence of the cells, Figure 3.16. Another negative control was performed in the presence of the NOS inhibitor, L-NAME. Incubation of the HUVEC cells with L-NAME for 5-10 minutes prior to bradykinin stimulation shows no significant change in background current at our NO microsensor as shown in Figure 3.17. Together, these results suggest that the observed current change is due to the oxidation of the NO released from the cells.

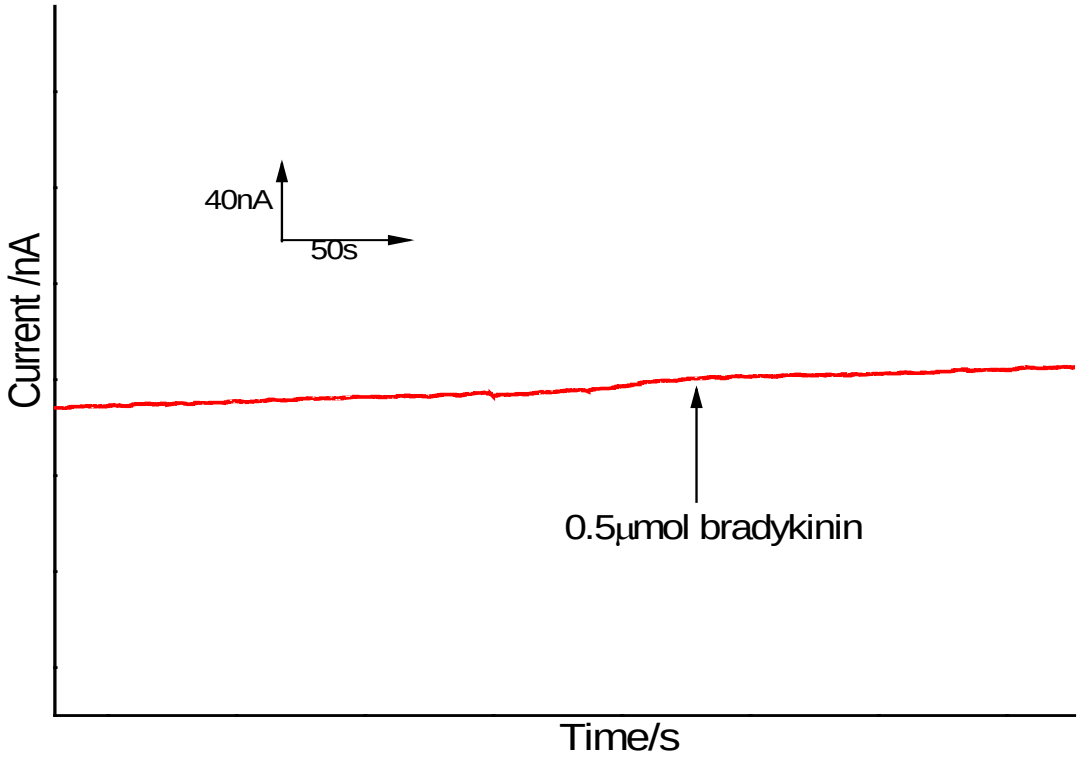

Figure 3.16. Amperometric response of our NO sensor upon addition of bradykinin to the buffer solution in the absence of cells.

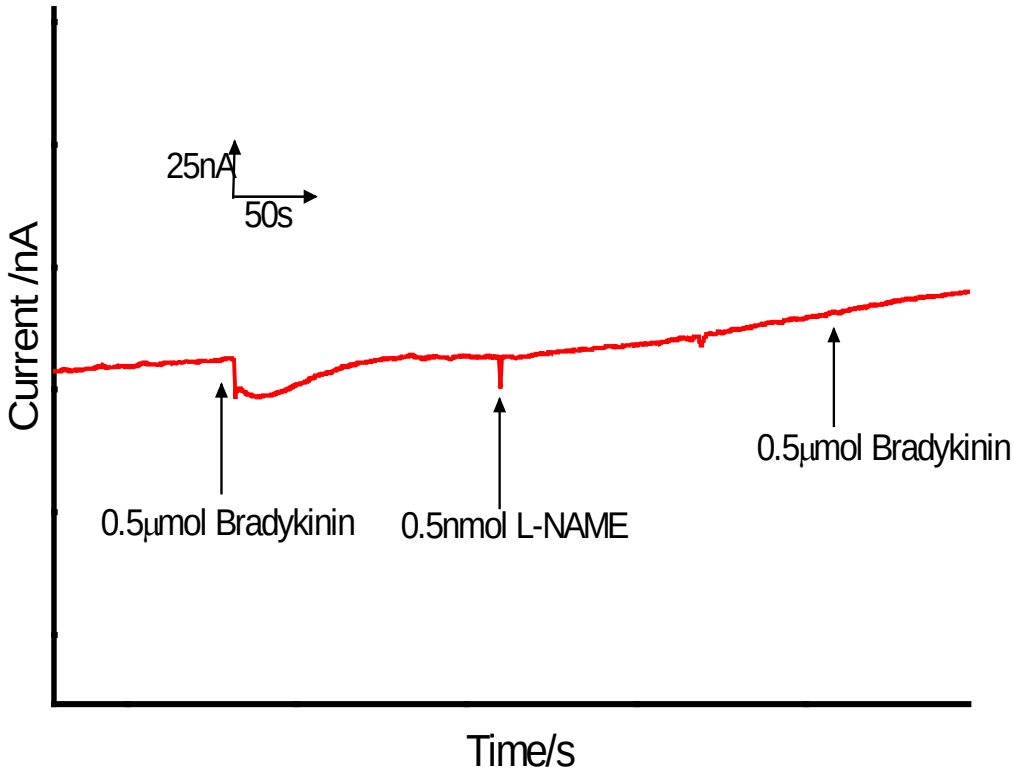

Figure 3.17. Amperometric response of our NO sensor upon addition of bradykinin to HUVEC cell culture before and after L-NAME inhibition.

3.3.3 NO detection in an isolated single Human Umbilical Vein Endothelial cells

Measurement of local NO concentration at a single endothelial cell is of particular interest in order to understanding the development and progress of NO-related diseases. Measuring analytes released from live single cells is critical to gaining fundamental understanding of many biological functions. Because of trace amount of NO produced by single cells, highly efficient, sensitive, and selective detection methods are necessary. In this regard, we investigated the performance of our modified sensor for NO detection and quantification at the level of live single human umbilical vein endothelial cell (HUVEC).

The amperometric response of our NO microsensor upon stimulation of single HUVEC cells by bradykinin is shown in Figure 3.18. The bradykinin stimulation of an isolated single cell changed the baseline current by giving 1.97 ± 0.53 nA, which is much less than the change in current observed for a population of cells (ca. 15 nA). Control experiments similar to what was described for the collection of cells were also performed. The response is consistent with the amount of NO released from a single cell as compared to a collection of cells. The NO amounts calculated using Ficks' law shows the ~14.0 attomoles (n=6) of NO produced by a normal single HUVEC cell upon bradykinin stimulation under the conditions described (the detail calculation is repoted in next

section). While the current change recorded is small, it can still be accurately measured with our highly sensitive NO microsensor.

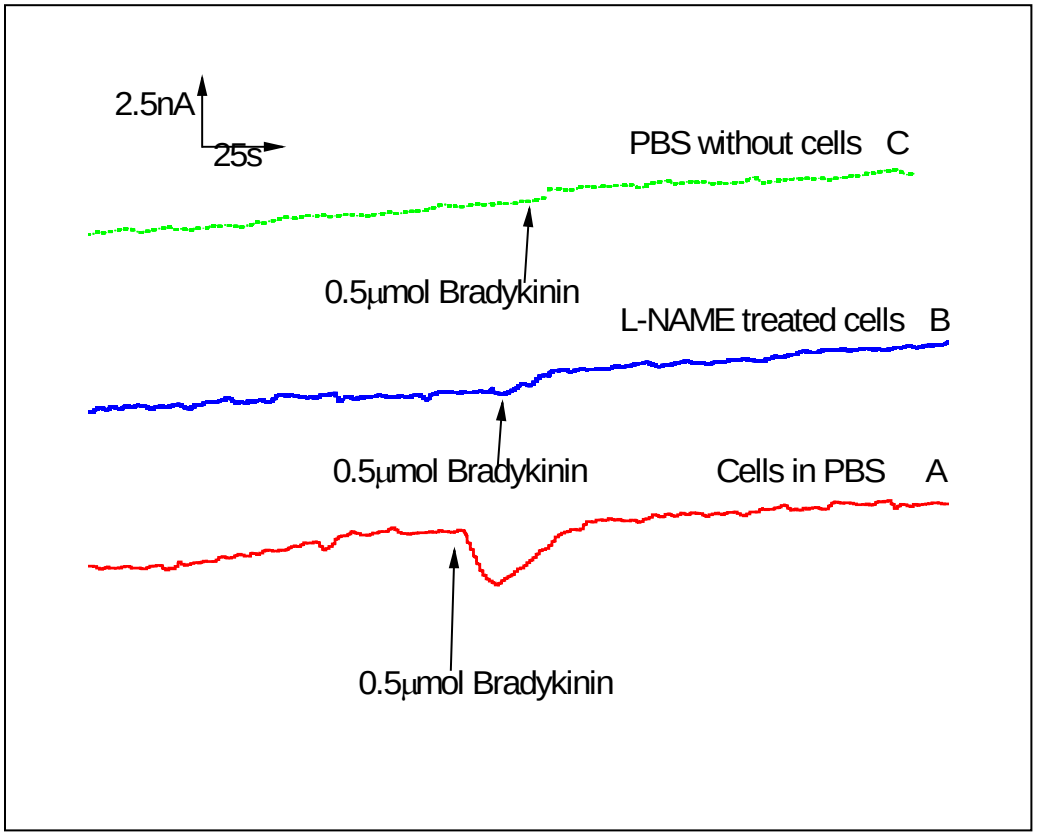

Figure. 3.18. Amperometric response of our NO sensor upon addition of bradykinin to an isolated single cell (A) Same as (A) but with L-NAME pretreated cells (B) Same as (A) but in the absence of cells to the buffer solution (C).

Appendix. Calculation of the amount of NO released from isolated single cell

The theoretical NO diffusion profile from a single cell surface is shown in scheme 3.1.

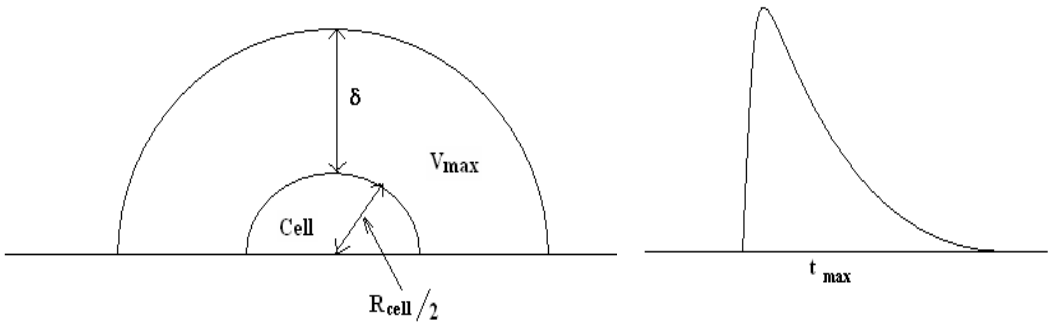

Scheme. 3.1. Schematic diagram showing the NO diffusion from a cell surface.

The amount of NO released from a single cell can be calculated using Einstein-Smoluchowski diffusion equation [32] as shown in equation 3.1.

$2Dt_{max} = \delta^2$ Equation 3.1

Where D is the diffusion coefficient, t_{max} is the time and δ is the radial distance from the cell surface.

The following assumptions are used in our calculations:

(i) Diffusion and resulting diffusion currents are governed by Fick's Laws (i.e. only concentration gradients are involved).

(ii) The diffusion coefficient of NO is constant and not a function of concentration or distance. From the experiment, time (t_{max}) is known and the diffusion coefficient of NO (D_{NO}) is reported [33] as 3300 $\mu m^2 s^{-1}$ hence, the distance from the cell surface can be calculated. Using the diffusion distance (δ), one can derive the maximum diffusion volume of NO ($½V_{max}$).

$$2Dt_{max} = \delta^2$$

$$\text{Mean } D_{NO} = 3300\ \mu m^2 s^{-1}$$

$$\delta = (2D_{NO}t_{max})^{1/2} = (2 \times 3300\ \mu m^2 s^{-1} \times 50s)^{1/2}$$

$$\delta = 0.5 \times 10^{-3}\ m$$

$$V_{max} = V_{total} - V_{cell}$$

Where, V_{total} is the total volume and the V_{cell} is the volume of cell.

Based on the typical HUVEC dimentions;

$$V_{max} = (4/3)*\pi\ (0.5 \times 10^{-3}\ m + 5x10^{-6}m)^3 - (4/3)*\pi\ (5x10^{-6}m)^3$$

$$V_{max} = 2.722 \times 10^{-13}\ m^3$$

$$½V_{max} = 1.36 \times 10^{-13}\ m^3$$

The diffusion volume of NO released from the single cell is therefore: $V = 1.36 \times 10^{-10}$ L

The average current response = 1.97 ± 0.53 nA (n=6); our standard calibration curve in the same experimental conditions gives a corresponding NO concentration of ~0.1μM; therefore the number of moles of NO is captured at the electrode surface is:

moles NO = 0.1×10^{-6} $molL^{-1} \times 1.36 \times 10^{-10}$ L

= 13.6×10^{-18} mol

= ~14.0 attomoles

It is a great advantage to know the range of NO amounts produced in normal endothelial cells to identify the diseases in early stages that are associated with NO [29].

3.4. Summary of Chapter III

The results demonstrate that the performance of our Ru-PEDOT-Ru NO sensor is great for quantitative and real-time analysis of NO release from live cells. The NO sensor allowed us to monitor NO synthesis and release from cultured mouse embryonic fibroblast cells, cultured human umbilical vein endothelial cells (HUVEC), and from single HUVEC cells. The calculations show the amount of NO released from an isolated healthy HUVEC is ~14.0 attomoles, which may be used as the set value for the early determination of disease status that correlates with NO. These direct analysis performance of the modified NO sensor allows us to measure NO released from NOS entrapped in liposomes as described in Chapter IV.

3.5. References

1. Johnson, R.A., and Freeman, R.H. (1992). Sustained hypertension in the rat induced by chronic blockade of nitric oxide production. Am J Hypertens *5*, 919-922.
2. Lahera, V., Salazar, J., Salom, M.G., and Romero, J.C. (1992). Deficient production of nitric oxide induces volume-dependent hypertension. J Hypertens Suppl *10*, S173-177.
3. Brock, G., Nunes, L., Padma-Nathan, H., Boyd, S., and Lue, T.F. (1993). Nitric oxide synthase: a new diagnostic tool for neurogenic impotence. Urology *42*, 412-417.
4. McGuffey, E. (1993). Can nitric oxide be used to treat impotence? Am Pharm *NS33*, 20.
5. Koglin, J., Glysing-Jensen, T., Mudgett, J.S., and Russell, M.E. (1998). Exacerbated transplant arteriosclerosis in inducible nitric oxide-deficient mice. Circulation *97*, 2059-2065.
6. Weis, M., Kledal, T.N., Lin, K.Y., Panchal, S.N., Gao, S.Z., Valantine, H.A., Mocarski, E.S., and Cooke, J.P. (2004). Cytomegalovirus infection impairs the nitric oxide synthase pathway: role of asymmetric dimethylarginine in transplant arteriosclerosis. Circulation *109*, 500-505.
7. Kamei, K., Mie, M., Yanagida, Y., Aizawa, M., and Kobatake, E. (2004). Construction and use of an electrochemical NO sensor in a cell-based assessing system Sensors and Actuators B *99* 106-112.

8. Hengstenberg, A., Blochl, A., Dietzel, I.D., and Schuhmann, W. (2001). Spatially Resolved Detection of Neurotransmitter Secretion from Individual Cells by Means of Scanning Electrochemical Microscopy. Angew Chem Int Ed Engl *40*, 905-908.

9. Dawson, T.M., and Dawson, V.L. (1996). Nitric oxide synthase: role as a transmitter/mediator in the brain and endocrine system. Annu Rev Med *47*, 219-227.

10. Choi, J.W. (2003). Nitric oxide production is increased in patients with rheumatoid arthritis but does not correlate with laboratory parameters of disease activity. Clin Chim Acta *336*, 83-87.

11. Moncada, S., Radomski, M.W., and Palmer, R.M. (1988). Endothelium-derived relaxing factor. Identification as nitric oxide and role in the control of vascular tone and platelet function. Biochem Pharmacol *37*, 2495-2501.

12. Erdogan, H., Fadillioglu, E., and Emre, M.H. (2006). Protection from renal ischemia reperfusion injury by an endothelin-A receptor antagonist BQ-123 in relation to nitric oxide production. Toxicology *228*, 219-228.

13. Martinez, C., Juarranz, Y., Abad, C., Arranz, A., Miguel, B.G., Rosignoli, F., Leceta, J., and Gomariz, R.P. (2005). Analysis of the role of the PAC1 receptor in neutrophil recruitment, acute-phase response, and nitric oxide production in septic shock. J Leukoc Biol *77*, 729-738.

14. Pieper, G.M. (1998). Review of alterations in endothelial nitric oxide production in diabetes: protective role of arginine on endothelial dysfunction. Hypertension *31*, 1047-1060.

15. Johanning, J.M., Franklin, D.P., Han, D.C., Carey, D.J., and Elmore, J.R. (2001). Inhibition of inducible nitric oxide synthase limits nitric oxide production and experimental aneurysm expansion. J Vasc Surg *33*, 579-586.

16. Lavnikova, N., and Laskin, D.L. (1995). Unique patterns of regulation of nitric oxide production in fibroblasts. J Leukoc Biol *58*, 451-458.

17. Wang, S., Paton, J.F., and Kasparov, S. (2006). The challenge of real-time measurements of nitric oxide release in the brain. Auton Neurosci *126-127*, 59-67.

18. Kiechle, F.L., and Malinski, T. (1996). Indirect detection of nitric oxide effects: a review Annals of Clinical and Laboratory Science *26*, 501-511.

19. Leone, A.M., Furst, V.W., Foxwell, N.A., Cellek, S., and Moncada, S. (1996). Visualisation of nitric oxide generated by activated murine macrophages. Biochem Biophys Res Commun *221*, 37-41.

20. Yoshimura, T., Yokoyama, H., Fujii, S., Takayama, F., Oikawa, K., and Kamada, H. (1996). In vivo EPR detection and imaging of endogenous nitric oxide in lipopolysaccharide-treated mice. Nat Biotechnol *14*, 992-994.

21. Vasquez-Vivar, J., Martasek, P., Hogg, N., Karoui, H., Masters, B.S., Pritchard, K.A., Jr., and Kalyanaraman, B. (1999). Electron spin resonance spin-trapping detection of superoxide generated by neuronal nitric oxide synthase. Methods Enzymol *301*, 169-177.

22. Nakatsubo, N., Kojima, H., Sakurai, K., Kikuchi, K., Nagoshi, H., Hirata, Y., Akaike, T., Maeda, H., Urano, Y., Higuchi, T., and Nagano, T. (1998). Improved nitric oxide detection using 2,3-diaminonaphthalene and its application to the

evaluation of novel nitric oxide synthase inhibitors. Biol Pharm Bull *21*, 1247-1250.

23. Lim, M.H., Wong, B.A., Pitcock, W.H., Jr., Mokshagundam, D., Baik, M.H., and Lippard, S.J. (2006). Direct nitric oxide detection in aqueous solution by copper(II) fluorescein complexes. J Am Chem Soc *128*, 14364-14373.

24. Ye, X., Rubakhin, S.S., and Sweedler, J.V. (2008). Detection of nitric oxide in single cells. Analyst *133*, 423-433.

25. Blackwell, T.S., Blackwell, T.R., Holden, E.P., Christman, B.W., and Christman, J.W. (1996). In vivo antioxidant treatment suppresses nuclear factor-kappa B activation and neutrophilic lung inflammation. J Immunol *157*, 1630-1637.

26. Furchgott, R.F., and Zawadzki, J.V. (1980). The obligatory role of endothelial cells in the relaxation of arterial smooth muscle by acetylcholine. Nature *288*, 373-376.

27. Ignarro, L.J., Byrns, R.E., Buga, G.M., and Wood, K.S. (1987). Endothelium-derived relaxing factor from pulmonary artery and vein possesses pharmacologic and chemical properties identical to those of nitric oxide radical. Circ Res *61*, 866-879.

28. Palmer, R.M., Ferrige, A.G., and Moncada, S. (1987). Nitric oxide release accounts for the biological activity of endothelium-derived relaxing factor. Nature *327*, 524-526.

29. Ignarro, L.J. (2002). Nitric oxide as a unique signaling molecule in the vascular system: a historical overview. J Physiol Pharmacol *53*, 503-514.

30. Nathan, C. (1992). Nitric oxide as a secretory product of mammalian cells. Faseb J *6*, 3051-3064.

31. Ignarro, L.J. (1989). Biological actions and properties of endothelium-derived nitric oxide formed and released from artery and vein. Circ Res *65*, 1-21.

32. Islam, M.A. (2004). Einstein–Smoluchowski Diffusion Equation: A Discussion. Physica Scripta. *70*, 120-125.

33. Malinski, T., Taha, Z., Grunfeld, S., Patton, S., Kapturczak, M., and Tomboulian, P. (1993). Diffusion of Nitric-Oxide in the Aorta Wall Monitored in-Situ by Porphyrinic Microsensors. Biochemical and Biophysical Research Communications *193*, 1076-1082.

CHAPTER IV

THE NOS-LOADED LIPOSOME AS A PLATFORM FOR THE TREATMENT OF NO/NOS DEFICIENT TARGETS

4.1. Introduction

As explained in Chapter I, nitric oxide (NO) is an extremely important and versatile messenger in the biological system. At first, it was recognized as an endothelium-derived relaxing factor in the vascular system [1]. It has also been identified as a neurotransmitter or neuromodulator in the neuronal system [2] and a cytotoxic factor in the immune system [3, 4]. In addition, it is believed to be that NO is related to some tissue damage, such as ischemia/reperfusion tissue damage [3, 5] and excitatory neuronal death [6-8].

Nitric oxide is produced from the guanidino group of L-arginine in an NADPH-dependent reaction catalyzed by a family of nitric oxide synthase (NOS) enzymes [9]. There are three distinct isoforms of NOS: neuronal NOS (nNOS), inducible NOS (iNOS), and endothelial NOS (eNOS) [10]. All three NOS isoforms have a similar molecular structure and require multiple cofactors, including flavins (FMN,FAD), NADPH, and tetrahydrobiopterin (BH_4) that are required to maintain the active dimeric form of the enzyme.

As described in previous chapters, NO is involved in many important physiological processes. Although the remedy for circumstances with insufficient NO production is a supply of NO to targets, it is not feasible because of the short lifetime and high reactivity of NO in biological systems. Thus, the treatment with NOS delivery to the targets is a promising method to overcome NO deficiency. NOS gene delivery has been reported for several years to cure NO deficiency. The deficiency of NO production in the cardiovascular system is an early aspect of atherosclerosis and other vascular injury [11]. Since the amount of NO plays an important role in phathogenesis of above diseases, eNOS gene transfer has a potential as a therapeutic strategy for treatments [12, 13]. NO produced by iNOS is responsible of angiogenesis [14, 15] and endothelial and epithelial cell proliferation and migration, which is associated with the wound healing [16-18]. To promote wound healing in NO deficient states, iNOS gene transfer showed some potential as a strategy [19].

Despite the fact that the NOS gene therapy shows prospective benefits, several obstacles have to be defeated for the clinical practice. The foremost concerns of NOS gene therapy are the limitations of currently available vectors, the need of suitable delivery methods to targets, and the difficulties of control of the NOS expression. To surmount those problems associated with gene therapy, delivery of NOS enzyme itself to targets may provide alternative routes for temporary remediation of NO deficiency.

Liposomes are considered as effective delivery systems owing to their unique properties. Liposomes were first described by Alec Bangham in 1965 while studying cell membranes. He found that lipsomes are vesicular structures consisting of hydrated bilalyers, which form spontaneously when phospholipids are dispersed in water. At that moment in time, neither the name nor their eventual efficacies as drug carriers were recognized. Ever since, further studies into liposomes and their relevance in diverse areas such as medicine and research have been explored. The question was whether these lipid structures were closed membranes bearing similar properties as biological cell membranes. As the most copious lipids in the cell membrane, phosphotidylcholine received much attention in the studying of cell model system formation. Subsequently, the liposome research area was extended to several other lipids, such as cholesterol and sphingolipids.

The most important quality of liposomes is the ability to enclose an aqueous medium separate from the external aqueous medium. Since liposomes are formed with lipid bilayer membranes that are identical to the natural cell membrane, they are

considered a simple-model system to study cellular properties. Liposomes encapsulate an aqueous solution inside a hydrophobic membrane. Dissolved hydrophilic solutes cannot readily pass through the lipids. This property makes liposomes more effective biocompatible carriers in the development of delivery systems. Hydrophobic compounds can be dissolved in the membrane, and, in this way, liposomes can carry both hydrophobic molecules as well as hydrophilic molecules. To deliver the molecules to sites of action, the lipid bilayer fuses with other bilayers, such as the cell membrane, and liberate the liposome contents.

The encapsulation of proteins in liposomes has gained great interest. Encapsulation provides stabilization and it prevents denaturation and proteolysis of proteins inside the liposome. Thus, as explained in Chapter I, liposome with encapsulated is a promising approach in carrying and delivering protein to targets for medical and pharmoceuticle perspectives. The aim of this study is the investigation of the efficacy of liposomes for carrying NOS enzymes and preserving their native structure and function for potential delivery to targets deficient in NO. To this end, conventional and NOS-embedded liposomes will be evaluated. NOS-loaded liposomes will be prepared by means of the thin-film hydration method in the presence of the target enzyme. The mild operative conditions allow the preservation of enzymatic structural integrity and activity.

4.2 Experimental Section

4.2.1 Materials

1,2-distearoyl--glycero-3-phosphocholine (DSPC) was obtained from Avanti Polar Lipids (Alabaster, Alabama). Cholesterol, Trizma base, K_3PO_4, KH_2PO_4, $MgSO_4$, EDTA, Triton-X, and glycerol were purchased from Sigma-Aldrich (St Louis, MO). Nanopure deionized water (specific resistance >18.2 MΩ.cm) used is supplied by a Barnstead water purification system model D8961. All chemicals are reagent grade and used as received. Bradford assay kit for protein analysis was obtained from Bio-Rad Laboratories (Hercules, CA). The Griess assay kit was purchased from Promega (Madison, WI).

4.2.2 Apparatus

Amperometric measurements are carried out using the CHI-440 electrochemical workstation. Electrochemical experiments of NOS-loaded liposomes are carried out on the stage of an Olympus IX-71 inverted microscope (Center Valley, PA) with the microelectrode positioned 10-15 μm above an isolated single liposome. The micropositioning was done with the help of a micromanipulator. An atomic force microscope (AFM) (Molecular Imaging Corp, Tampe, AZ) was used for characterizing the liposomes. Buchi Rotavapor from Buchi Corporation (New Castle, DE) was used for the evaporation. A mini-extruder obtained from Avanti Polar Lipids (Alabaster, Al). The

average particle size of vesicles was obtained by dynamic light scattering (DLS) using a 90 plus particle size analyzer, Brookhaven Instruments Corporation (Holtsville, NY). UV-visible absorbance spectra were recorded on an Agilent 8453 spectrophotometer using 1-cm path UV-visible cells.

4.2.3 Liposome Preparation

Liposomes are obtained by the thin-film hydration method followed by an extrusion process through a 10 nm pore size membrane [20]. Briefly, phosphatedyl - choline lipids (PC, 5 mg) and cholesterol (0.5 mg) are diluted with chloroform to a lipid concentration of 10 mg/mL. This solution is transferred to a round-bottom flask and the solvent is removed on a rotary evaporator for ~6 h at room temperature to form a dry, thin lipid film on the walls of the flask. To this film, a PBS buffer (Trizma base 5 mM, K_3PO_4 30 mM, KH_2PO_4 30 mM, $MgSO_4$ 1 mM, EDTA 0.5 mM, pH 7.4.) containing 1% v/v glycerol is carefully added to a lipid concentration of 5 mg/mL. The lipid film is allowed to swell overnight at 4 ° C. Finally, the sample is subjected to 10 freeze thaw cycles in liquid nitrogen and warm water. The unilamellar vesicles are then extruded through 0.1 μm pore-size polycarbonate filters to obtain liposomes with uniform-size. The unilamilar vesicle (UV) suspension is then stored at 4 °C for several days.

4.2.4 NOS encapsulation in liposomes

The thin lipid film is further dried by flowing dry nitrogen gas into the flask and ensure complete evaporation of the organic solvent. An aqueous solution of iNOS (or other isoforms) enzyme (0.45 μM) is then used to hydrate the lipid film before dilution with a pH 7.4 buffer solution. In order to eliminate unencapsulated NOS protein, the liposome suspension is passed through an activated Ni^{2+} column, which traps only the free histidine-tagged NOS proteins. The fractions containing NOS-encapsulated liposomes are collected and used for further analysis.

4.2.5 Size determination and the stability of NOS-loaded liposome

The mean liposome diameter and the size distribution of the vesicles were determined by dynamic Light Scattering (DLS). A 20 μl portion of the liposome dispersion was diluted with 1 ml of filtered buffer solution (0.2-μm pore size polycarbonate filters) and measurements were made at 25 ^{o}C. The stability of the liposome dispersion upon storage at 4 ^{o}C was monitored periodically by DLS.

4.2.6 Visualization of NOS inside the liposome

4.2.6.1 Formation of Ni-NTA-Gold tag NOS

Ni-NTA-Gold and His-taggged protein in TBST (20 mM Tris, pH 7.6, 150 mM NaCl and 0.05 % Tween 20) were mixed together in 10:1 molar ratio. The mixture was kept at room temperature for 2 hours and then centrifuged to remove unlabeled Ni-NTA-gold by reducing the volume to 0.05 ml using 50,000 cutoff centricon (Millipore Amicon Ultra-4; 50 kD). The above step was repeated three times and the modified protein was collected in TBST and stored at $-4\ ^{o}C$.

4.2.6.2 Gold enhanced (EM) Ni-NTA-Gold labeled NOS

The gold labeled NOS suspension was concentrated using centricon, and then redissolved in 3 ml deionized water followed by centrifugation to reduce the volume to 0.05 ml. The gold enhancement (20μl of each solution) was added to the protein mixture. After 5 minutes, the gold-labeled proteins were centrifuged at 35000 g. The gold-labeled proteins were rinsed five times with water by resuspension, in 1.5 ml water followed by removing the supernatant. The labeled proteins were redissoved in buffer solution and used as the rehydating medium on dried lipid film for formation of liposomes containing labeled-NOS.

4.2.7. Bradford Assay procedure

The total amount of NOS encapsulated was determined by the difference of NOS in liposome suspension and NOS inside the liposomes. The liposome suspension was treated with Triton X-100 (10% w/v aqueous solution) at 37 ^{o}C. The vesicle/Triton mixture was subjected to brief sonication to disrupt and empty liposomes of protein content. The vesicle debris was separated by centrifugation at 4000 rpm for 15 min. The supernatant was collected and analyzed for protein content by the Bradford microassay reading the purple complex at 595 nm.

4.2.8. Griess Assay procedure

The Griess assay reagent kit was used with the instruction provided. Briefly, the NADPH-treated 100 μl of NOS-loaded liposome sample was incubated with 100 μl of sulfanilamide for 10 minutes in the dark followed by 10-minute reaction with 100 μl *N*-1-napthylethylenediamine dihydrochloride (NAD) in the dark at room temperature. The absorbance was recorded at 540 nm.

4.2.9 Measuring of the NOS activity in liposomes

The enzyme activity of NOS-encapsulated liposomes was determined by the detection of NO released upon stimulation by NADPH using our modified sensor. All the materials for electrochemistry were used as indicated in Section 2.2.1. Similar

experimental set-up and instrumentation were used as outlined in the Section 2.2.2. The NOS-loaded liposomes were incubated with a PBS buffer solution. A micromanipulator attached to the stage of an inverted microscope allowed us to position the NO-selective micro-sensor 10-15 μm above the liposome surface as previously shown in Figure 3.4. A potential of +0.5 V vs. Ag/AgCl is typically applied to our NO-sensitive electrode. Once a steady background current is obtained, 150 μM of NADPH was injected into the vicinity of an isolated single liposome surface to stimulate NO release.

4.3 Results and Discussion

4.3.1 Characterization of Liposomes

4.3.1.1 AFM images of Liposomes

Atomic force microscopy (AFM) enables the direct visualization of liposomes and their morphological structure on mica surfaces in liquid and partially dry samples. The shape of the liposome depends on the time between the deposition of the sample on a mica surface and the imaging. AFM images obtained immediately after the deposition have spherical shapes as expected for lipid vesicles. After some time in air, we observe a shortening of the lipid vesicular height with broader diameters giving disk-like appearances as shown in Figure 4.1. The composition and size of the liposomes influence both the adsorption onto the mica layer and the vesicle deformation. Most of the observed liposomes in Figure 4.1 show a structure with an outer deformed layer,

probably associated with a flattened spherical vesicle. However, the central part of vesicles still hold and did not rupture.

The most common structure corresponds to a liposome formed by the aggregation of multiple vesicles as seen in Figure 4.2. Aggregation occurs when a larger vesicle is formed from the joining of two or more smaller vesicles. During the adsorption process, the liposome formed by the aggregation of various vesicles has the lower part of its structure in contact with the mica substrate. Due to mica-liposome interaction, the bottom part of the structure may be partially open with stronger interaction with the surface, resulting in the formation of a flattened bilayer that adheres to the surface. The aggregated liposome structure has to be considered when developing liposomes to be applied to the field of drug delivery systems since the selective permeability is substantially modified in aggregated vesicles when compared to single spherical ones.

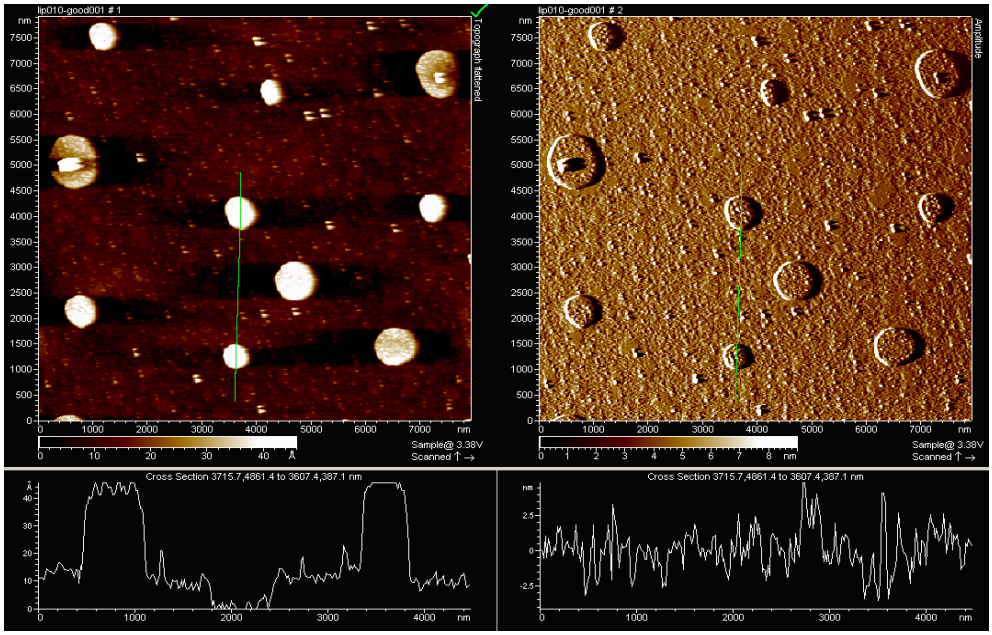

Figure 4.1. Representative AFM images of liposomes on mica surfaces.

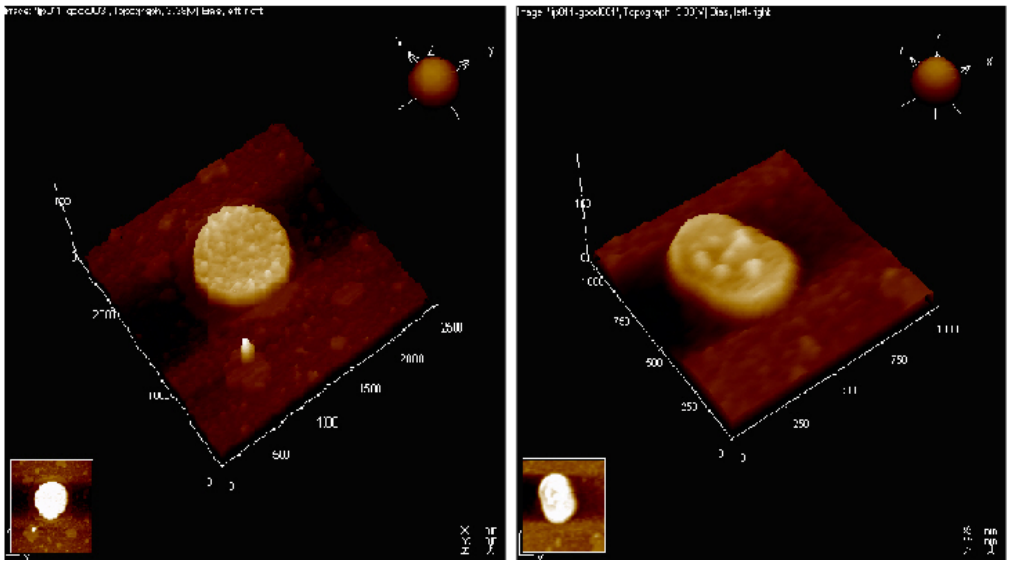

Figure 4.2. Three-dimensional images of the typical aggregated vesicle formed from multiple liposomes.

4.3.1.2 Microscopic images of Liposomes

The morphology of NOS-loaded giant liposomes can also be routinely observed under an inverted microscope immediately after the preparation. Figure 4.3 shows large NOS-loaded vesicles with an average size of 1μm diameter (before being subjected to the extrusion that reduce their size).

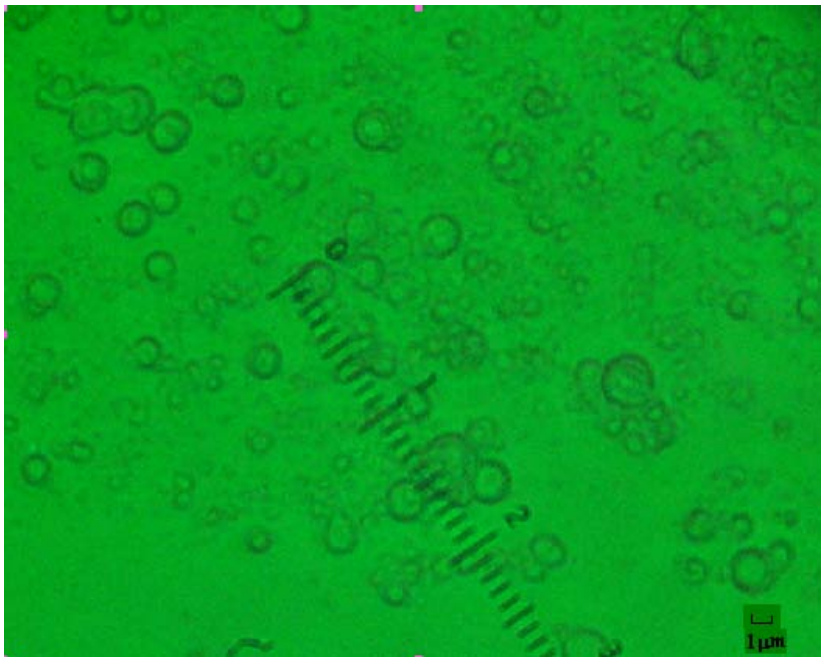

Figure 4.3. Inverted microscope images of large liposomes.

4.3.2 Size determination and the stability of NOS-loaded liposome

The size distribution of the vesicles was determined by Dynamic Light Scattering (DLS). In this technique, the Brownian motion of liposomes influence the scattering of laser light that corresponds to measure of diffusion coefficient, which can be used to calculate the diameter of liposomes. Homogeneous size distribution of vesicle suspension is achieved by performing sequential extrusions at moderately low pressure through polycarbonate membranes with desired pore size.

DLS analysis of liposomes immediately after preparation shows monodispersed vesicles with the mean size of about 140 ± 30 nm (polydispersity index of less than 0.1) ((Figure 4.4).

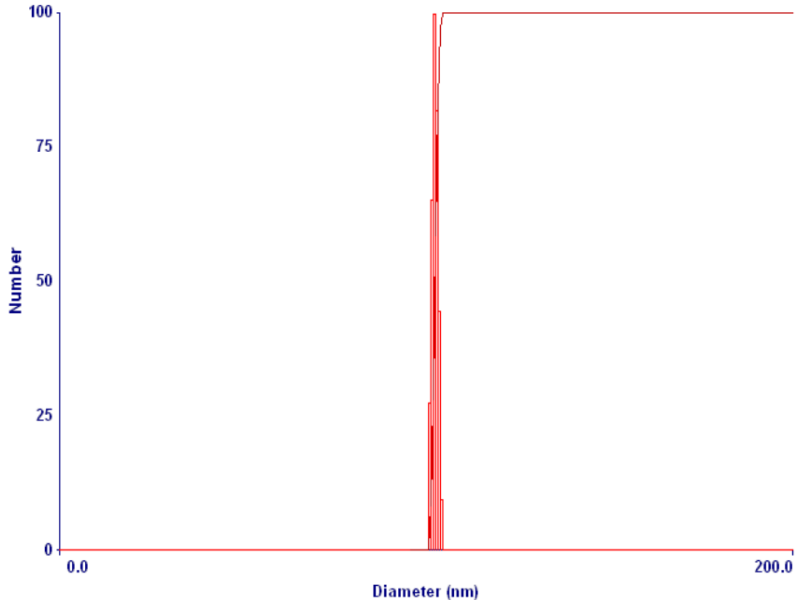

Figure 4.4. Size distribution for vesicles in suspension measured in DLS.

Monitoring of the size of liposomes is a great advantage and it can be reflect on the stability of liposomes. The size characterization and the stability of liposomes have the foremost effect of their fate (such as the application and the targets that liposomes can be used for). Therefore, formation of predictable and reproducible particle size distribution in each batch of liposomes is a great importance for medical applications.

NOS-loaded liposomes were stored at 4 ^{o}C and the stability as a function of time storage was tested using DLS analysis. The liposome stability was obtained by the diameter of vesicles as a function of time and is reported in Figure 4.5. The first 15 days demonstrate an excellent stability of vesicles, and after 30 days the mean diameter of vesicles increased by around 1.2 fold. The results reveal that liposomes tend to fuse and aggregate each other as a function of storage time in 4 ^{o}C. At the point of 30 days, the vesicle dispersion was heterogeneous with an increasing polydispersity index (more than 1.0) that pointed out wider diameter vesicles.

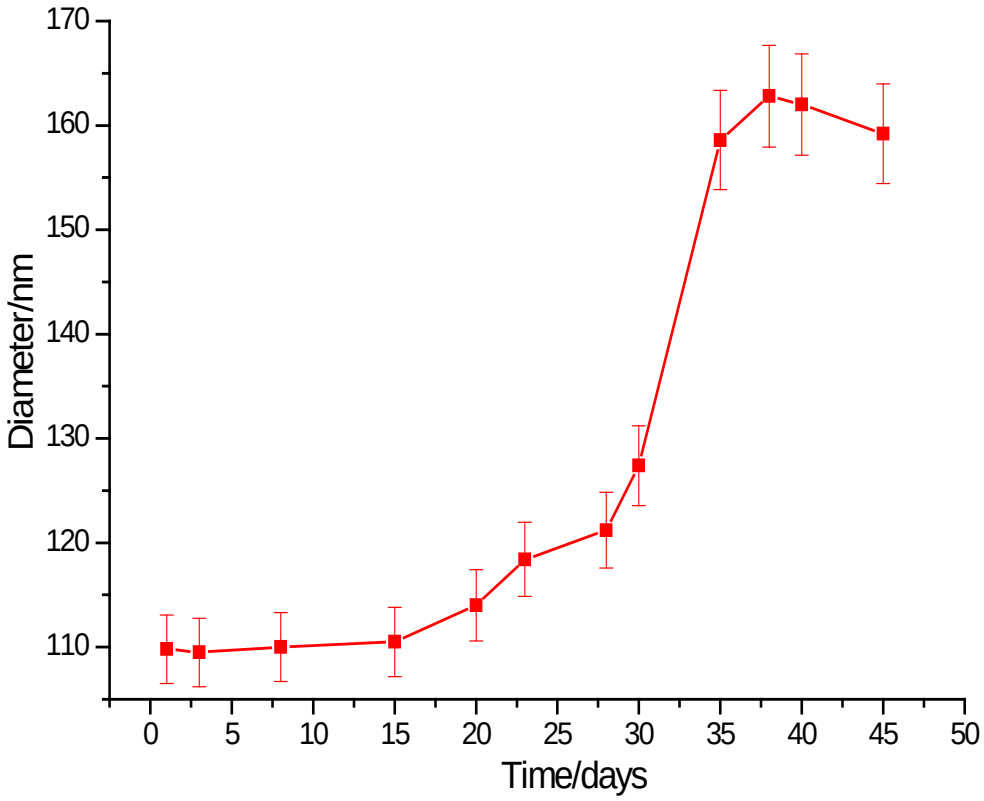

Figure. 4.5. Mean size variation of liposomal suspension as a function of time.

4.3.3. Visualization of NOS inside the liposome

The histidine tage has an extremely high affinity for metal ions, which can be employed to purify His-tagged protein by immobilized metal ion affinity chromatography. The nickel is chelated to nitrilotriacetic acid (NTA), and histidine resides in protein make a stable, six-coordinated octahedral compound. NTA can bind specifically to nanogold particles and therefore used to label His-tag proteins as shown in Scheme 4.1. Since the Ni-NTA group is quite small compared to an antibody, the gold particle can reach more closely the 6-His-tag site and give high resolution labeling with less ambiguity or floppiness. Another advantage of this type of label is the size compatibility of Ni-NTA group with cells and tissues, which can diffuse more easily [21]. The nanogold-labeled protein can be visualized by an electron microscope for higher resolution studies; it can also be visible with a light microscope after treatment with gold enhancement.

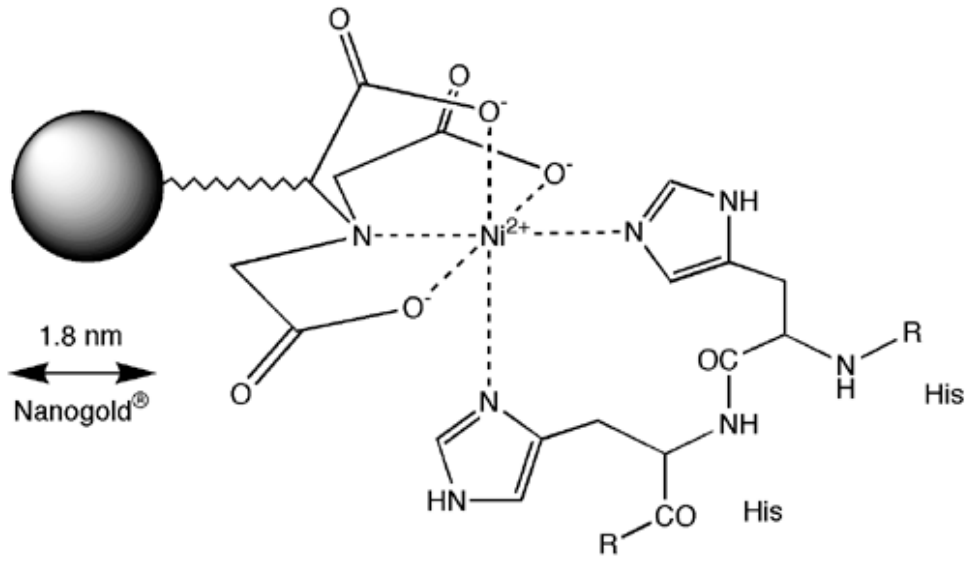

Scheme. 4.1. The diagram of His-tagged protein and Ni-NTA-Nanogold complex Adapted from ref. [21].

Ni-NTA-nanogold was used as a tool for localizing and visualizing His-tagged nitric oxide synthase enzyme inside liposomes. The NOS protein was first modified with Ni-NTA-nanogold group, and, after gold enhancement, the modified NOS was loaded inside the liposome.

Liposomes enclosed with gold labeled proteins were visualized under a microscope. Darker membranes and darker hollow surfaces were observed under the magnification of 400X as shown in Figure 4.6. The liposomes loaded with labeled NOS were much darker compared with the unlabeled NOS-loaded liposomes, which indicate

that the NOS enzyme is successfully entrapped inside the hollow surface and the membrane of liposome.

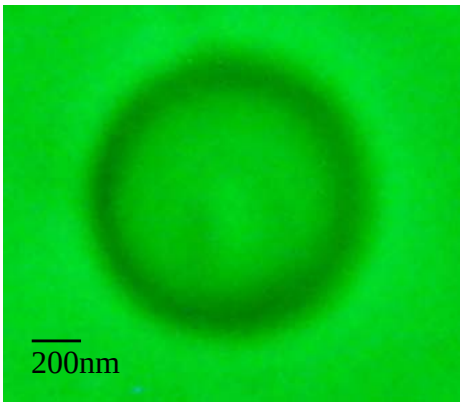

Figure. 4.6. Microscopic image of NOS-Ni-NTA-Gold loaded liposome.

4.3.4 Protein content inside the liposome

For liposomes to be a feasible pharmaceutical delivery system, not only the liposome stability but also the encapsulation efficiency or the loading capacity also needs to be considered. The total amount of NOS encapsulated was determined either in the supernatant or in liposome suspensions. Figure 4.7 shows the absorbance vs. wavelength plot using the Bradford assay and the resultant calibration plot is presented in Figure 4.8. The encapsulation efficiency (%) of liposomes is defined as the ratio of the total encapsulant in the liposome and the total initial input of the encapsulant is shown in equation 4.1 [22].

$$\text{Encapsulation efficiency (\%)} = \frac{\text{NOS in vesicles}}{\text{Total NOS added}} \qquad \text{Equation 4.1}$$

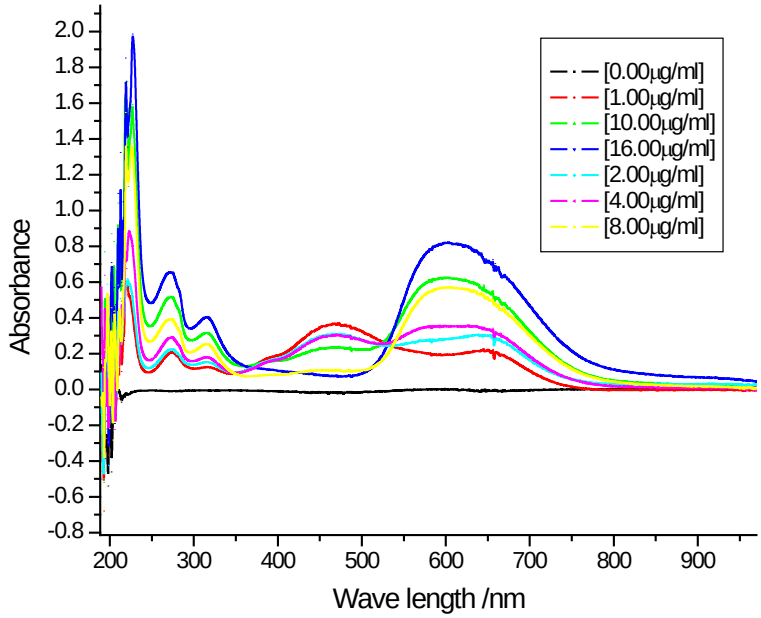

Figure 4.7. The absorbance vs. wavelength curve for the standard for the Bradford protein assay.

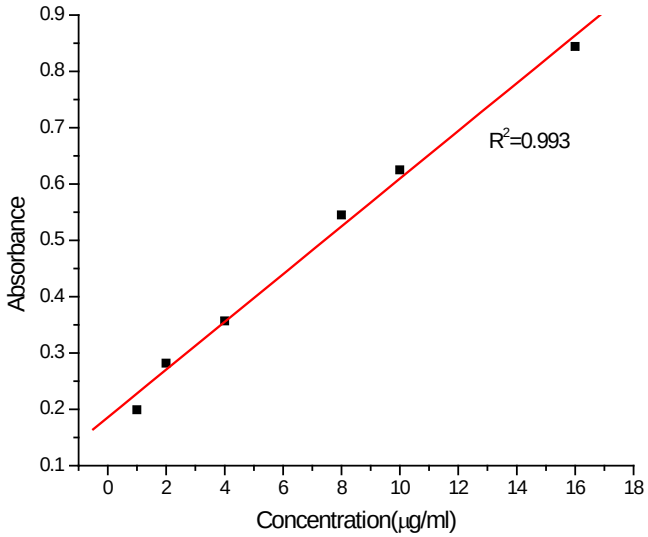

Figure 4.8. The calibration plot for Bradford protein assay.

Table 4.1 The values obtained from Bradford assay.

Sample	ΔAbsorbance	[Enzyme] (μg̃/ml)
NOS*	0.5354 ± 0.2	8.064 ± 2.3
NOS-loaded Liposome(intact)	2.279×10^{-2}	~0.00
NOS After liposome disruption	0.3187 ± 0.28	2.993 ± 2.1

NOS* - Input NOS concentration after subtracting the unloaded NOS.

Five replicate experiments were used determining the encapsulation efficiencies. The % encapsulation efficiency for NOS-loaded liposomes was obtained as 40 ± 25%. The loading capacity remains constant over 15 days upon storage in 4 ^{o}C. After 15 days low loading capacity of the enzyme observed and indicates the vesicle disruption and aggregation. instability of the vesicles.

4.3.5 Quantification of NO production (NOS activity) using the Griess Assay

The Griess assay is commonly used for the detection of NO synthesis from NOS and hence can determine the NOS turnovers [23, 24]. In the Griess assay, the nitrite, the steady breakdown product of NO, is quantified. The Griess reaction is based on the reaction of nitrite with sulfanilamide under acidic conditions to form diazonium cation. This cation then couples with *N*-1-napthylethylenediamine dihydrochloride (NED) to form a purple azo dye with maximum absorbance at 540 nm [25]. The calibration curve is constructed using standard nitrite using the same reaction conditions (Figure 4.9).

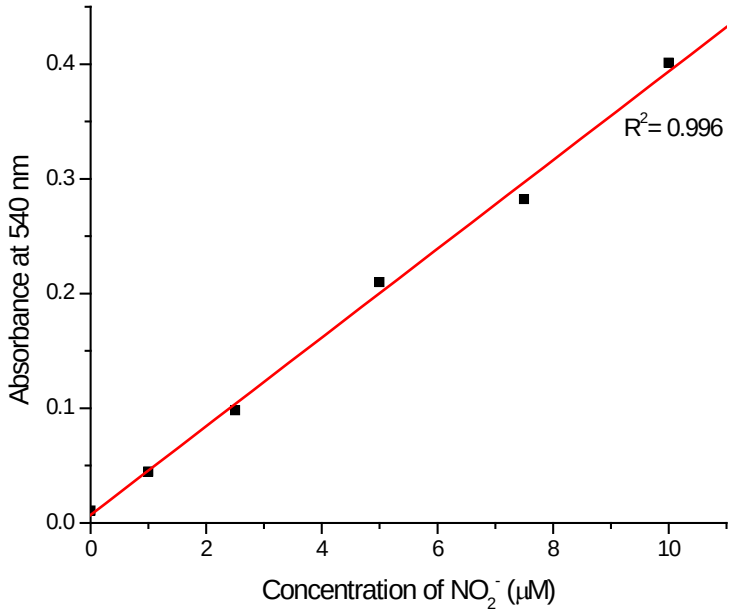

Figure 4.9. The calibration plot for the Griess assay.

Table 4.2 The values obtain from the Griess assay.

Sample	Absorbance	Concentration of NO (nM)
NOS *	0.0639	1.519×10^3
NOS-Loaded liposome	0.0517	1.153×10^3

NOS*- Input NOS after subtracting unloaded NOS

According to the Griess assay results, each batch produces 3.5 μM of NO (with consideration the dilution factor of 3). Compared to the initial protein activity, the percentage of the protein activity inside the liposomes is 75.91% (n=3). The high % value demonstrates the retaining of the NOS activity is mostly retained inside the vesicles.

4.3.6 Dynamic measurement of NO released by NOS-loaded liposomes using the NO sensor

The detection of NO released by stimulated NOS-encapsulated liposomes enables us to determine the NO release capability activity of NOS enzymes entrapped in liposomes. If NO synthesis and release is to be triggered within an isolated single NOS-loaded liposomes we expect a change in current signal as a function of time after addition of NADPH. This is indeed what is observed as indicated in Figure 4.10. The sharp drop in current signal after the addition of 45 nmol of NADPH is due to the oxidation of NO released from single NOS-encapsulated liposome. In fact control experiments (e.g. the addition of 10 μl of buffer solution to NOS-liposomes) do not give this positive responses, as shown in Figure 4.10. Each NOS-loaded liposome produced a 19.8 nM concentration of NO. Since liposomes are spherical, they can be considered as cell-mimics. Using similar calculations as in (Section 3.3.4), the amount of NO produced from one liposome is around 3.7 attomoles and this value is constant for all same size NOS-loaded liposomes (Figure 4.11).

As explained in Chapter 3, Section 3.3 a set of control experiments were carried out to confirm that the current response is due to NO released from NOS-loaded liposomes. When the enzyme is inhibited by adding L-NAME, no current response was observed upon the addition of NADPH, as shown in Figure 4.12. the addition of NADPH to the bulk solution does not give any significant signal indicating that the sensor response is due to NO released from NOS encapsulated in liposomes.

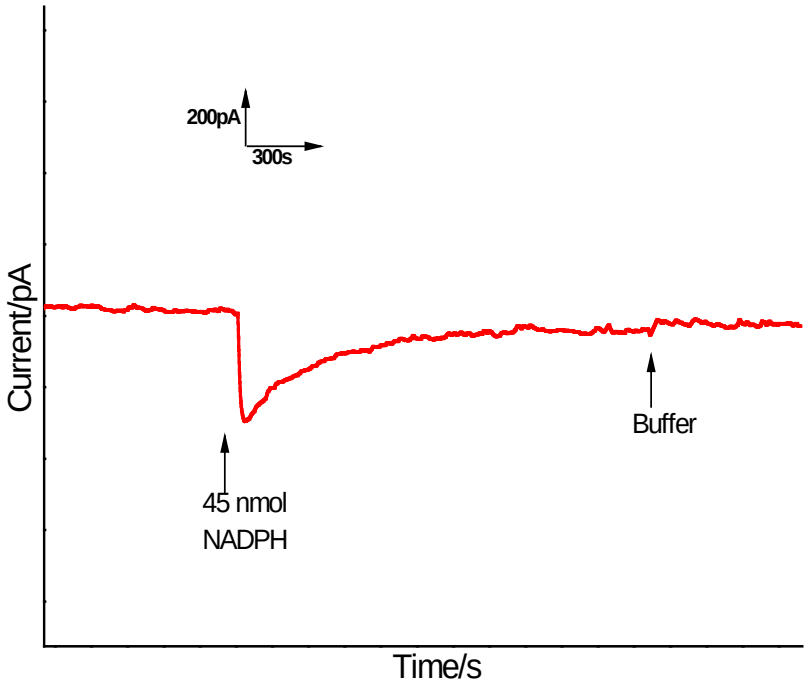

Figure 4.10. Amperometric response of our NO sensor after addition of NADPH and PBS buffer solution to the NOS-encapsulated liposome.

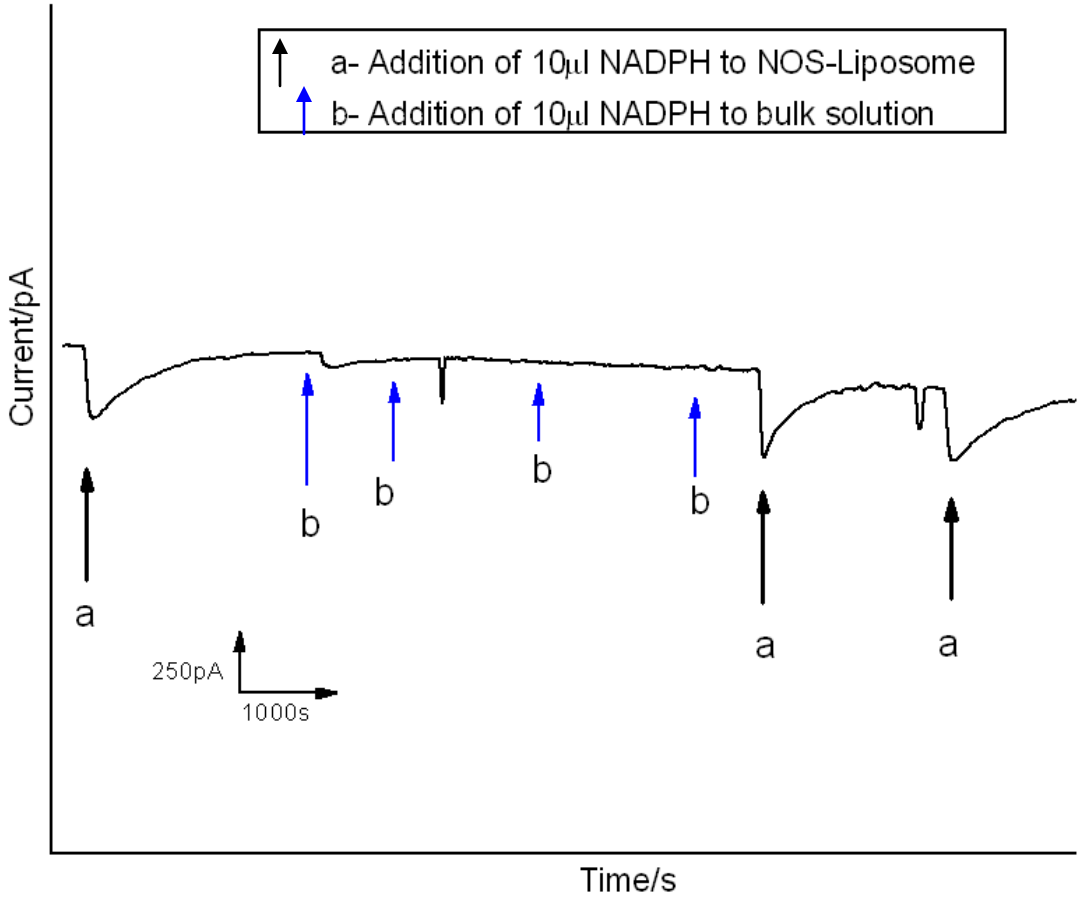

Figure. 4.11. Amperometric response of our NO sensor for the addition of NADPH close to the NOS-encapsulated liposomes and in bulk solution.

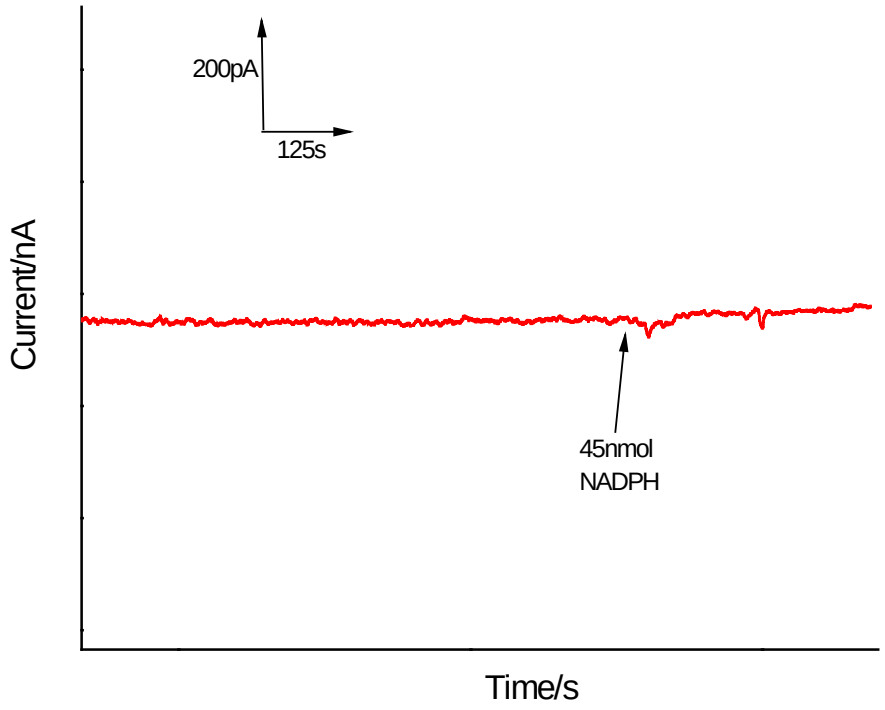

Figure 4.12. Amperometric response of the modified electrode for the addition of NADPH to the NOS-encapsulated liposome after the L-NAME treatment.

4.4 Summary of Chapter IV

The NOS-loaded liposomes were obtained by the thin film hydration method. We were able to prepare stable liposomes loaded with NOS enzyme with an encapsulation efficiency of 40 ± 25%. Size monitoring with DLS demonstrate the excellent stability of NOS-loaded liposome for around 15 days upon storage and NOS-enzyme activity also retained. The Griess assay results revealed that each batch of NOS-loaded liposomes can produce 3.5 μM of NO. Dynamic electrochemical measurement of NO indicates that 19.8 nM of NO are released from an isolated single liposome. These positive results confirmed that the enzyme activity is retained inside the liposome, and it can release NO upon stimulation.

4.5 References

1. Palmer, R.M., Ferrige, A.G., and Moncada, S. (1987). Nitric oxide release accounts for the biological activity of endothelium-derived relaxing factor. Nature *327*, 524-526.
2. Nathan, C. (1992). Nitric oxide as a secretory product of mammalian cells. Faseb J *6*, 3051-3064.
3. Moncada, C., Lekieffre, D., Arvin, B., and Meldrum, B. (1992). Effect of No Synthase Inhibition on Nmda-Induced and Ischemia-Induced Hippocampal-Lesions. Neuroreport *3*, 530-532.
4. Friedemann, M.N., Robinson, S.W., and Gerhardt, G.A. (1996). o-Phenylenediamine-modified carbon fiber electrodes for the detection of nitric oxide. Anal Chem *68*, 2621-2628.
5. Jaeschke, H., Schini, V.B., and Farhood, A. (1992). Role of Nitric-Oxide in the Oxidant Stress during Ischemia Reperfusion Injury of the Liver. Life Sciences *50*, 1797-1804.
6. Dawson, T.M., Dawson, V.L., and Snyder, S.H. (1992). A Novel Neuronal Messenger Molecule in Brain - the Free-Radical, Nitric-Oxide. Annals of Neurology *32*, 297-311.
7. Manchester, K.S., Jensen, F.E., Warach, S., and Lipton, S.A. (1993). Chronic Administration of Nitroglycerin Decreases Cerebral Infarct Size. Neurology *43*, A365-A365.

8. Lipton, S.A., Choi, Y.B., Pan, Z.H., Lei, S.Z.Z., Chen, H.S.V., Sucher, N.J., Loscalzo, J., Singel, D.J., and Stamler, J.S. (1993). A Redox-Based Mechanism for the Neuroprotective and Neurodestructive Effects of Nitric-Oxide and Related Nitroso-Compounds. Nature *364*, 626-632.

9. Beckman, J.S. (1996). The physiological and pathological chemistry of nitric oxide-Nitric Oxide-Principles and Actions. 1-83.

10. Forstermann, U., Closs, E.I., Pollock, J.S., Nakane, M., Schwarz, P., Gath, I., and Kleinert, H. (1994). Nitric oxide synthase isozymes. Characterization, purification, molecular cloning, and functions. Hypertension *23*, 1121-1131.

11. Luscher, T.F., Tanner, F.C., Tschudi, M.R., and Noll, G. (1993). Endothelial dysfunction in coronary artery disease. Annu Rev Med *44*, 395-418.

12. Chen, A.F., Ren, J., and Miao, C.Y. (2002). Nitric oxide synthase gene therapy for cardiovascular disease. Jpn J Pharmacol *89*, 327-336.

13. Channon, K.M., Blazing, M.A., Shetty, G.A., Potts, K.E., and George, S.E. (1996). Adenoviral gene transfer of nitric oxide synthase: High level expression in human vascular cells. Cardiovascular Research *32*, 962-972.

14. Ziche, M., Morbidelli, L., Masini, E., Amerini, S., Granger, H.J., Maggi, C.A., Geppetti, P., and Ledda, F. (1994). Nitric oxide mediates angiogenesis in vivo and endothelial cell growth and migration in vitro promoted by substance P. J Clin Invest *94*, 2036-2044.

15. Leibovich, S.J., Polverini, P.J., Fong, T.W., Harlow, L.A., and Koch, A.E. (1994). Production of angiogenic activity by human monocytes requires an L-

arginine/nitric oxide-synthase-dependent effector mechanism. Proc Natl Acad Sci U S A *91*, 4190-4194.

16. Morbidelli, L., Chang, C.H., Douglas, J.G., Granger, H.J., Ledda, F., and Ziche, M. (1996). Nitric oxide mediates mitogenic effect of VEGF on coronary venular endothelium. Am J Physiol *270*, H411-415.

17. Benrath, J., Zimmermann, M., and Gillardon, F. (1995). Substance P and nitric oxide mediate would healing of ultraviolet photodamaged rat skin: evidence for an effect of nitric oxide on keratinocyte proliferation. Neurosci Lett *200*, 17-20.

18. Noiri, E., Peresleni, T., Srivastava, N., Weber, P., Bahou, W.F., Peunova, N., and Goligorsky, M.S. (1996). Nitric oxide is necessary for a switch from stationary to locomoting phenotype in epithelial cells. Am J Physiol *270*, C794-802.

19. Yamasaki, K., Edington, H.D., McClosky, C., Tzeng, E., Lizonova, A., Kovesdi, I., Steed, D.L., and Billiar, T.R. (1998). Reversal of impaired wound repair in iNOS-deficient mice by topical adenoviral-mediated iNOS gene transfer. J Clin Invest *101*, 967-971.

20. Kono, K., Nakai, R., Morimoto, K., and Takagishi, T. (1999). Thermosensitive polymer-modified liposomes that release contents around physiological temperature. Biochim Biophys Acta *1416*, 239-250.

21. Hainfeld, J.F., Liu, W., Halsey, C.M., Freimuth, P., and Powell, R.D. (1999). Ni-NTA-gold clusters target His-tagged proteins. J Struct Biol *127*, 185-198.

22. Kaiser, N., Kimpfler, A., Massing, U., Burger, A.M., Fiebig, H.H., Brandl, M., and Schubert, R. (2003). 5-Fluorouracil in vesicular phospholipid gels for

anticancer treatment: entrapment and release properties. Int J Pharm *256*, 123-131.

23. Maurer, T.S., and Fung, H.L. (2000). Evaluation of nitric oxide synthase activity and inhibition kinetics by chemiluminescence. Nitric Oxide *4*, 372-378.

24. Pfeiffer, S., Gorren, A.C., Schmidt, K., Werner, E.R., Hansert, B., Bohle, D.S., and Mayer, B. (1997). Metabolic fate of peroxynitrite in aqueous solution. Reaction with nitric oxide and pH-dependent decomposition to nitrite and oxygen in a 2:1 stoichiometry. J Biol Chem *272*, 3465-3470.

25. Tsikas, D. (2000). Simultaneous derivatization and quantification of the nitric oxide metabolites nitrite and nitrate in biological fluids by gas chromatography/mass spectrometry. Anal Chem *72*, 4064-4072.

CHAPTER V

FUTURE DIRECTIONS - THE INVESTIGATION OF CELLULAR UPTAKE OF NOS ENZYME FROM NOS-LOAD LIPOSOMES

5.1. Introduction

As discussed in previous chapters, a change in physiological concentration of NO causes severe problems in biological systems. The logical therapy for NO deficient conditions such as, hypertension [1, 2], impotence [3, 4], hyperglycaemia, arteriosclerosis [5, 6], is the supply of NO or NOS to targets. In Chapter IV, we described the development of an effective method to entrap NOS enzymes in liposomes as a prospective vehicle for onsite NO delivery. Liposomes have emerged as efficient and versatile carrier system due to their capability to entrap a verity of substances, such as drugs, proteins, antibodies, etc. By virtue of their biocompatible lipid exterior, liposomes are considered as a powerful tools for delivery as they can introduce various biologically

active materials into cells both *in vivo* and *in vitro*. Initial studies of vesicle-cell interactions demonstrated that the compounds in the vesicles can be released to cells, and hence affect cell functions. Although several studies have investigated the cellular interactions with liposomes, less attention has been given to the mechanism of liposomes' incorporation into cells [7-9].

There are several ways of interaction of liposomes and cells for delivering liposomal content inside cells. Without interruption of liposomes integrity phospholipid bilayers can approach close to cell membrane and foster intermembrane transfer. Four mechanisms have been proposed that can explain the liposome-cell interactions by which liposomes can deliver their content to cells (Figure 5.1). Liposomes can adsorb onto the cell membrane and then promote the extracellular release of the liposomal content, which can transfer into the cells by active or passive transport (path 1 in Figure 5.1) [11]. Secondly, adsorbed liposome can selectively transfer lipophilic compounds from the liposomal bilayer to the cell interior as shown in Figure 5.1, path 2 [12]. The most common mechanism is the endocytosis (Figure 5.1, path 3), where the endocytotic internalization of the liposome occurs, followed by the intracellular degradation and subsequent intracellular delivery of substances [9, 13, 14]. Fusion is the fourth method and consist of direct and simple delivery mechanism (Figure 5.1, path 4). In fusion, the plasma membrane and the vesicle membrane fuse and incorporate together, which results in the release of the content into the cytoplasm [15].

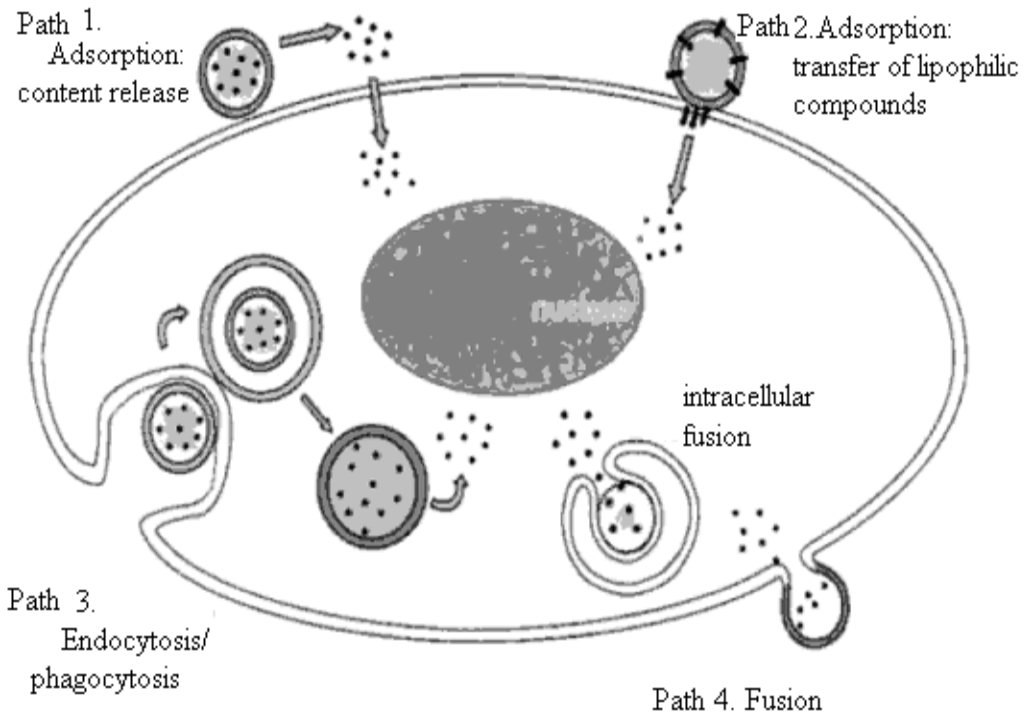

Figure 5.1. Schematic representation of the possible mechanism by which the liposomes can interact with cells *in vitro* and deliver their content (Adapted from [10])

The aim of this chapter is the investigation of the effectiveness of NOS loaded liposome for intracellular delivery. The goal is to deliver liposome-entrapped NOS inside the cells while retaining enzyme activity. The NOS-loaded liposomes prepared as pointed out in Chapter IV will be used for the intracellular NOS delivery into cultured human embroyonic kidney cells (HEK 293). The procedure and the preliminary results are discussed.

5.2 Experimental Section

5.2.1 Materials and Apparatus

All the materials for electrochemistry are used as indicated in Section 2.2.1 and similar experimental set-up and instrumentation is used as outlined in Section 2.2.2. Cell experiments were carried out on the stage of an Olympus IX 71 inverted microscope, Center Valley, PA.

5.2.2 Liposome Preparation

Liposomes were prepared by thin-film hydration method as described in Chapter IV, Section, 4.2.3. All experiments were done in sterilized conditions. Liposome preparation was also carried out under aseptic conditions. After the liposome extrution the suspension was sterile-filtered through 0.2 μm membranes (Millipore, Jaffrey, NH).

5.2.3 Cell Culture Preparation

Human embryonic kidney cell cultures (HEK-293) were grown in Eagle's Minimum Essential Medium (MEM) with 4 mM L-glutamine, 4.5 g/L glucose, 10% fetal bovine serum and adjusted to contain 1.5 g/L sodium bicarbonate. The cells were grown and sub-cultured as described in the Section, 3.2.3.

5.2.4. *In vitro* liposome-cell interaction

HEK cells were grown in petri dishes (3.0 cm diameter) in the MEM medium and at the confluence (4.2×10^5 cells/ml), the media was removed and replaced with MEM containing 1% Insulin-transfering-sodium selenite (MEM + ITS) [16]. The sterilized NOS- loaded liposomes at the concentration of 0.5 μmol lipids/ml were incubated with HEK cells. After 2 days of incubation at 37 ^{o}C, the media was removed and the cells were washed three times with a PBS buffer. As controls, HEK cells were grown with the addition of empty liposomes (without NOS) and without the addition of any liposomes.

5.2.5. Electrochemical Experiments

Electrochemical experiments of NOS-loaded liposomes were carried out as described previously (Section 4.2.2) for HEK cells incubated with liposomes and for controls. NO synthesis was triggered by adding the NOS substrate L-Arginine (1.5 mM) [17].

5.3. Preliminary Results and Discussion

After injecting 1.5mM of L-arginine close to the collection of HEK cells, the changes in the current signal were monitored as described in Section 3.3.1. The typical current-time plot obtained for HEK cells without NOS-loaded liposomes is shown in Figure 5.2. We observed a change in current immediately after the addition of L-arginine. The HEK cells incubated with empty liposomes (without NOS) also gave the similar current response as Figure 5.2. This indicates that there is no effect from the liposomes for the functions of HEK cells.

To make sure that the NO released comes from stimulated HEK cells, a set of control experiments were carried out as explained before. First, the cells were treated with the nitric oxide synthase (NOS) inhibitor, L-NAME, prior to the experiment. As shown in Figure 5.3, no significant change in current response is observed for the addition of L-arginine to the L-NAME treated HEK cells. To ensure that the injection

process did not cause the current change, an equivalent volume (50 μl) of phosphate buffer (PBS) was injected into the solution close to the cells in lieu of L-arginine and no significant change in the background current was observed. Also as shown in Figure 5.4, when L-arginine was injected to buffer solution without cells, there was no current change. These results indicate that the current response obtained in Figure 5.3 was totally due to the NO produced from HEK cells.

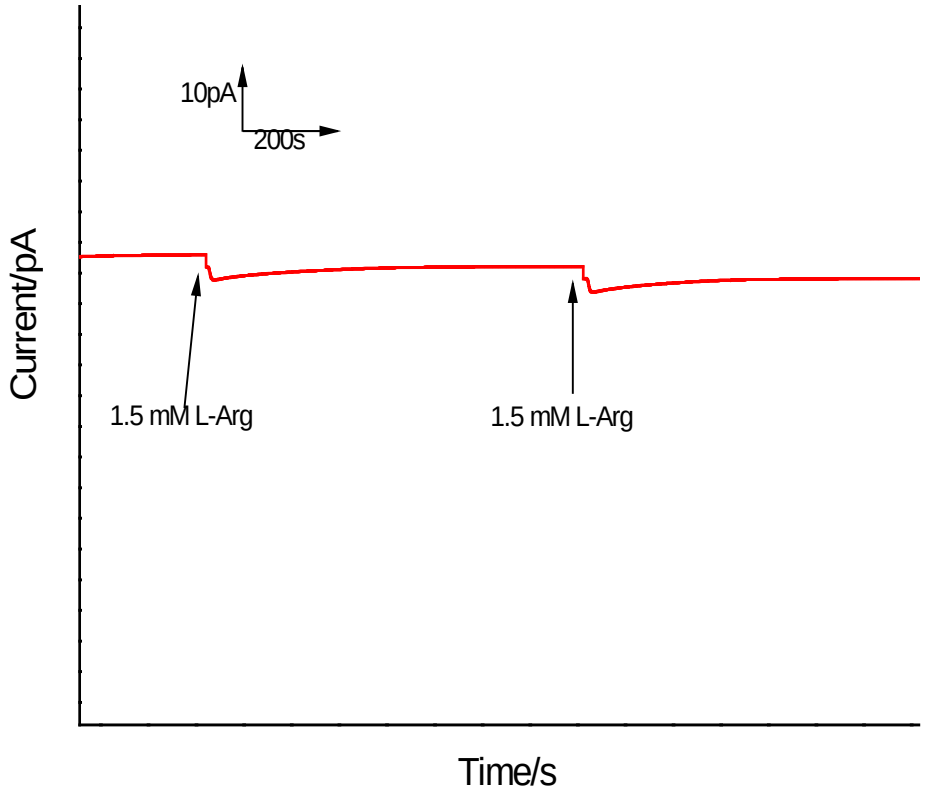

Figure 5.2. Amperometric response of NO sensor after addition of L-Arginine to the HEK cell culture.

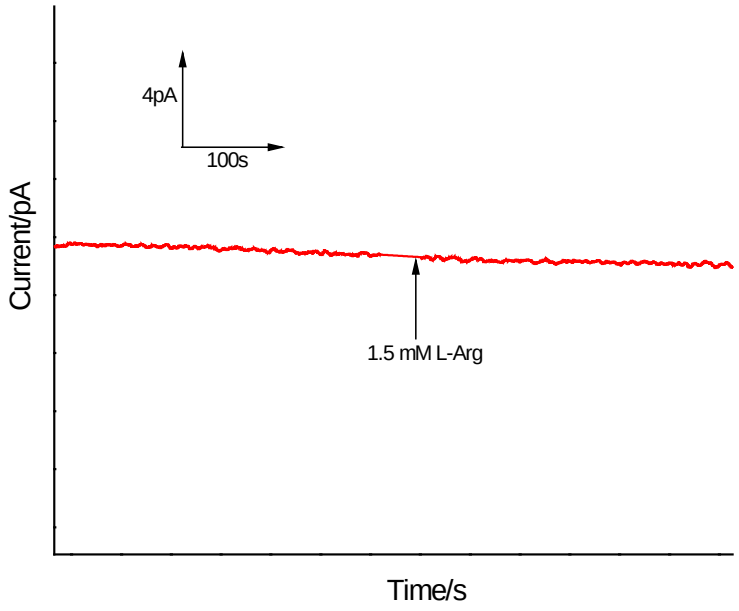

Figure 5.3. Amperometric response of our NO sensor after addition of L-Arginine to the cell culture treated with the NOS inhibitor L-NAME

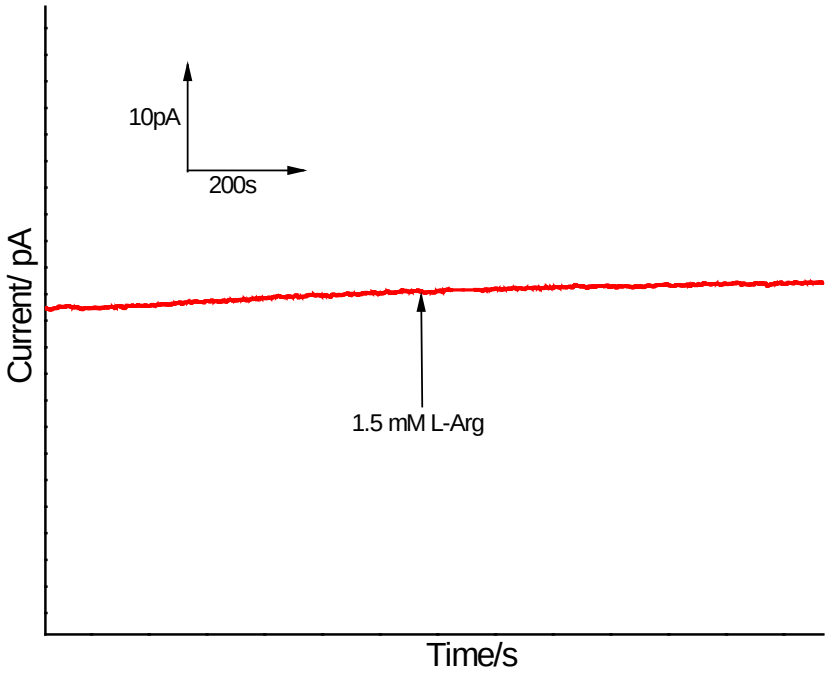

Figure 5.4 Amperometric response of our NO sensor after addition of L-Arginine to the PBS solution.

The same electrochemical experiments were carried out for the HEK cells that were incubated with 0.5 μmol lipids/ml NOS-loaded liposomes. When L-arginine was injected near to the cell surface, a current response greater than cells not subjected to liposome treatment was observed (Figure 5.5). According to the calibration plot obtained in the same experimental conditions (Chapter III, Figure 3.10), the NO generated from HEK cells incubated with NOS-loaded liposomes is about 10 nM. Compared to the normal production of NO by HEK cells (1 nM), this value is about 10 times higher, supporting the idea that NOS enzyme from liposomes were delivered inside HEK cells from the NOS-loaded liposomes.

The amount of NO produced by transferring the NOS enzyme from liposomes to cells is much lower compared to the total amount of NO production by NOS-loaded liposomes themselves. Our results show that only about 10 % of active enzymes are delivered from NOS-loaded liposomes to cell interior. This can be explained by analyzing the NO production from the medium and the washings that removed from HEK cells after incubation with NOS-loaded liposomes. Griess assay analysis results shows that about 0.56 μM of NO produced from the washings. This indicates a potential leakage of NOS enzymes from the liposomes in the experimental conditions described above. Some of the possible modifications and conditions for optimized enzyme delivery are discussed bellow. Although the values are in the low end of internalization of NOS, our method provide novel platform for targeted NOS delivery.

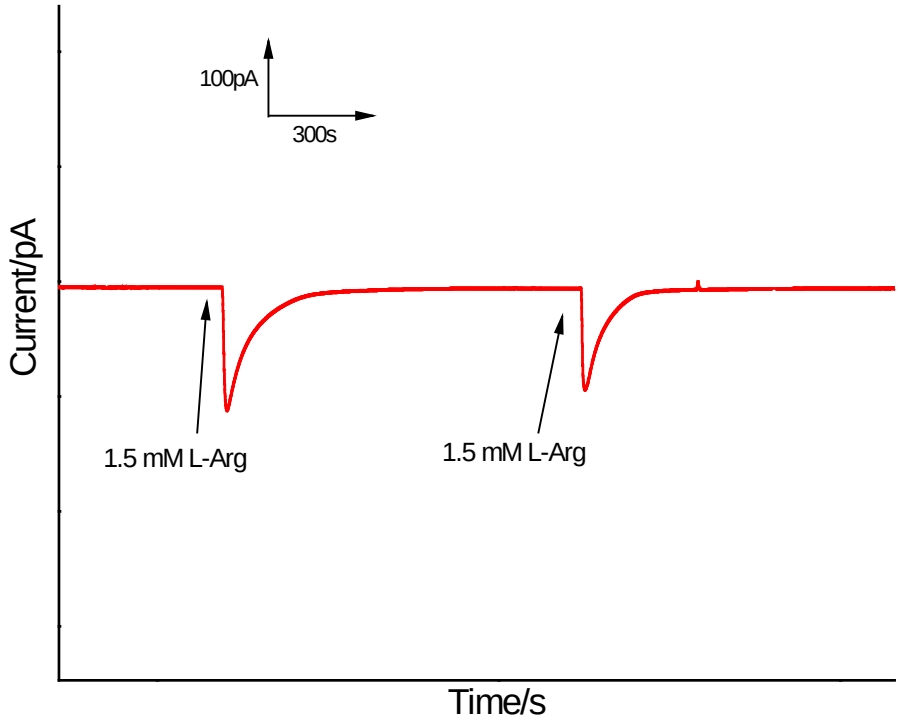

Figure 5.5. Amperometric response of our NO sensor after addition of L-Arginine to the HEK cell culture that incubated with NOS-loaded liposome.

As an effective drug delivery system, liposomes must reach the target site after passing through the blood flow and release their content to the target site. Then the target tissues /cells should uptake the liposomal content to cure the disease or change the functions. As explained in the introduction, fusion, adsorption and the endocytosis occur when delivering liposomal content into cells. It has been found that the optimum condition of intracellular delivery of liposomal content to cells is similar *in vivo* and *in vitro* [13]. Therefore, the study of cellular uptake of liposomes in vitro condition is vital. Liposomes bearing a negative charge (such as liposomes formed with phosphatidylserine (PS), phosphatidylglycerol (PG), or phosphatidic acid (PA) lipids) were observed to be endocytosed in macrophages to a greater extent than neutral liposomes [9, 13, 14]. Some cell types, including macrophages, can recognize negatively charged liposomes more successfully [7, 13, 14, 18]. The Hela cells have been found to uptake positively charged liposomes more preferentially and this interaction is reliable with nonspecific binding rather than involving a specific receptor [19]. However, the factors that affect the binding of liposome into cells have not yet been clearly deliniated. Therefore, using a similar approach, we will develop NOS-loaded liposomes by varying the charge, the composition of lipids, to maximize uptake of liposomal content.

The biocompatible polymer, poly (ethylene glycol) (PEG) is a good candidate for preparation of satirically stabilized liposomes. PEG modified membrane can prevent the clearance of liposomes in the blood stream [19]. Immobilizing liposomes onto biodegradable solid materials, can result in effective delivery to targets, with low dosage, minimal side effects, and long term circulation. As an approach of the clinical

applications, PEG-Biotin-tag NOS-loaded liposomes will be prepared as shown in Figure 5.6. The solution phase AFM characterization of such a Biotin-tag NOS-loaded liposomes on streptavidine modified mica surface shown in Figure 5.7. Further studies are in process to optimize the stability and delivery to achieve more stable vesicles for on-site NO delivery.

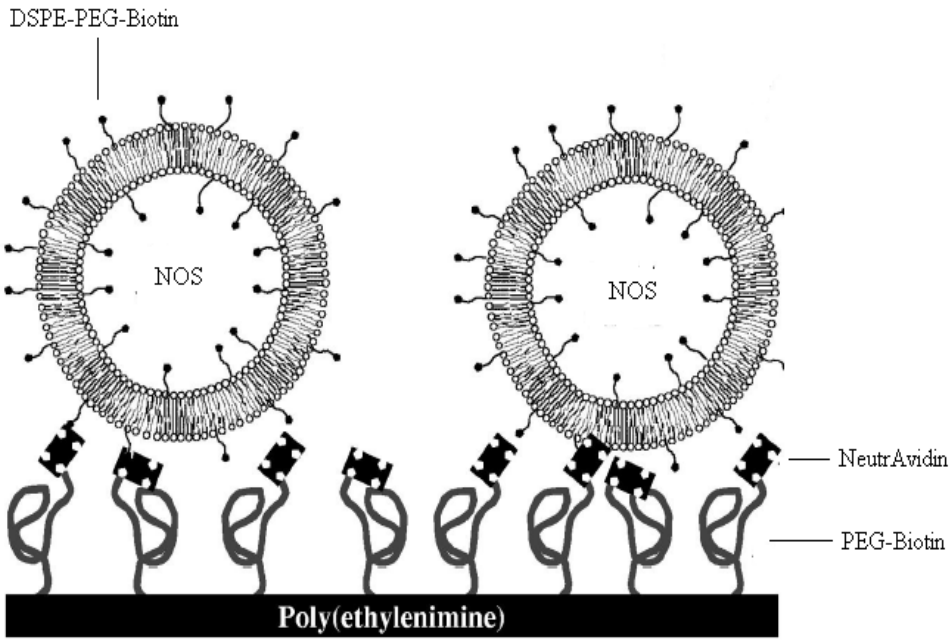

Figure 5.6. Schematic representation of immobilized Biotin-tag NOS-loaded liposome on solid carrier. (Reprinted from [20])

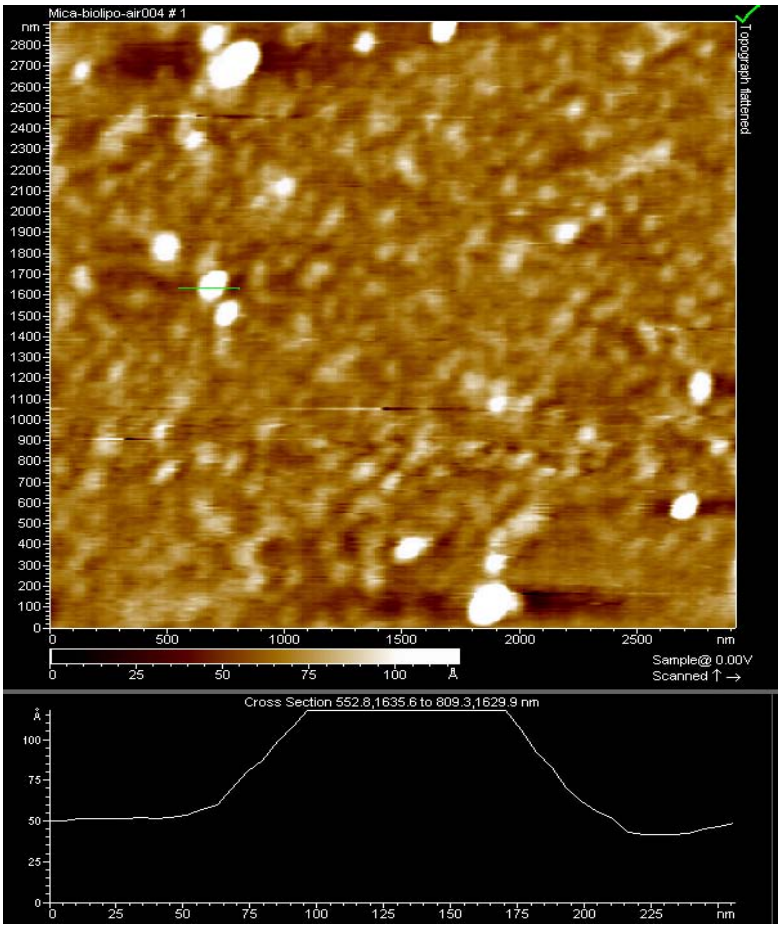

Figure 5.7. Solution phase AFM image of biotin-tag NOS-loaded liposome on mica surface

5.4. References

1. Johnson, R.A., and Freeman, R.H. (1992). Sustained hypertension in the rat induced by chronic blockade of nitric oxide production. Am J Hypertens *5*, 919-922.
2. Lahera, V., Salazar, J., Salom, M.G., and Romero, J.C. (1992). Deficient production of nitric oxide induces volume-dependent hypertension. J Hypertens Suppl *10*, S173-177.
3. Brock, G., Nunes, L., Padma-Nathan, H., Boyd, S., and Lue, T.F. (1993). Nitric oxide synthase: a new diagnostic tool for neurogenic impotence. Urology *42*, 412-417.
4. McGuffey, E. (1993). Can nitric oxide be used to treat impotence? Am Pharm *NS33*, 20.
5. Koglin, J., Glysing-Jensen, T., Mudgett, J.S., and Russell, M.E. (1998). Exacerbated transplant arteriosclerosis in inducible nitric oxide-deficient mice. Circulation *97*, 2059-2065.
6. Weis, M., Kledal, T.N., Lin, K.Y., Panchal, S.N., Gao, S.Z., Valantine, H.A., Mocarski, E.S., and Cooke, J.P. (2004). Cytomegalovirus infection impairs the nitric oxide synthase pathway: role of asymmetric dimethylarginine in transplant arteriosclerosis. Circulation *109*, 500-505.
7. Allen, T.M., Williamson, P., and Schlegel, R.A. (1988). Phosphatidylserine as a determinant of reticuloendothelial recognition of liposome models of the erythrocyte surface. Proc Natl Acad Sci U S A *85*, 8067-8071.

8. Papahadjopoulos, D., Allen, T.M., Gabizon, A., Mayhew, E., Matthay, K., Huang, S.K., Lee, K.D., Woodle, M.C., Lasic, D.D., Redemann, C., and et al. (1991). Sterically stabilized liposomes: improvements in pharmacokinetics and antitumor therapeutic efficacy. Proc Natl Acad Sci U S A *88*, 11460-11464.

9. Lee, K.D., Nir, S., and Papahadjopoulos, D. (1993). Quantitative analysis of liposome-cell interactions in vitro: rate constants of binding and endocytosis with suspension and adherent J774 cells and human monocytes. Biochemistry *32*, 889-899.

10. Trubetskoy, V.S., Dormeneva, E.V., Tsibulsky, V.P., Repin, V.S., and Torchilin, V.P. (1988). Use of enzyme label for quantitative evaluation of liposome adhesion on cell surface: studies with J774 macrophage monolayers. Anal Biochem *172*, 185-189.

11. Weinstein, J.N., Yoshikami, S., Henkart, P., Blumenthal, R., and Hagins, W.A. (1977). Liposome-cell interaction: transfer and intracellular release of a trapped fluorescent marker. Science *195*, 489-492.

12. Szoka, F.C., Jr., Jacobson, K., and Papahadjopoulos, D. (1979). The use of aqueous space markers to determine the mechanism of interaction between phospholipid vesicles and cells. Biochim Biophys Acta *551*, 295-303.

13. Allen, T.M., Austin, G.A., Chonn, A., Lin, L., and Lee, K.C. (1991). Uptake of liposomes by cultured mouse bone marrow macrophages: influence of liposome composition and size. Biochim Biophys Acta *1061*, 56-64.

14. Lee, K.D., Hong, K., and Papahadjopoulos, D. (1992). Recognition of liposomes by cells: in vitro binding and endocytosis mediated by specific lipid headgroups and surface charge density. Biochim Biophys Acta *1103*, 185-197.

15. Pagano, R.E., and Huang, L. (1975). Interaction of phospholipid vesicles with cultured mammalian cells. II. Studies of mechanism. J Cell Biol *67*, 49-60.

16. Perugini, P., Hassan, K., Genta, I., Modena, T., Pavanetto, F., Cetta, G., Zanone, C., Iadarola, P., Asti, A., and Conti, B. (2005). Intracellular delivery of liposome-encapsulated prolidase in cultured fibroblasts from prolidase-deficient patients. J Control Release *102*, 181-190.

17. Rodriguez-Juarez, F., Aguirre, E., and Cadenas, S. (2007). Relative sensitivity of soluble guanylate cyclase and mitochondrial respiration to endogenous nitric oxide at physiological oxygen concentration. Biochem J *405*, 223-231.

18. Allen, T.M., Hong, K., and Papahadjopoulos, D. (1990). Membrane contact, fusion, and hexagonal (HII) transitions in phosphatidylethanolamine liposomes. Biochemistry *29*, 2976-2985.

19. Miller, C.R., Bondurant, B., McLean, S.D., McGovern, K.A., and O'Brien, D.F. (1998). Liposome-cell interactions in vitro: effect of liposome surface charge on the binding and endocytosis of conventional and sterically stabilized liposomes. Biochemistry *37*, 12875-12883.

20. Vermette, P., Meagher, L., Gagnon, E., Griesser, H.J., and Doillon, C.J. (2002). Immobilized liposome layers for drug delivery applications: inhibition of angiogenesis. J Control Release *80*, 179-195.